THE UNIVERSITY OF OKLAHOMA

GRADUATE COLLEGE

THE EFFECT OF BULK VISCOSITY ON COMPRESSIBLE COUETTE FLOW WITH BLOWING

A THESIS

SUBMITTED TO THE GRADUATE FACULTY

in partial fulfillment of the requirement for the

degree of

MASTER OF SCIENCE

by

Hugo Gonzalez

Norman, Oklahoma

1992

THE EFFECT OF BULK VISCOSITY ON COMPRESSIBLE COUETTE FLOW WITH BLOWING

A THESIS

APPROVED FOR THE SCHOOL

OF

AEROSPACE AND MECHANICAL ENGINEERING

BY

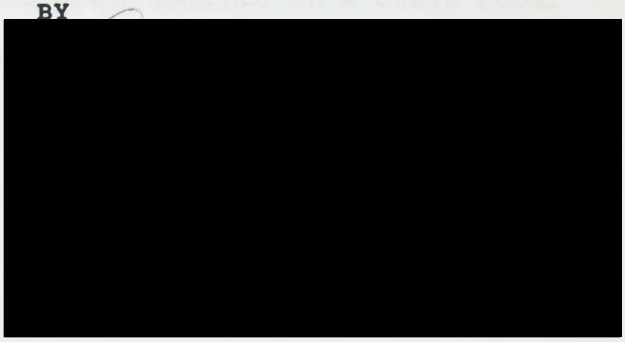

ACKNOWLEDGMENTS

The author wishes to express his sincere appreciation to Dr. G. Emanuel for his supervision, guidance and encouragement throughout the course of this research. He has been a great inspiration and one of the main reason for my success in the completion of my higher education. Thanks is also in order for Dr. W. Upthegrove for his utmost guidance and assistance throughout my graduate education advisement. I would like to extend my gratitude toward my committee members, Dr. W. Sutton and Dr. M. Rasmussen.

Special recognition is directed toward my family "Los González", especially my parents Cosme and Carmen Gonzalez, for their caring, encouragement and sacrifices. I would have wished my mother could be here with us to witness and enjoy the successes of her children. She has taught me so much about life, that I would have never learned in a class room. Finally and not least, I owe all my accomplishments to God for giving me the ability, strength and perseverance required for life.

TABLE OF CONTENTS

Page

LIST OF TABLES

LIST OF FIGURES

FIGURES **Page**

FIGURES **Page**

FIGURES **Page**

FIGURES **Page**

THE EFFECT OF BULK VISCOSITY ON COMPRESSIBLE COUETTE FLOW WITH BLOWING

ABSTRACT

The effect of bulk viscosity on a compressible couette flow is considered between two porous parallel walls in which the lower wall is at rest and the upper wall is moving at a constant velocity. The flow between the walls is steady, two-dimensional, and the gas is perfect. At the lower wall, there is vertically oriented blowing; suction occurs at the upper wall.

The bulk viscosity μ_b is introduced through the second viscosity coefficient, $\lambda = \mu_b - 2/3\mu$, where μ is the shear viscosity and μ_b provides the viscous stresses due to dilatational motion of the gas. Typically μ_b is set equal to zero (Stokes' hypothesis). This case is generally true for monatomic gases and air, but for certain polyatomic gases, such as CO_2, the ratio μ_b/μ can exceed 10^3. Such a large value can significantly effect the flow field.

Compressible couette flow with blowing is governed by four first-order ODE's which are formulated from the conservation equations. These equations are numerically

solved using a fourth-order Runge-Kutta method with variable step size and the shooting method, which transforms a two-point boundary value problem into an equivalent initial value problem. The shooting method is applied to the temperature boundary conditions to assist in determining the initial temperature gradient. This same method also assists in defining an initial x-velocity gradient that governs the determination of the distance between the walls. The physical significance of computed results for both subsonic and supersonic blowing are discussed.

CHAPTER I

INTRODUCTION

1.1 Background

Since the 19th century, couette flow has universally been encountered in fluid dynamic courses at the undergraduate level. It was first studied by M. Couette, a French scientist who helped establish the analysis of viscous shear flows between parallel plates and rotating cylinders. This simple flow model provides researchers with a method for analyzing the behavior of fluids, i.e., velocity and temperature profiles. Although couette flow has been in existence for over a century, it is still an active research topic in the scientific community. For example, two current papers are references [1] and [2]. A major reason for this long-standing interest is because couette flow allows for an analytical solution of the Navier-Stokes equations.

1.2 Purpose of Study

In studying compressible couette flow with blowing, the effect of bulk viscosity μ_b on the flow field is of primary interest. There are few studies that investigate the effect of bulk viscosity on a flow [3,4]. The reason for this limited interest is because bulk viscosity is a third-order boundary-layer effect [3]. When the ratio of bulk viscosity, μ_b, relative to the shear viscosity, μ, is of order unity, bulk viscosity does not enter either the first- or second-order boundary-layer equations. Secondly, common gases, such as air, are well served by Stokes' hypothesis, which states that $\mu_b = 0$. If the flow is incompressible, the terms containing the bulk viscosity in the Navier-Stokes equations are zero because the dilatation, $\nabla \cdot \vec{W}$, equals zero, where $\vec{W}$ is the velocity vector. Therefore, in order for bulk viscosity to have an effect, the flow must be compressible. However, compressible couette flow is uneffected by bulk viscosity unless there is blowing at one porous wall and suction at the other.

Although many gases are adequately served by Stokes' hypothesis, certain polyatomic gases such as CO_2 and N_2O have extremely large μ_b values relative to μ. In fact, these two

gases can have an $\alpha = \mu_b/\mu \approx 2000$ or greater, according to estimates produced using acoustic attenuation experiments. For gases possessing such a large bulk viscosity value, one can anticipate a non-negligible effect in a compressible, viscous flow.

In analyzing couette flow with blowing, a two-dimensional flow of a perfect gas is considered between two parallel porous walls in which the lower wall is stationary, and the upper wall is moving at a constant velocity. The flow is compressible with blowing at the lower wall and suction occurring at the upper wall. The effect of two separate cases are contrasted: Stokes' hypothesis with $\alpha = 0$, and an $\alpha = 2000$.

Discussion regarding the formulation and examination of the governing equations are furnished in the following chapters. Chapter II concentrates on the conservation equations and leads to the derivation of the governing equations using dimensionless parameters and variables. Chapter III reviews the numerical methods used to solve the governing equations. Chapter IV analyzes and compares numerical results involving CO_2 with blowing at either subsonic or supersonic conditions. The last chapter provides a summary and discussion of the physical significance of couette flow with blowing.

CHAPTER II

FORMULATION OF COMPRESSIBLE COUETTE FLOW WITH BLOWING

2.1 Introduction

The behavior of fluids are analyzed by utilizing the conservation equations regardless of the nature of the flow. These equations are the continuity equation, the momentum equation and the energy equation. They are essential in order to completely examine the nature of the flow in question.

The formulation of the governing equations used to study the effect of bulk viscosity on a compressible couette flow with blowing, stems from applying the conservation equations involving mass, momentum and energy. To keep the study simple, the flow is assumed to be steady, two-dimensional and compressible with blowing occurring at a lower porous wall. The lower wall is kept fixed while the upper porous wall is moving at a constant velocity. The gas is assumed thermally and calorically perfect. At the lower porous wall, the gas is injected at either a subsonic or supersonic condition, while suction is occurring at the upper porous wall.

2.2 Compressible Couette Flow with Blowing

Couette flow is assumed to be steady, two-dimensional, compressible, and laminar as illustrated in **Figure 2.2.1.** Gas is uniformly injected into the lower porous wall which is kept stationary, while uniform suction is occurring at the upper porous wall which is moving at a constant velocity, u_o.

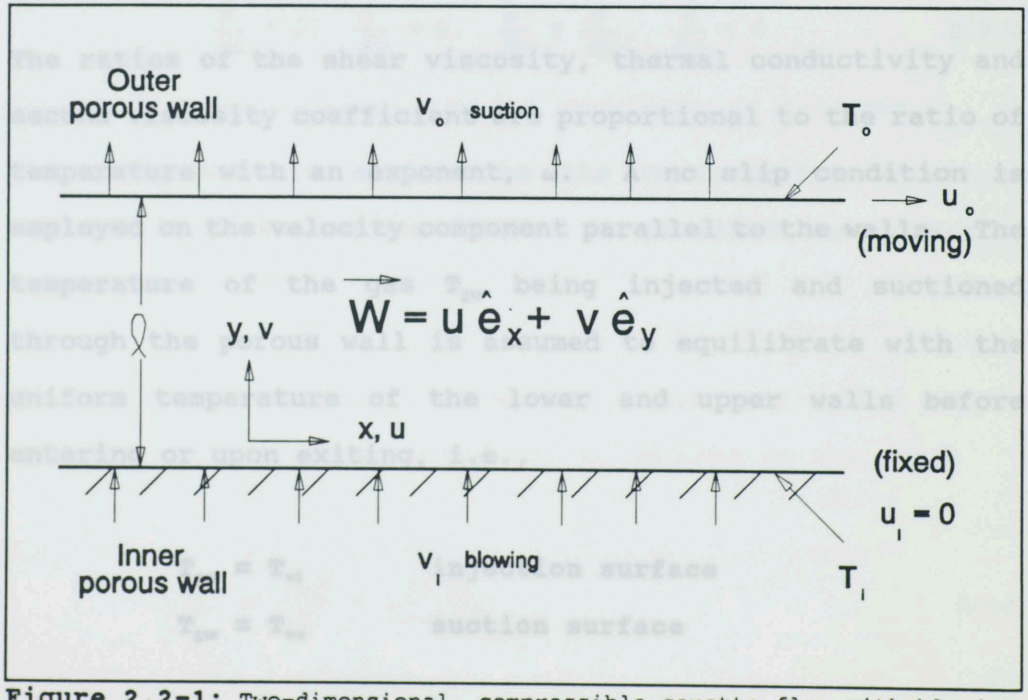

Figure 2.2-1: Two-dimensional, compressible couette flow with blowing at the lower porous wall and suction at the upper wall.

The fluid's velocity vector is indicated as:

$$\vec{W} = u\hat{e}_x + v\hat{e}_y \qquad (2.2\text{-}1)$$

and is a function only of the **y**-coordinate system. The two parallel walls are separated by a vertical distance, ℓ, which contains a perfect gas with the following properties:

$$\frac{\mu}{\mu_i} = \frac{\kappa}{\kappa_i} = \frac{\lambda}{\lambda_i} = \left(\frac{T}{T_i}\right)^{\omega} \qquad (2.2\text{-}2)$$

The ratios of the shear viscosity, thermal conductivity and second viscosity coefficient are proportional to the ratio of temperature with an exponent, ω. A no slip condition is employed on the velocity component parallel to the walls. The temperature of the gas T_{gas} being injected and suctioned through the porous wall is assumed to equilibrate with the uniform temperature of the lower and upper walls before entering or upon exiting, i.e.,

$T_{gas} = T_{wi}$ **injection surface**

$T_{gas} = T_{wo}$ **suction surface**

The gas injected at the lower porous wall is introduced at either a subsonic or supersonic condition. Theoretical and experimental studies confirm that subsonic and supersonic blowing conditions through a porous plate are possible [14, 15]. Therefore, the assumption of either subsonic or supersonic blowing is valid.

Blowing allows for a velocity component, u, which is in the x-direction parallel to the walls and v, which is in the y-direction perpendicular to the walls. Since the flow only depends on y, we have

$$\frac{\partial}{\partial t} = 0, \quad \frac{\partial}{\partial x} = 0, \quad \frac{\partial}{\partial y} = \frac{d}{dy}, \quad \frac{\partial}{\partial z} = 0 \qquad \text{(2.2-3)}$$

The relations are applied to the conservation equations written in Cartesian coordinates to provided the governing equations.

2.3 Dimensionless Parameters and Variables

Dimensionless parameters are valuable and essential for analyzing and correlating results. Some of the most common parameters are the Reynolds number, **Re**; Prandtl number, **Pr**; Mach number, **M**; and Stanton number, **St**. In addition, newly developed dimensionless variables, discussed later in the section, are introduced to reduce the complexity of the governing equations.

The Reynolds number is based on the wall separation ℓ and the transverse blowing velocity component as follows:

$$\mathbf{Re} = \left(\frac{\rho V}{\mu}\right)_i \ell \qquad (2.3\text{-}1)$$

where the subscript **i** denotes the lower wall and ρ is the density. The Prandtl number can be written in the form:

$$\mathbf{Pr} = \frac{C_p \mu}{\kappa} = \frac{\gamma R \mu_i}{(\gamma-1)\kappa_i} \qquad (2.3\text{-}2)$$

where $\mathbf{C_p}$ is the specific heat at constant pressure, κ is the

thermal conductivity, γ is the specific heat ratio, and **R** is the gas constant. The Stanton number is provided as follows:

$$St = \frac{q}{\rho C_p u_o [T - T_t]} \tag{2.3-3}$$

where **q** is the heat flux, u_0 is the upper wall speed, and T_t is the stagnation temperature.

A dimensionless blowing parameter is given by:

$$b = \frac{v_i}{u_o} \tag{2.3-4}$$

To relate the effect of the fluid's bulk viscosity, μ_b, to the shear viscosity, μ, the following ratio is used:

$$\alpha = \left(\frac{\mu_b}{\mu}\right)_i \tag{2.3-5}$$

which is evaluated at the lower wall. The speed of the injected gas is obtained from a blowing Mach number:

$$M_{yi} = \frac{v_i}{(\gamma R T_i)^{1/2}} \tag{2.3-6}$$

The dimensionless velocity component in the x-direction is

$$U = \frac{u}{u_o} \tag{2.3-7}$$

The dimensionless velocity component in the y-direction is

$$V = \frac{v}{v_i} \tag{2.3-8}$$

The temperature distribution of the fluid is given by:

$$\theta = \frac{T}{T_i} \tag{2.3-9}$$

The fluid's transport properties are transformed into dimensionless form as

$$\mu = \mu_i \theta^{\omega} \tag{2.3-10a}$$

$$\kappa = \kappa_i \theta^{\omega} \tag{2.3-10b}$$

$$\lambda = \lambda_i \theta^{\omega} \tag{2.3-10c}$$

The dimensionless vertical distance, measured from the lower wall, is given as a Reynolds number

$$Y = \left(\frac{\rho V}{\mu}\right)_i y \qquad \textbf{(2.3-11)}$$

The **y** derivative is obtained from rearranging **(2.3-11)** and taking the derivative as a function of **y**

$$\frac{d}{dy} = \left(\frac{\rho V}{\mu}\right)_i \frac{d}{dY} = \left(\frac{\rho V}{\mu}\right)_i ( )' \qquad \textbf{(2.3-12)}$$

where a prime denotes d /dY.

These dimensionless parameters and variables are incorporated into the derivation of the governing equations.

2.4 The Continuity Equation

The continuity equation is obtained by taking a mass transfer balance on the fluid entering and exiting the boundaries of a volume element selected within the flow field. In vectorial form, the continuity equation is written as:

$$\frac{D\rho}{Dt} + \rho\nabla\cdot\vec{W} = 0 \qquad \text{(2.4-1)}$$

where **D /Dt** is the substantial derivative. Equations written in vectorial form are independent of any particular coordinate system. In a Cartesian coordinate system, the continuity equation is given by

$$W_i\frac{\partial\rho}{\partial x_i} + \rho\frac{\partial W_i}{\partial x_i} = 0 \qquad \text{(2.4-2)}$$

The equation simplifies to

$$v\frac{d\rho}{dy} + \rho\frac{dv}{dy} = 0 \qquad \text{(2.4-3)}$$

or

$$\frac{d}{dy}(v\rho) = 0$$

The final form produces a constant mass flux between the walls

$$v\rho = v_i\rho_i = v_o\rho_o = constant \qquad (2.4\text{-}4)$$

The density in dimensionless form is determined by equation (2.4-4) by substituting the dimensionless y-velocity component (2.3-8)

$$\rho = \frac{v_i\rho_i}{v}$$

$$\rho = \frac{\rho_i}{V} \qquad (2.4\text{-}5)$$

2.5 The Momentum Equation

The momentum equation is derived from Newton's second law of motion, which states that the sum of external forces acting on a fluid element is equal to the mass times the acceleration of that element. The external forces are comprised of both surface and body forces such as: viscous and pressure forces, gravitational and surface tension effects and, electrical and magnetic fields. The linear momentum equation expressed in vectorial form is given by

$$\rho \frac{D\vec{W}}{Dt} = -\nabla p + \vec{F}^{s} + \nabla(\lambda \nabla \cdot \vec{W}) \qquad (2.5\text{-}1)$$

where

λ = second viscosity coefficient = $\mu_b - \frac{2}{3}\mu$

$\vec{F}^{s}$ = viscous stress term = $F_i^s \hat{e}_i = 2\nabla \cdot (\mu \bar{\epsilon})$

$\bar{\epsilon}$ = strain rate tensor = $\epsilon_{ki}\hat{e}_k\hat{e}_i = \frac{1}{2}[\nabla\vec{W} + (\nabla\vec{W})^T]$

p = pressure

In a Cartesian coordinate system, the linear momentum equation transforms to:

$$\rho W_i \frac{\partial W_j}{\partial x_i} = -\frac{\partial p}{\partial x_j} + \frac{\partial}{\partial x_i}\left[\mu\left(\frac{\partial W_j}{\partial x_i} + \frac{\partial W_i}{\partial x_j}\right)\right] + \frac{\partial}{\partial x_j}\left(\lambda \frac{\partial W_j}{\partial x_i}\right) \qquad \textbf{(2.5-2)}$$

For this flow study, we have:

- Longitudinal momentum equation:

$$\rho v \frac{du}{dy} = \frac{d}{dy}\left[\mu \frac{du}{dy}\right] \qquad \textbf{(2.5-3a)}$$

- Transverse momentum equation:

$$\rho v \frac{dv}{dy} = -\frac{dp}{dy} + \frac{d}{dy}\left[(2\mu + \lambda)\frac{dv}{dy}\right] \qquad \textbf{(2.5-3b)}$$

The derivation of the dimensionless longitudinal and transverse momentum equations are separately discussed in the next sections.

2.6 The Longitudinal Momentum Equation

The longitudinal momentum equation **(2.5-3a)** is integrate with respect to **y**, and the continuity equation **(2.4-4)** is used

$$(\rho v)_i (u-u_i) = \mu \frac{du}{dy} - \left(\mu \frac{du}{dy}\right)_i \qquad \textbf{(2.6-1)}$$

The dimensionless **y** derivative **(2.3-12)**, the dimensionless **x**-velocity, **U** **(2.3-7)** and the dimensionless shear viscosity term, **(2.3-10a)** are substituted to obtain

$$(\rho v)_i u_o U = \mu_i \theta^\omega \left(\frac{\rho v}{\mu}\right)_i u_o \frac{dU}{dY} - \mu_i \left(\frac{\rho v}{\mu}\right)_i u_o \left(\frac{dU}{dY}\right)_i \qquad \textbf{(2.6-2)}$$

After simplification of equation **(2.6-2)**, we have

$$U = \theta^\omega U' - U_i' \qquad \textbf{(2.6-3)}$$

Equation **(2.6-3)** is solved for **U′** to obtain a first-order ordinary differential equation

$$U' = \frac{1}{\theta^\omega}\left(U + U_i'\right) \qquad \textbf{(2.6-4)}$$

2.7 The Transverse Momentum Equation

The transverse momentum equation **(2.5-3b)** is integrate with respect to **y**, and the continuity equation **(2.4-4)** is used

$$(\rho v)_i (v - v_i) = -p + p_i + 2\left[\mu \frac{dv}{dy} - \left(\mu \frac{dv}{dy}\right)_i\right] + \lambda \frac{dv}{dy} - \left(\lambda \frac{dv}{dy}\right)_i \qquad \textbf{(2.7-1)}$$

The dimensionless **y** derivative **(2.3-12)**, the dimensionless **y**-velocity, **V** **(2.3-8)**, the dimensionless shear viscosity and second viscosity coefficient **(2.3-10a,c)** are substituted to provide

$$(\rho v)_i (v_i V - v_i) = -p + p_i + 2\left[\mu_i \theta^{\omega} \left(\frac{\rho v}{\mu}\right)_i v_i \frac{dV}{dY} - \mu_i \left(\frac{\rho v}{\mu}\right)_i v_i \left(\frac{dV_i}{dY}\right)_i\right] + \lambda_i \theta^{\omega} \left(\frac{\rho v}{\mu}\right)_i v_i \frac{dV}{dY} - \lambda_i \left(\frac{\rho v}{\mu}\right)_i v_i \left(\frac{dV_i}{dY}\right)_i \qquad \textbf{(2.7-2)}$$

After dividing by $(\rho v/\mu)_i v_i$, simplification, and rearrangement, the following is obtained

$$\mu_i (V - 1) = \frac{\mu_i (p_i - p)}{\rho v_i^2} + \theta^\omega (2\mu_i + \lambda_i) V' - (2\mu_i + \lambda_i) V_i' \qquad (2.7\text{-}3)$$

Equation **(2.7-3)** is solved for V' to obtain the following first-order ordinary differential equation

$$V' = \frac{V_i'}{\theta^\omega} + \frac{\mu_i}{\theta^\omega (2\mu_i + \lambda_i)} \left[(V - 1) - \frac{(p_i - p)}{\rho_i v_i^2} \right] \qquad (2.7\text{-}4)$$

The pressure difference using the perfect gas assumption in dimensionless form is determined and later employed in equation, **(2.7-4)**, i.e.,

Perfect Gas: $p = \rho R T$

$$p_i - p = R (\rho_i T_i - \rho T)$$

Applying the continuity equation and dimensionless temperature $\theta = T/T_i$, the pressure difference becomes

$$p_i - p = R\left(\rho_i T_i - \frac{\rho_i}{V} T_i \theta\right)$$

$$p_i - p = \rho_i R T_i \left(1 - \frac{\theta}{V}\right) \qquad \textbf{(2.7-5)}$$

For equation **(2.7-4)**, the bulk viscosity is introduced through second viscosity coefficient using the relation in **(2.5-1)**

$$2\mu_i + \lambda_i = 2\mu_i + \left(\mu_{bi} - \frac{2}{3}\mu_i\right) = \mu_{bi} + \frac{4}{3}\mu_i$$

$$2\mu_i + \lambda_i = \left(\frac{\mu_{bi}}{\mu_i} + \frac{4}{3}\right)\mu_i = \mu_i\left(\alpha + \frac{4}{3}\right) \qquad \textbf{(2.7-6)}$$

After substituting the dimensionless pressure difference **(2.7-5)**, the bulk-shear viscosity ratio in **(2.7-6)** into equation **(2.7-4)**, and simplifying, the following is produced

$$V' = \frac{V_i'}{\theta^\omega} + \frac{1}{\theta^\omega\left(\alpha + \frac{4}{3}\right)}\left[V - 1 - \frac{R T_i\left(1 - \frac{\theta}{V}\right)}{v_i^2}\right] \qquad \textbf{(2.7-7)}$$

The blowing Mach number **(2.3-6)** is substituted to obtain the final dimensionless first-order ordinary differential equation for **V'**

$$V' = \frac{1}{\theta^{\omega}} \left\{ V_i' + \frac{1}{\left(\alpha + \frac{4}{3}\right)} \left[V - 1 + \frac{\left(\frac{\theta}{V} - 1\right)}{\gamma M_{yi}^2} \right] \right\} \qquad \textbf{(2.7-8)}$$

2.8 The Energy Equation

The energy equation is derived from taking an energy balance on a volume element within the flow field. It is derived from the first law of thermodynamics, which states that the heat added to a system minus the work done by the system is equal to the difference of the internal energy of the initial and final states. In vectorial form, the energy equation is given by

$$\rho \frac{Dh}{Dt} = \frac{Dp}{Dt} + \Phi - \nabla \cdot \vec{q} \qquad \text{(2.8-1)}$$

where

h = enthalpy = $C_p T = \frac{\gamma}{\gamma - 1} RT$

$\vec{q}$ = heat flux = $-\kappa \nabla T$

Φ = viscous dissipation

$$= \mu \left[2 \sum_{i=1}^{3} \epsilon_{ii}^2 + 4 \left(\epsilon_{12}^2 + \epsilon_{23}^2 + \epsilon_{31}^2 \right) \right] + \lambda \left(\nabla \cdot \vec{W} \right)^2$$

For the heat flux, Fourier's equation is used.

In a Cartesian coordinate system, the energy equation is expressed as:

$$\rho W_i \frac{\partial h}{\partial x_i} = W_i \frac{\partial p}{\partial x_i} + \Phi + \frac{\partial}{\partial x_i}\left(\kappa \frac{\partial T}{\partial x_i}\right) \qquad \textbf{(2.8-2)}$$

$$\Phi = \mu\left[2\sum_{i=1}^{3}\left(\frac{\partial W_i}{\partial x_i}\right)^2 + \left(\frac{\partial W_1}{\partial x_2} + \frac{\partial W_2}{\partial x_1}\right)^2 + \left(\frac{\partial W_2}{\partial x_3} + \frac{\partial W_3}{\partial x_2}\right)^2 + \left(\frac{\partial W_3}{\partial x_1} + \frac{\partial W_1}{x_3}\right)^2\right] + \lambda\left(\sum_{i=1}^{3}\frac{\partial W_i}{\partial x_i}\right)^2 \qquad \textbf{(2.8-2a)}$$

For this study, the equations simplify to

$$\rho v \frac{dh}{dy} = v \frac{dp}{dy} + \Phi + \frac{d}{dy}\left(\kappa \frac{dT}{dy}\right) \qquad \textbf{(2.8-3)}$$

$$\Phi = \mu\left(\frac{du}{dy}\right)^2 + (2\mu + \lambda)\left(\frac{dv}{dy}\right)^2 \qquad \textbf{(2.8-3a)}$$

The viscous dissipation term **(2.8-3a)** is transformed into dimensionless form by substituting the dimensionless **y**-derivative **(2.3-12)**, the dimensionless **x**-velocity, **U (2.3-7)**, the dimensionless **y**-velocity, **V (2.3-8)**, the dimensionless shear viscosity **(2.3-10a)** and the second viscosity coefficient **(2.3-10c)**

The bulk-shear viscosity relationship **(2.7-6)**, obtained in section 2.7, is substituted into equation **(2.8-4)** and after simplifying and rearranging, the following is produced

$$\Phi = \mu_i \theta^{\omega} \left(\frac{\rho V}{\mu}\right)_i^2 \left[u_o^2 (U')^2 + \left(\alpha + \frac{4}{3}\right) v_i^2 (V')^2 \right]$$

(2.8-5)

Now for equation **(2.8-3)**, the dimensionless **y**-derivative **(2.3-12)**, the continuity equation **(2.4-4)**, the dimensionless **y**-velocity, **V** **(2.3-8)**, the dimensionless shear viscosity and thermal conductivity (**2.3-10a** and **2.3-10b**, respectively) and the dimensionless viscous dissipation term **(2.8-5)** are substituted to provide

$$(\rho v)_i \left(\frac{\rho V}{\mu}\right)_i \frac{dh}{dY} = v_i V \left(\frac{\rho V}{\mu}\right)_i \frac{dp}{dY} + \mu_i \theta^{\omega} \left(\frac{\rho V}{\mu}\right)_i^2 \left[u_o^2 (U')^2 + \left(\alpha + \frac{4}{3}\right) v_i^2 (V')^2 \right] + \left(\frac{\rho V}{\mu}\right)_i^2 \kappa_i T_i \frac{d}{dY}\left(\theta^{\omega} \frac{d\theta}{dY}\right) \qquad \textbf{(2.8-6)}$$

After dividing by $(\rho v/\mu)_i$, simplification, and rearrangement, the following is obtained

$$\mu_i \frac{dh}{dY} = \frac{v_i V}{\left(\frac{\rho v}{\mu}\right)_i} \frac{dp}{dY} + \mu_i \theta^{\omega} \left[u_o^2 (U')^2 + \left(\alpha + \frac{4}{3}\right) v_i^2 (V')^2 \right]$$

$$+ \kappa_i T_i \frac{d}{dY}\left(\theta^{\omega} \frac{d\theta}{dY}\right) \qquad \textbf{(2.8-7)}$$

The enthalpy for equation **(2.8-7)** is written as

$$h = c_p T = \frac{\gamma}{\gamma - 1} R T = \frac{Pr \kappa_i}{\mu_i} T_i \theta$$

The derivative of enthalpy is taken with respect to the dimensionless **Y** variable as

$$\frac{dh}{dY} = \frac{Pr \kappa_i T_i}{\mu_i} \frac{d\theta}{dY} = \frac{Pr \kappa_i T_i}{\mu_i} \overline{\theta}$$

(2.8-8)

where

$$\overline{\theta} = \frac{d\theta}{dY}$$

The perfect gas assumption is converted to dimensionless variables as provided

$$p = \rho R T = \frac{\rho_i}{V} \frac{(\gamma - 1) Pr \kappa_i}{\gamma \mu_i} T_i \theta = \frac{(\gamma - 1) \rho_i Pr \kappa_i T_i}{\gamma \mu_i} \frac{\theta}{V}$$

The derivative of pressure is taken with respect to the dimensionless **Y** variable as

$$\frac{dp}{dY} = \frac{(\gamma - 1) \rho_i Pr \kappa_i T_i}{\gamma \mu_i} \left(\frac{1}{V} \frac{d\theta}{dY} - \frac{\theta}{V^2} \frac{dV}{dY} \right)$$

$$= \frac{(\gamma - 1) \rho_i Pr \kappa_i T_i}{\gamma \mu_i V} \left(\overline{\theta} - \frac{\theta}{V} V' \right) \qquad \textbf{(2.8-9)}$$

The derivative with respect to the dimensionless **Y** variable is applied to the following term taken from equation **(2.8-7)** as

$$\frac{d}{dY} \left(\theta^{\omega} \frac{d\theta}{dY} \right) = \omega \theta^{\omega - 1} \left(\frac{d\theta}{dY} \right)^2 + \theta^{\omega} \frac{d^2 \theta}{dY^2}$$

$$= \theta^{\omega} \left(\omega \frac{\overline{\theta}^2}{\theta} + \overline{\theta}' \right) \qquad \textbf{(2.8-10)}$$

After substituting the dimensionless enthalpy **(2.8-8)**, the

After substituting the dimensionless enthalpy **(2.8-8)**, the dimensionless pressure **(2.8-9)**, the term **(2.8-10)** into equation **(2.8-7)** and simplifying, the following is obtained

$$Pr\,\kappa_i\,T_i\,\overline{\theta} = \frac{(\gamma - 1)\,Pr\,\kappa_i\,T_i}{\gamma}\left(\overline{\theta} - \frac{\theta}{V}V'\right) + \mu_i\,\theta^{\omega}\left[u_o^2\,(U')^2 + \left(\alpha + \frac{4}{3}\right)v_i^2\,(V')^2\right] + \kappa_i\,T_i\,\theta^{\omega}\left(\omega\,\frac{\overline{\theta}^2}{\theta} + \overline{\theta}'\right)$$

(2.8-11)

Equation **(2.8-11)** is solved for $\overline{\theta}'$ and rearrange to obtain the following first-order ordinary differential equation

$$\overline{\theta}' = Pr\frac{\overline{\theta}}{\theta^{\omega}} + \frac{Pr\,(\gamma - 1)}{\gamma\,\theta^{\omega}}\left(\frac{\theta}{V}V' - \overline{\theta}\right) - \frac{\mu_i}{\kappa_i\,T_i}\left[u_o^2\,(U')^2 + \left(\alpha + \frac{4}{3}\right)v_i^2\,(V')^2\right] - \omega\,\frac{\overline{\theta}^2}{\theta}$$

(2.8-12)

The blowing Mach number **(2.3-6)** is transformed into dimensionless variables as provided by

$$M_{yi}^2 = \frac{v_i^2}{\gamma R T_i} = \frac{v_i^2}{\gamma \left[\frac{(\gamma - 1) Pr \kappa_i}{\gamma \mu_i} \right] T_i}$$

$$= \frac{v_i^2 \mu_i}{(\gamma - 1) Pr \kappa_i T_i}$$

(2.8-13)

This equation is rearranged to obtain the following form

$$\frac{\mu_i}{\kappa_i T_i} = \frac{(\gamma - 1) Pr M_{yi}^2}{v_i^2} \qquad \textbf{(2.8-14)}$$

After substituting **(2.8-14)** into **(2.8-12)** and rearranging, the first-order ODE becomes

$$\overline{\theta}' = \frac{Pr}{\theta^\omega} \left\{ \overline{\theta} + \frac{\gamma - 1}{\gamma} \left[\frac{\theta}{V} V' - \overline{\theta} - \gamma M_{yi}^2 \theta^\omega \left(\left(\frac{u_o}{v_i} \right)^2 (U')^2 \right. \right. \right.$$

$$\left. \left. \left. + \left(\alpha + \frac{4}{3} \right) (V')^2 \right) \right] \right\} - \omega \frac{\overline{\theta}^2}{\theta} \qquad \textbf{(2.8-15)}$$

The following terms are taken from **(2.8-15)** and combined as

$$\overline{\theta} - \frac{\gamma - 1}{\gamma}\overline{\theta} = \frac{\overline{\theta}}{\gamma} \qquad \textbf{(2.8-16)}$$

The blowing parameter **(2.3-4)** and combined terms **(2.8-16)** are substituted into equation **(2.8-15)** to obtain the final dimensionless first-order ordinary differential equation for $\overline{\theta}'$

$$\overline{\theta}' = \frac{Pr}{\theta^{\omega}}\left\{\frac{\overline{\theta}}{\gamma} + \frac{\gamma - 1}{\gamma}\left[\frac{\theta}{V}V' - \gamma M_{yi}^2\theta^{\omega} * \left(\frac{1}{b^2}U'^2 + \left(\alpha + \frac{4}{3}\right)V'^2\right)\right]\right\} - \omega\frac{\overline{\theta}^2}{\theta}$$

(2.8-16)

2.9 Stokes' Hypothesis and Bulk Viscosity

For a century and a half, numerous discussions have focused on the limitations of Stokes' hypothesis introduced by G.G. Stokes in 1845 [5]. The relation between, μ_b, λ and the shear viscosity coefficient, μ, is

$$\mu_b = \lambda + \frac{2}{3}\mu \qquad (2.9\text{-}1)$$

Stokes' hypothesis sets the bulk viscosity equal to zero

$$\lambda + \frac{2}{3}\mu = \mu_b = 0 \qquad (2.9\text{-}2a)$$

or

$$\lambda = -\frac{2}{3}\mu \qquad (2.9\text{-}2b)$$

This hypothesis is exact for monatomic gases in accordance with the kinetic theory [7], and works quite well for air, where $(\mu_b/\mu = 0.6)$ can be considered negligible.

In situations where Stokes' hypothesis is not valid, the effect of bulk viscosity may be important and should be

considered. It is associated with the viscous stresses produced by the dilatational motion of the fluid, as opposed to shear viscosity which is associated with the shear deformation of the fluid. The dilatational stresses are associated with the collisional relaxation of the vibrational and rotational energy modes of the molecules.

If the flow is incompressible, the continuity equation **(2.4-1)** becomes:

$$\nabla \cdot \vec{W} = 0 \qquad \textbf{(2.9-3)}$$

which states that the dilatation equals zero. The influence of dilatation appears in the momentum equation **(2.5-1)** and in the energy equation **(2.8-1)** through the viscous dissipation term. Therefore, in order for bulk viscosity, μ_b, to have an effect, the flow must be compressible. However, there must also be transverse blowing in the **y**-direction to assure that the effect of bulk viscosity is present. This is noticed when the flow is two-dimensional, since in the momentum equation

$$\frac{d}{dy}\left[\left(\mu_b - \frac{2}{3}\mu\right)\frac{dv}{dy}\right]$$

and in the energy equation

$$\left(\mu_b - \frac{2}{3}\mu\right)\left(\frac{dv}{dy}\right)^2$$

The μ_b terms disappear unless **dv/dy** is not zero.

Although Stokes' relation **(2.9-1)** has been in existence for some time, there are few studies that extensively investigate the effect of bulk viscosity on a flow **[3]**. One reason for this limited area of research is because the bulk viscosity is a third-order effect within boundary-layer theory **[3,4]**. Another reason is that for over a century, Stokes' hypothesis, $\mu_b = 0$, has become a common assumption in fluid dynamics and has proven to be adequate for numerous flow problems, even at extreme conditions. For certain polyatomic gases (such as CO_2 and N_2O), μ_b relative μ is extremely large. In fact, these two gases have a viscosity ratio of $\mu_b/\mu \approx 2 \times 10^3$ at room temperature, according to Tisza **[6]** and Truesdell **[10]** using acoustic attenuation measurements. Monchik and Mason **[7]** applied kinetic theory to a polyatomic gas with the result

$$\alpha = \frac{\mu_b}{\mu} = \frac{C_{int}}{C_v}\frac{\tilde{R}}{C_v}\frac{p\tau}{\mu} \qquad (2.9\text{-}4)$$

where C_{int} is the specific heat for the vibrational or

rotational energy mode of interest, C_v is the specific heat at constant volume, $\tilde{R}$ is the universal gas constant, and τ is the relaxation time for the mode of interest. Due to gas laser research, a considerable amount of vibrational relaxation data is available for CO_2 [6,10]. This data shows that $\alpha \approx 2 \times 10^3$ for CO_2 is realistic [9].

One reason for analyzing flows with a large bulk viscosity is that several planetary atmospheres are mainly composed of a gas having a large α value [8]. Two planets with such an atmosphere are Venus and Mars, which have about 96% CO_2 with a small trace of water vapor [9]. Recently, there is interest in using these planetary atmospheres for hypersonic space vehicle maneuvers to change the vehicle's trajectory. This area of study is known as Aero-Gravity-Assist [11, 12, 13]. When this type of situation is experienced, Stokes' hypothesis may not be valid, since the heat transfer or other fluid characteristics may be governed by the influence of bulk viscosity.

2.10 Governing Equations for Compressible Couette Flow with Blowing

The conservation equations, discussed earlier in sections 2.4 through 2.8, are the basis used to derive the governing equations associated with this study. These equations are generated for a two-dimensional, compressible flow with transverse blowing in the **y**-direction. The effect of bulk viscosity μ_b is introduced through the second viscosity coefficient term, λ. The transverse momentum equation **(2.5-1)** and the energy equation **(2.8-1)** both involve bulk viscosity.

After algebraic manipulation, simplification and substitution of all the dimensionless parameters and variables discussed in section 2.3 through 2.8, the final derived form of the governing equations and their boundary conditions are provided as follows:

1. Continuity Equation

$$\rho = \frac{\rho_i}{V} \qquad \textbf{(2.10-1)}$$

2. Linear Momentum Equations

a. Longitudinal momentum equation (provides the x-velocity profile)

$$U' = \frac{1}{\theta^{\omega}} \left(U + U_i' \right) \qquad \textbf{(2.10-2a)}$$

b. Transverse momentum equation (provides the y-velocity profile)

$$V' = \frac{1}{\theta^{\omega}} \left\{ V_i' + \frac{1}{\alpha + \frac{4}{3}} \left[V - 1 + \frac{1}{\gamma M_{yi}^2} \left(\frac{\theta}{V} - 1 \right) \right] \right\} \qquad \textbf{(2.10-2b)}$$

3. Energy Equation (provides the temperature profile)

$$\overline{\theta} = \theta' \qquad \textbf{(2.10-3a)}$$

$$\overline{\theta}' = \frac{Pr}{\theta^{\omega}} \left\{ \frac{\overline{\theta}}{\gamma} + \frac{\gamma - 1}{\gamma} \left[\frac{\theta}{V} V' - \gamma M_{yi}^2 \theta^{\omega} \right.\right.$$

$$\left.\left. * \left(\frac{1}{b^2} U'^2 + \left(\alpha + \frac{4}{3} \right) V'^2 \right) \right] \right\} - \omega \frac{\overline{\theta}^2}{\theta}$$

(2.10-3b)

4. Boundary Conditions

a. inner wall at Y = 0:

$$U_i = 0 \qquad \textbf{(2.10-4a)}$$

$$V_i = 1 \qquad \textbf{(2.10-4b)}$$

$$\theta_i = 1 \qquad \textbf{(2.10-4c)}$$

b. outer wall at Y = Y_o = Re:

$$U_o = 1 \qquad \textbf{(2.10-5)}$$

The momentum equation is derived as first-order ODE's **(2.10-2a and 2.10-2b)**. These equations introduce integration constants as follows: U_i' for the longitudinal momentum equation **(2.10-2a)** and V_i' for the transverse momentum equation **(2.10-2b)**. The energy equation is derived as a second-order ODE which is reduced to two first-order ODE's **(2.10-3a and 2.10-3b)**. Both the transverse momentum equation and energy equations involve the effect of bulk viscosity, μ_b, through α and the blowing Mach number M_{yi}. The energy equation is the only governing equation that involves the dimensionless blowing parameter, **b (2.3-4)**.

The system for compressible couette flow with blowing and bulk viscosity is now composed of four first-order ODE's with

boundary conditions applied at both the lower and upper walls (2.10-4 and 2.10-5). To solve the governing equations, a numerical scheme can be applied to determine the flow's distribution profiles

$$U,\ V \text{ and } \theta$$

which are dimensionless functions of **Y** taken from the lower wall to the upper wall. The governing equations are integrated until the upper wall boundary condition, $U_o = 1$, is satisfied. When this criteria is meet, the Reynolds number is determined since $Y_o = Re$ at the upper wall. Therefore, the vertical wall separation distance, ℓ, is subsequently determined by the Reynolds number, **Re**. The Reynolds number is numerically dependent upon the input parameters, especially the initial **x**-velocity integration constant, U_i', which influences convergence of the boundary condition, $U_o = 1$. This makes for a solution that is dependent upon the selection of the initial gradients (U_i', V_i' and θ_i'), and the dimensionless input parameters. To help minimize the number of free parameters, the upper wall temperature can be prescribed and a shooting method applied to determine the initial temperature gradient, θ_i', required to satisfy θ_o. The shooting method is also used to determine, U_i', in order to compare $\alpha = 0$ and 2000 cases that pertain to the same Reynolds

number. The shooting method is effective only if a solution exists based upon the selection of the numerical parameters for both α cases.

The numerical solution, the upper wall heat transfer and the skin friction coefficient depends on the following input parameters and variables γ, ω, **Pr**, α, **b**, M_{yi}, **Re**, θ_o, and V_i' or γ, ω, **Pr**, α, **b**, M_{yi}, θ_i', U_i', and V_i'. For variable property couette flow without blowing, the fluid's properties are constant within each streamline which are parallel to the walls, but vary from streamline to streamline. Now for compressible couette flow with blowing, the stream line are not parallel to the walls and the fluid's properties vary within each streamline, but are constant for each streamline when taking a reference line parallel to the walls. To illustrate, **Figure 2.10-1** is given below:

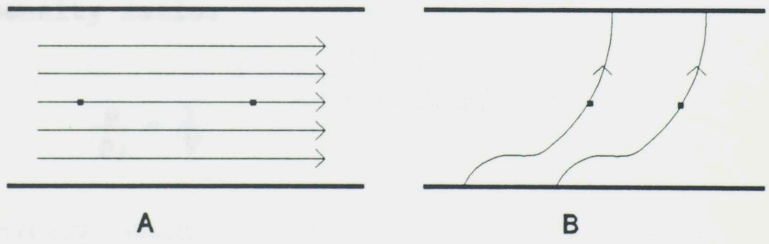

Figure 2.10-1: Streamlines A.) Simple couette flow without blowing
B.) Compressible couette flow with blowing

2.11 Auxiliary Equations

Once the governing equations are solved for the flow's **U**, **V** and θ profiles, auxiliary equations as functions of $0 \leq Y \leq Re$ are utilized to analyze the flow field in greater detail. These auxiliary relations include density ratio, pressure ratio, Mach number, normalized vorticity, normalized viscous dissipation, rate of entropy production, Stanton number, and skin friction coefficient. The Stanton number and the skin friction coefficient are analyzed only at the lower and upper walls. The auxiliary equations are formulated by implementing the dimensionless parameters defined in section 2.3. They are provided in their dimensionless form as follows:

Density ratio:

$$\frac{\rho}{\rho_i} = \frac{1}{V} \tag{2.6-1}$$

Pressure ratio:

$$\frac{p}{p_i} = \frac{\theta}{V} \tag{2.6-2}$$

Mach number:

$$M^2 = M_{yi}^2 \frac{\frac{1}{b^2} U^2 + V^2}{\theta} \tag{2.6-3}$$

Normalized Vorticity:

$$\hat{\omega} = U' \tag{2.6-4}$$

Normalized Viscous Dissipation:

$$\hat{\Phi} = \theta^{\omega} \left[\frac{1}{b^2} U'^2 + \left(\alpha + \frac{4}{3} \right) V'^2 \right] \tag{2.6-5}$$

Rate of Entropy Production:

$$\hat{s}_{irr} = \frac{p_i}{p} \hat{\Phi} + \frac{V \theta^{\omega - 1} \theta'^2}{(\gamma - 1) Pr M_{yi}^2} \tag{2.6.6}$$

Stanton Number:

$$St = \frac{q}{\rho c_p u_o [T - T_t]} = \frac{2}{\gamma - 1} \frac{b}{Pr} \frac{V \theta^{\omega - 1} \theta'}{M^2} \tag{2.6.7}$$

Skin Friction Coefficient:

$$C_f = \frac{2\tau}{\rho u_o^2} = 2\, b\, \theta^{\omega}\, V U' \qquad (2.6\text{-}8)$$

A detailed derivation is provided in **Appendix A.** The density and pressure ratios examine the compressibility characteristics of the fluid. The normalized viscous dissipation analyzes the heat dissipated from viscous stresses produced by the deformation and the dilatational motion of the fluid. The rate of entropy production is used to examine the overall dissipation due to heat transfer and viscous effects. The Stanton number and the skin friction coefficient, which are examined only at the lower and upper walls, are used to analyze the heat transfer and frictional forces encountered on the two walls.

CHAPTER III

NUMERICAL METHOD

3.1 Introduction

The revolution of computer technology and numerical techniques has become an essential tool for solving complicated and tedious mathematical problems. Depending upon the selection of the computer and the numerical method chosen, numerical solutions of ordinary and partial differential equations can be determined in a small fraction of the time, as compared to elaborate hand calculations. The computer is only considered a tool which requires the assistance of someone to provided computer language programs. These computer programs are crucial instructions that allows the computer to generate solutions to an infinite number of complex scientific problems.

Numerical methods contribute enormous power to the mathematical analysis of modeled problems. They provide the ability for accurately simulating many real physical situations by handling nonlinearities, large systems of coupled equations, complicated geometries and many other

applications. Numerical methods assist in solving problems which do not have analytical solutions and provide accurate estimates for those problems which do have analytical solutions.

The numerical methods selected to solve the governing equations for compressible couette flow with blowing will be discussed in the following sections. Section 3.2 discusses the fourth-order Runge-Kutta method used to solve the governing equations. Section 3.3 reviews the input parameter required to solve the equations numerically. Section 3.4 discuses an application of a variable step size method to handle situations where the governing equations are stiff based upon certain numerical input parameters. Section 3.5 introduces the shooting method used to determine the initial temperature gradient, θ_i', and the initial x-velocity gradient, U_i', by converting a two-point boundary value problem into an equivalent initial value problem.

3.2 Fourth-Order Runge-Kutta Method

This study is governed by four first-order ODE's **(2.10-2a, 2.10-2b, and 2.10-3)**. A fourth-order Runge-Kutta method is selected to solve these ODE's. It is one of the easiest numerical methods to program for initial value problems. Advantages include simplicity, self-starting, and the ability to vary it's step size without any difficulty. This approach has good stability characteristics and behaves quite well with nonlinear equations. The general fourth-order Runge-Kutta formulas obtained from Hornbeck **[16]** are provided below for the generic equation, **dy/dt = f(y,t)**:

$$y_{i+1} = y_i + \Delta t \left[\frac{1}{6} f(y_i, t_i) + \frac{1}{3} f(y^*_{i+1/2}, t_{i+1/2}) + \frac{1}{3} f(y^{**}_{i+1/2}, t_{i+1/2}) + \frac{1}{6} f(y^*_{i+1}, t_{i+1}) \right] \qquad \textbf{(3.2-1)}$$

where

$$y^*_{i+1/2} = y_i + \frac{\Delta t}{2} f(y_i, t_i) \qquad \textbf{(3.2-1a)}$$

$$y^{**}_{i+1/2} = y_i + \frac{\Delta t}{2} f(y^*_{i+1/2}, t_{i+1/2}) \qquad \textbf{(3.2-1b)}$$

$$y^*_{i+1} = y_i + \Delta t f(y^{**}_{i+1/2}, t_{i+1/2}) \qquad \textbf{(3.2-1c)}$$

Since the equations in section 2.10 already exist as four coupled set of first-order ODE's:

$$U' = f_1 \tag{3.2-2}$$

$$V' = f_2 \tag{3.2-3}$$

$$\theta' = \overline{\theta} = f_3 \tag{3.2-4}$$

$$\overline{\theta}' = f_4 \tag{3.2-5}$$

the fourth-order Runge-Kutta formulas can be applied directly to them. The intermediate quantities $\mathbf{y}^{*}_{i+1/2}$, $\mathbf{y}^{**}_{i+1/2}$, and $\mathbf{y}^{*}_{i+1}$ **(3.2-1a, 3.2-1b,** and **3.2-1c;** respectively) are determined in sequential order, since they are interdependent of each other.

3.3 Numerical Input Parameters

To solve the ODE's that govern compressible couette flow with blowing, certain initial input parameters and variables are required. For the fluid properties, they are

γ, specific heat ratio

ω, power law temperature exponent

Pr, Prandtl number

α, bulk-shear viscosity ratio

For the fluid dynamic properties, they are

b, blowing parameter

M_{yi}, blowing Mach number

The integration constants (initial gradient values) introduced from integrating the momentum equation **(2.10-2)** are

U_i', from x-momentum equation (2.10-2a)

V_i', from y-momentum equation (2.10-2b)

The energy equation **(2.10-3)** requires an initial gradient value for the temperature which is:

$$\theta_i', \qquad \textbf{initial temperature gradient}$$

The initial gradient values (U_i', V_i' and θ_i') are unknown but are required in order to solve the derived governing equations. The shooting method assists in eliminating two of these unknowns, which are U_i' and θ_i'. This leaves V_i' to be considered as a hypothetical value based upon the required input parameters mentioned at the beginning of this section.

Certain limits are placed on the input parameters to assure that there are no unwarranted physical characteristics of the fluid or flow. The limitations are provided as shown below in **Table 3.3-1:**

Table 3.3-1: Limitation conditions placed on input parameters

$\gamma \geq 1$	$\omega \geq 0$	$Pr > 0$
$\alpha \geq 0$	$b > 0$	$M_{y1} > 0$
$U > 0$	$V > 0$	$\theta > 0$
$U_i' > 0$	$\theta_i' > 0$	

3.4 Variable Step Size

Depending on the numerical input values for **b**, M_{yi}, and **α**, the **y**-momentum equation **(2.10-2b)** can become stiff. This situation is encountered if either the blowing parameter or the blowing Mach number is relatively small, i.e.,

$$b < 0.1, \qquad M_{yi} < 0.2$$

In addition to these conditions, stiff behavior of the equations can be caused by a large bulk-shear viscosity ratio

$$\alpha >> 10$$

To adjust for stiffness, the step size **ΔY** required by the Runge-Kutta method is varied, using small increments on the order of 10^{-4}. To determine the variable step size, a method discussed in reference **[17]** is utilized. This method controls the step size by approximately evaluating the relaxation time for the stiffest equation. The **y**-momentum equation **(2.10-2b)**, which controls whether the equation is stiff or not, is

approximated by:

$$\frac{dV}{dY} = V' \approx \frac{\theta - V}{V\theta^{\omega}\left[\left(\alpha + \frac{4}{3}\right)M_{yi}^2\right]} \tag{3.4-1}$$

An approximate relaxation time is

$$Z \equiv V\theta^{\omega}\left[\left(\alpha + \frac{4}{3}\right)M_{yi}^2\right] \tag{3.4-2}$$

and a stable step size then is

$$\Delta Y = Z \tag{3.4-3}$$

The variation of the step size is also controlled by applying minimum and maximum limits

$$|\Delta Y|_{min} \leq \Delta Y \leq |\Delta Y|_{max} \tag{3.4-4}$$

3.5 Shooting Method

Application of the shooting method is used to transform a two-point boundary value problem into an equivalent initial value problem. This is accomplished by using a root solving procedure such as the bisection or secant methods. The shooting method is similar to a ballistic problem of shooting a cannon at a target. With known calculated misses, one can eventually predict the required initial condition to hit the target.

With the same logic, a boundary value problem is converted into an initial value problem by providing two estimated values of the unknown initial values. By utilizing these estimates, solutions for the initial value problem are determined utilizing any numerical method. At the distant point, the computed and known boundary values are compared, and new estimated initial values are found using the secant method. This process is continued until convergence is reached for the boundary values at the distant point. Depending on the complexity of the equations, this procedure may require only a few iterations until convergence is reached.

To illustrate the method consider a simple two-point boundary value problem given as:

$$y'' + Ay = B \tag{3.5-1}$$

with boundary conditions

$$y(0) = g(0) \tag{3.5-1a}$$

$$y(N) = g(N) \tag{3.5-1b}$$

By applying the shooting method, this boundary value problem is converted into the following initial value problem:

$$y'' + Ay = B \tag{3.5-2}$$

with initial conditions

$$y(0) = g(0) \tag{3.5-2a}$$

$$y'(0) = \delta(0) \tag{3.5-2b}$$

where the $\delta(0)$ value is to be determined based on the boundary condition provided by $y(N) = g(N)$. The general shooting method formulas using the secant method are given by:

$$\delta_j = \delta_{j-1} - \frac{R_{j-1}(\delta_{j-1} - \delta_{j-2})}{R_{j-1} - R_{j-2}}, \quad j = 3, \ldots, n \tag{3.5-3}$$

$$R_j = y_j(N) - g(N), \quad j = 1, \ldots, n \tag{3.5-3a}$$

Two estimated initial values δ_1 and δ_2 are required in order to determine $y_1(N)$ and $y_2(N)$ by a numerical method, followed by the calculation of R_1 and R_2. The iteration of the secant based formula converges when:

$$|R_j| \leq \epsilon$$

where

ϵ = specified minimum value

The shooting method is applied to the governing equations (2.10-2 and 2.10-3) along with the fourth-order Runge-Kutta method to convert

$$U_0 = 1$$

$$\theta_0 = g(N) = \text{prescribed value}$$

into an equivalent initial conditions

$$U'(0) = U_i'$$

$$\overline{\theta}(0) = \theta'(0) = \theta_i'$$

Values for U_i' and θ_i' are determined when the U_0 and θ_0 conditions are simultaneously satisfied at $Y_0 = Re$. Thus, U_i' can be varied until a prescribed value for Re is attained. Consequently, the wall separation, ℓ, is a computed quantity rather than a prescribed one. This approach leaves only V_i'

as a free parameter. Depending on the choice of parameters, such as b, M_{yi}, V_i', ..., convergence may not occur, in which case a solution does not exist.

Since θ_o is not an essential boundary condition, the shooting method can be used with just $U_o = 1$ replaced with $U'(0) = U_i'$. It is found to be more convenient, however, to prescribe θ_o rather than guess θ'_i, since we had a general idea of what θ_o should be. The process was not extended to replacing V_i' with V_o. One reason is that computation time increases rapidly as the number of boundary conditions requiring simultaneous satisfaction increases. A second reason was the uncertainty of appropriate values for V_o.

CHAPTER IV

DISCUSSION OF NUMERICAL RESULTS

4.1 Introduction

Cases are run with $\alpha = 0$ (Stokes' hypothesis) and with $\alpha = 2000$, which is appropriate for CO_2 at room temperature. At a temperature of $T_i = 300$ K, CO_2 has the properties

$$\gamma = 1.285, \quad \omega = 0.867, \quad Pr = 0.770$$

and these are used throughout this study. Thus, the effect of a large bulk viscosity is evaluated by comparing solution profiles with a comparable $\alpha = 0$ case. Both subsonic and supersonic injection is considered.

4.2 Numerical Computer Code

The numerical computer program created to analyze the influence of bulk viscosity on a compressible couette flow is written in Fortran 77 computer language. The program can be compiled on a main frame computer or a stand alone personal computer system (PC). Due to today's ever increasing technology advances in personal computers, the PC is the most suitable option for computer usage as opposed to main frames. Today's PC are portable and are continually increasing in speed, power and capability.

The numerical code is written in Ascii text and is provided in **Appendix B.** The Ascii code is complied using a DOS operating software known as "Microsoft Fortran 5.0". The numerical compiling of the Ascii code with this software produces a DOS executable file which can be used on any compatible "IBM" PC system. The advantage of compiling the numerical code on a personal computer is that the executable numerical code file can be transferred onto a storage media such as a floppy diskette. The floppy diskette allows the executable program to be used on any compatible "IBM" DOS operating personal computer.

Whenever the executable code is run, it asks the user to supply the following required numerical input data, discussed in section 3.3, provided below in **Table 4.2-1:**

Table 4.2-1: Questions asked for numerical code inputs

Do you want detailed print out of Runge-Kutta's intermediate formulas ? Type (0) for YES or (1) for NO.
Do you want detailed print out of U, U', V, V', θ, θ', θ" at each step size interval ? Type (0) for YES or (1) for NO.
Input number of printed steps wanted for solution ?
Input specific heat ratio $\gamma \geq 1$ for the gas ?
Input power law temperature exponent $\omega \geq 0$ for the gas ?
Input Prandtl number $Pr > 0$ for the gas ?
Input bulk-shear viscosity ratio $\alpha \geq 0$ for the gas ?
Input blowing parameter $b > 0$?
Input blowing Mach number $M_{y1} > 0$?
Input prescribed outer wall temperature $1 \leq \theta_o \leq 5$?
Input Reynolds number $10 \leq Re \leq 20$ for $U_o = 1$ condition ?
Input initial y-velocity gradient $-0.001 \leq V_1' \leq 0.001$?

The time required to run the numerical code depends on the microprocessor and clock speed of the PC used. **Table 4.2-2** provides the approximate time required to converge the numerical code using the following inputs:

γ = 1.285 ω = 0.867 Pr = 0.770

α = 2000 b = 0.25 M_{yi} = 1.0

θ_o = 2.5 Re = 12.0 V_i' = 0

U_i' = 0.000146 <= Determined by the Shooting Method

θ_i' = 0.008344 <= Determined by the Shooting Method

Table 4.2-2: Run time for different personal computers

PC System	486/33 Mhz	386/33 Mhz With Math Coprocessor	386/25 Mhz With No Math Coprocessor
Approximate Time	90 sec	300 sec	3 hrs-11 min

For this particular case, five iterations are required for the shooting method to converge to the prescribed upper wall temperature, θ_o = 2.5, and nine iteration to converge to a Reynolds number criteria of Re = 12.0 when U_o = 1. The number of iterations for convergence to a prescribed criteria will vary depending upon the closeness to the final result of the two initial guesses for the temperature and x-velocity gradients.

4.3 Temperature and Initial Gradient Limits

Limits are placed on the numerically determined temperature profiles to assure some degree of physical reality. The temperature limits are as follows:

$$0.6 \leq \theta \leq 10 \qquad (4.3\text{-}1)$$

$$0.6 \leq T/T_i \leq 10$$

$$0.6T_i \leq T \leq 10T_i$$

if T_i = 300 K $180\ K \leq T \leq 3000\ K$

When the temperature encountered in the flow field is extremely high, i.e. $\theta > 10$, the assumption of a perfect gas is no longer valid. Therefore, numerical solutions are not analyzed whenever the temperature value is greater than the maximum limit, i.e. $\theta > 10$. On the other hand, θ can not be negative either.

In order to numerically solve the governing equations, initial gradient values are required

$$U_i', \quad V_i' \quad \text{and} \quad \theta_i'$$

The initial temperature and **x**-velocity gradient, θ_i' and U_i', respectively, are obtained using the shooting method. Hence, the initial **y**-velocity gradient, V_i', is the only unknown value required.

In order for a numerical solution to converge, the temperature's initial gradient, θ_i', has to be either equal to zero or a small positive value, i.e.,

$$0 \leq \theta_i' \leq 0.1 \qquad (4.3\text{-}2)$$

If the initial temperature gradient is selected in the negative spectrum, on the order of -10^{-3} or less, the second law of thermodynamics is violated, since a negative temperature is encountered within the flow.

The initial **x**-velocity gradient, U_i', has to be positive and greater than zero to satisfy the upper wall boundary condition $U_o = 1$, i.e.,

$$0 < U_i' \leq 0.1 \qquad (4.3\text{-}3)$$

If the initial **x**-velocity gradient value is chosen as $U_i' = 0$, then the iteration for **U** remains zero and the numerical solution diverges. For $U_i' < 0$, the iteration of **U** remains negative preventing the upper wall boundary condition, $U_o = 1$, to be reached.

The Reynolds number, determined when the upper wall boundary condition, $U_o = 1$, is satisfied, is indirectly influenced by the initial **x**-velocity gradient, U_i'. As discussed before, the Reynolds number provides the vertical separation distance between the lower and upper walls. As the selected value for U_i' approaches zero, the Reynolds number steadily increases.

An illustration of the influence of U_i' on the Reynolds number is shown below in **Table 4.3.1** using the following inputs for CO_2 without using the shooting method:

γ = 1.285 ω = 0.867 Pr = 0.770

α = 2000 b = 0.1 M_{yi} = 0.2

U_i' = Varied V_i' = 0 θ_i' = 0.001

Table 4.3-1: The influence of U_i' on the Reynolds number, Re.

U_i'	Re	U_o	V_o	θ_o
0.0000001	47.2	1	1.4	27.7
0.000001	22.4	1.0	1.1	7.4
0.00001	13.7	1.0	1.0	2.4
0.0001	9.7	1.0	1.0	1.1
0.001	6.9	1.0	1.0	0.8
0.01	4.5	1.0	1.0	0.7
0.1	2.3	1.0	1.0	0.7

as U_i' approaches zero, **Re** increases but θ exceeds **10**, which

causes the perfect gas assumption to become invalid. Therefore, U_i' should be on the order of 10^{-5} to insure a realistic solution. When relatively low blowing Mach numbers are selected, such as $M_{yi} \leq 0.2$, the results obtained for **Re** tend to be higher as opposed to choosing larger values for M_{yi}.

The initial gradient, V_i', can either be a small positive, zero, or a small negative value, i.e.,

$$-0.1 \leq V_i' \leq 0.1 \qquad (4.3\text{-}4)$$

The initial gradient value of $V_i' = 0$ provides the widest convergence range for solutions when using $0 \leq \theta_i' \leq 0.03$ and $U_i' = 0.00005$ as shown in the next section with graphical results. If the initial gradient value is not selected as $V_i' = 0$, the possibility of a solution starts to decrease as the injected blowing condition increases into the supersonic regime.

4.4 Correlations for Bulk-Shear Viscosity Ratio $\alpha = \mu_b/\mu = 2000$

Without the use of the shooting method and a prescribed outer wall temperature, the numerical code is executed to produce several different numerical results by varying certain required input parameters. The numerical code is modified to allow only for iteration of the Runge-Kutta method until the outer boundary wall condition $U_o = 1$ is satisfied. Each individual input case consists of results for the outer wall values, which are the **Re**, V_o, and θ_o. In addition to the outer wall values, the minimum and maximum dimensionless temperature (θ_{min} and θ_{max}) encountered in the flow are extracted from each run.

The polyatomic gas, CO_2, is selected as the fluid with T_i = 300 K. The initial gradient values U_i' and V_i' selected for the input are 0.00005 and 0, respectively. The initial temperature gradient is allowed to vary as $0 \leq \theta_i' \leq 0.03$ in increments of 0.001. For each θ_i', the blowing parameter **b** is varied from 0.05 to 2 in increments of 0.05 for each blowing Mach number of M_{yi} = 0.1, 0.5, 1, 5, 10, 15.

By plotting results as **Re** verses M_{yi}^2/b^2, a graphical correlation for $\alpha = \mu_b/\mu = 2000$ is established (see **Figure**

4.4-1). Similar plots appear in **Figures 4.4-2** through **4.4-4** for θ_o, θ_{max}, and θ_{min}, respectively. These correlations are found only for the particular case of α = **2000** and V_i' = **0**. Linear correlations are produced by plotting the raw data for M_{yi}^2/b^2 relative to both **Re** and θ_o. The graphs are re-generated by applying a linear best fit method on the raw data to create **Figure 4.4-1** and **Figure 4.4-2**. Additional correlations are produced from the raw data of M_{yi}^2/b^2 relative to θ_{min} and θ_{max}. The raw data is best fitted to create **Figure 4.4-3** and **Figure 4.4-4**. These correlations help provide a guideline for predicting if solutions exist when α = **2000**. Information regarding a solution, such as it's **Re**, θ_o, θ_{min}, and θ_{max} can be graphically estimated using the correlations. The figures for θ_{min} and θ_{max} can be used to determine if temperature overshoot occurs within the flow. The ratio of M_{yi}^2/b^2 used for the graphical correlations can be translated as

$$\frac{M_{yi}^2}{b^2} = \frac{\left(\frac{v_i^2}{\gamma R T_i}\right)}{\left(\frac{v_i^2}{u_o^2}\right)} = \frac{u_o^2}{\gamma R T_i} \qquad (4.4\text{-}1)$$

When α >> **10** and V_i' = **0**, the **y**-velocity distribution remains virtually constant, i.e., **V** ≈ **1.0** and in turn **V'** ≈ **0**; thereby, causing the energy equation **(2.5-10)** to be governed by M_{yi} and

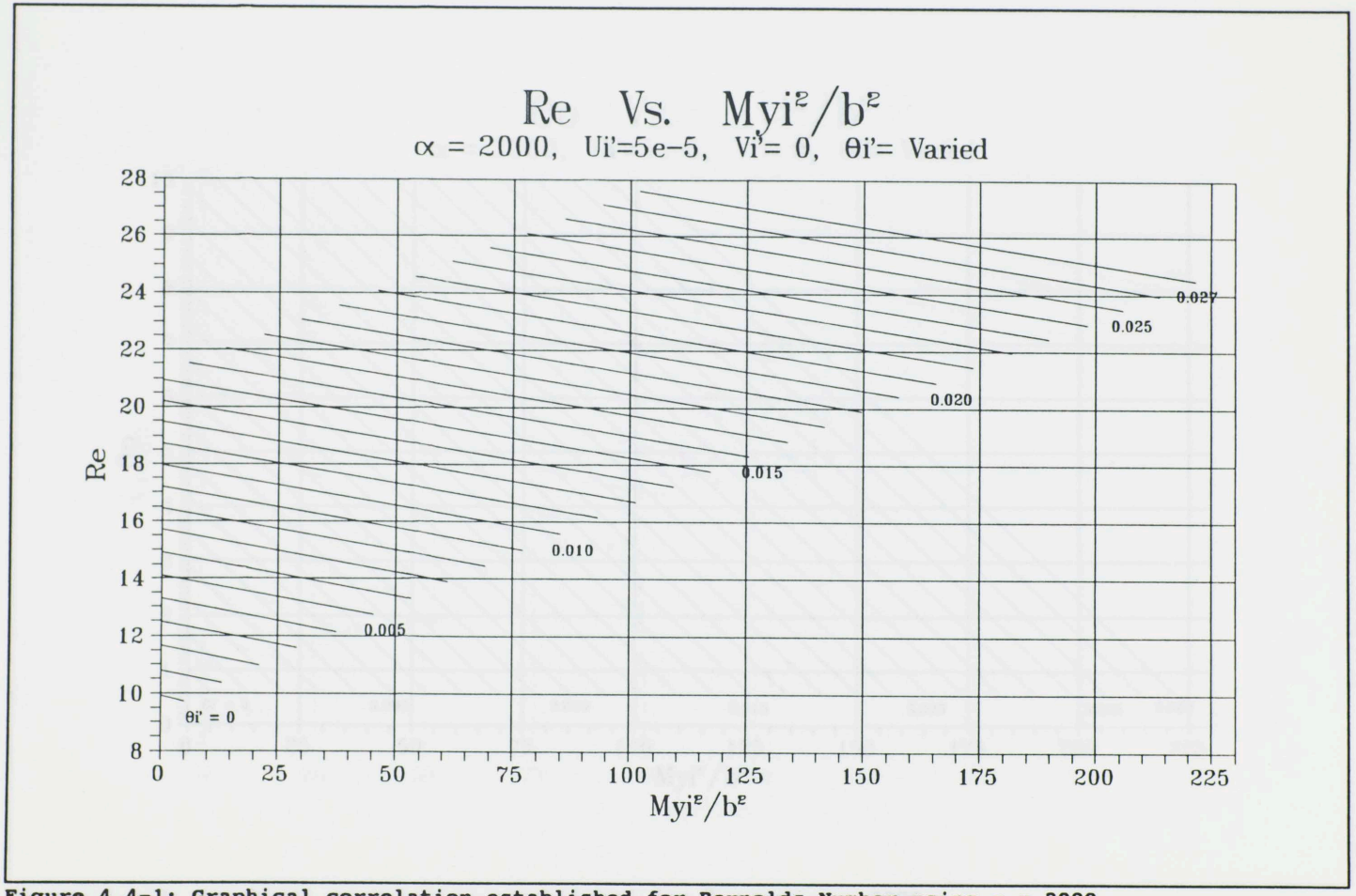

Figure 4.4-1: Graphical correlation established for Reynolds Number using α = 2000.

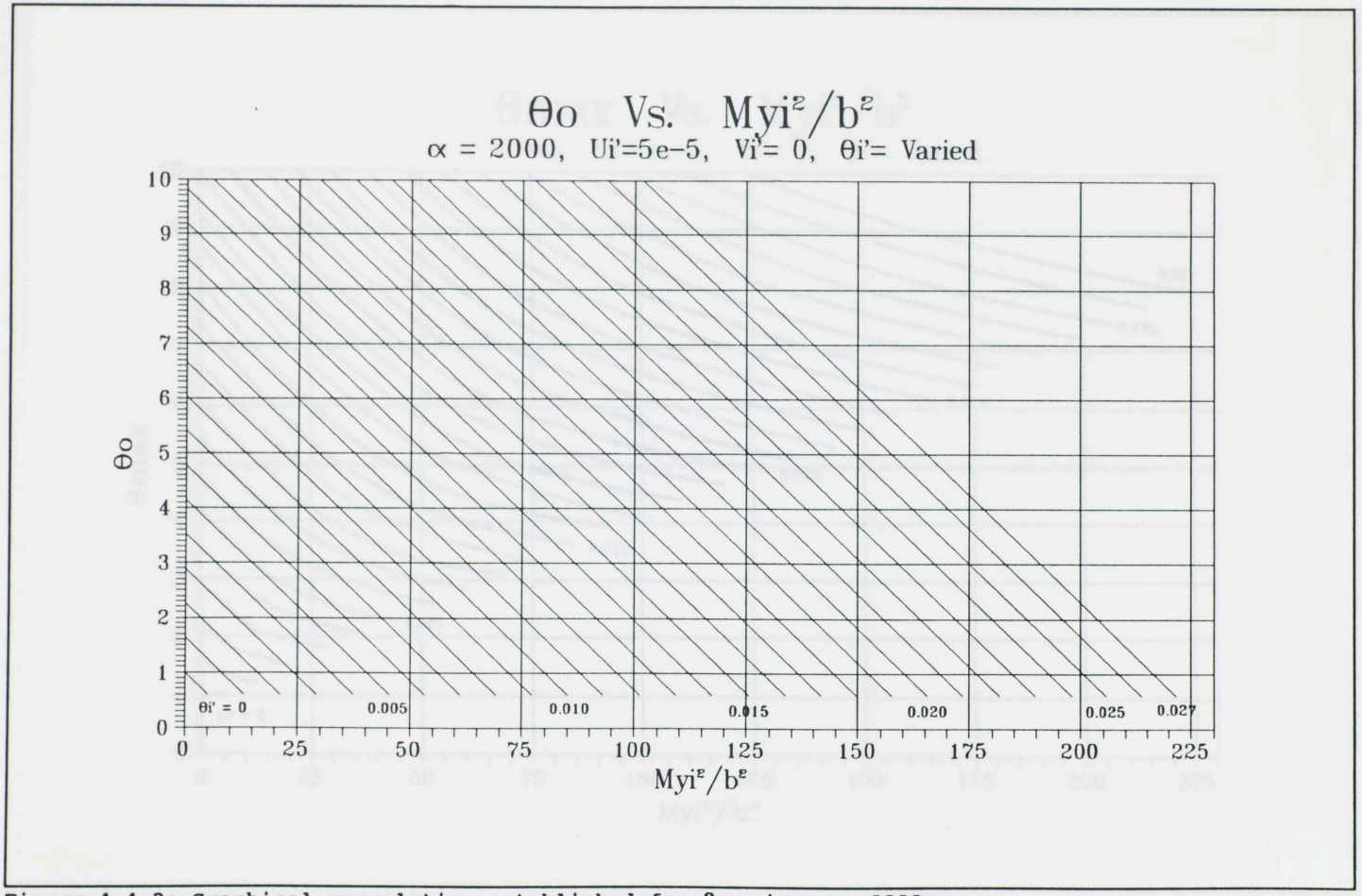

Figure 4.4-2: Graphical correlation established for θ_o using α = 2000.

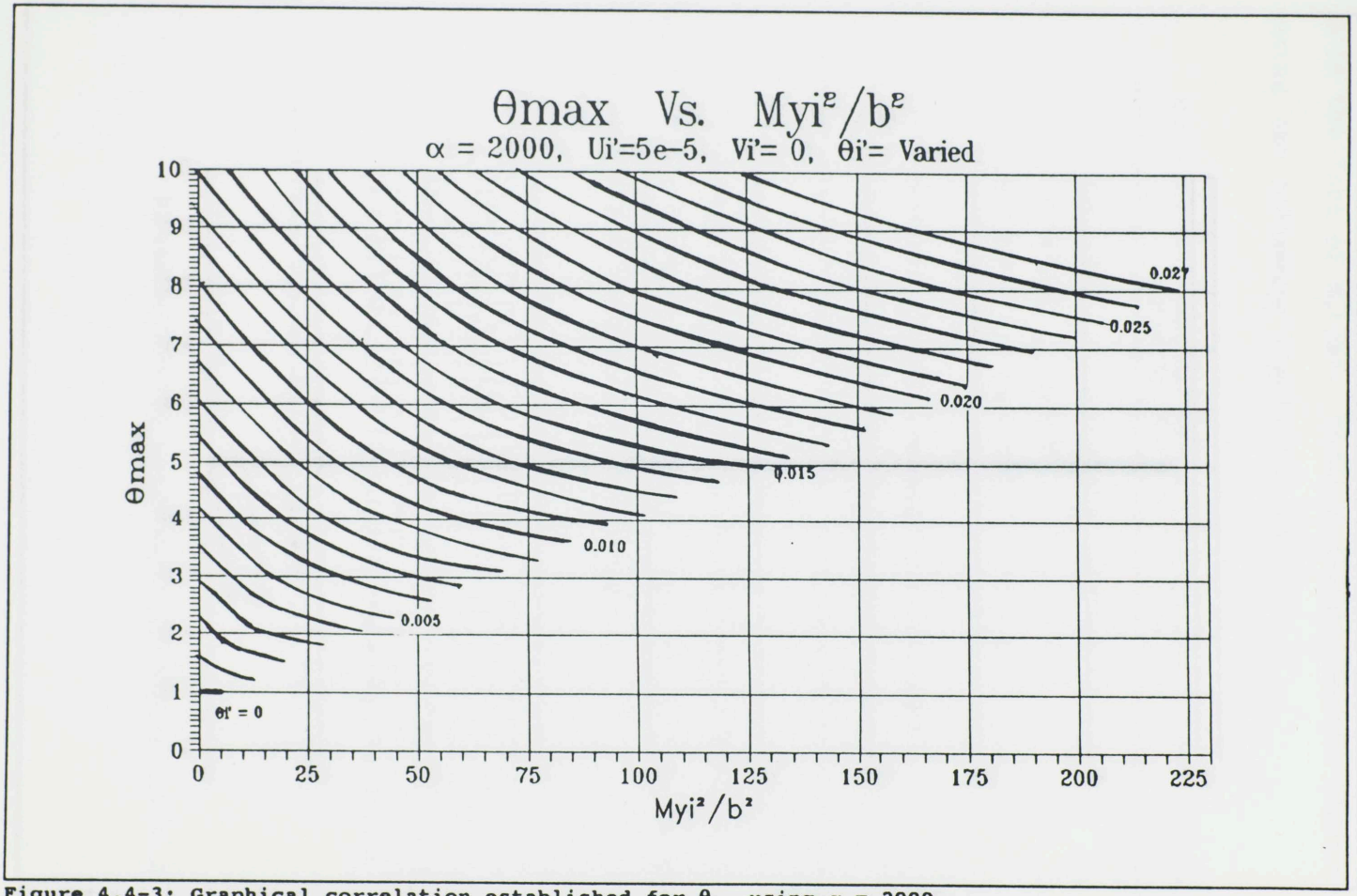

Figure 4.4-3: Graphical correlation established for θ_{max} using α = 2000.

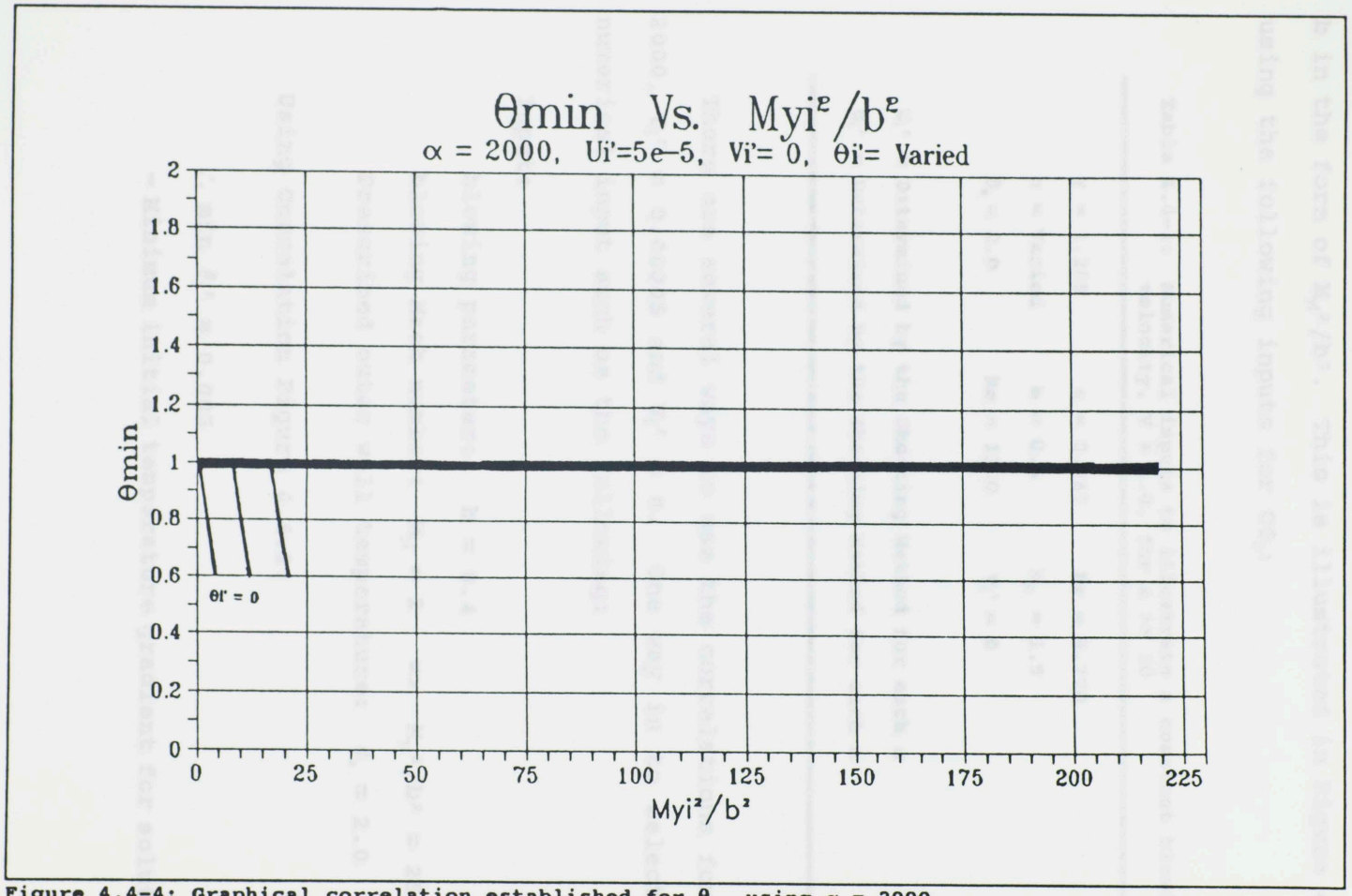

Figure 4.4-4: Graphical correlation established for θ_{min} using α = 2000.

b in the form of M_{yi}^2/b^2. This is illustrated in **Figure 4.4.5** using the following inputs for CO_2:

Table 4.4-1: Numerical inputs to illustrate a constant blowing velocity, V ≈ 1.0, for α >> 10

$\gamma = 1.285$	$\omega = 0.867$	$Pr = 0.770$
α = Varied	$b = 0.4$	$M_{yi} = 1.5$
$\theta_o = 2.0$	$Re = 12.0$	$V_i' = 0$

U_i' = Determined by the Shooting Method for each α

θ_i' = Determined by the Shooting Method for each α

There are several ways to use the correlations for α = 2000, $U_i' = 0.00005$ and $V_i' = 0$. One way is to select the numerical input such as the following:

Input:

blowing parameter: $b = 0.4$

blowing Mach number: $M_{yi} = 2 \Rightarrow M_{yi}^2/b^2 = 25$

Prescribed outer wall temperature: $\theta_o = 2.0$

Using Correlation Figure 4.4.2:

$\therefore$ min $\theta_i' \approx 0.005$

- Minimum initial temperature gradient for solutions

b in the form of M_{yi}^2/b^2. This is illustrated in **Figure 4.4.5** using the following inputs for CO_2:

Table 4.4-1: Numerical inputs to illustrate a constant blowing velocity, V ≈ 1.0, for α >> 10

$\gamma = 1.285$	$\omega = 0.867$	$Pr = 0.770$
α = Varied	$b = 0.4$	$M_{yi} = 1.5$
$\theta_o = 2.0$	$Re = 12.0$	$V_i' = 0$

U_i' = Determined by the Shooting Method for each α

θ_i' = Determined by the Shooting Method for each α

There are several ways to use the correlations for α = 2000, $U_i' = 0.00005$ and $V_i' = 0$. One way is to select the numerical input such as the following:

Input:

blowing parameter: $b = 0.4$

blowing Mach number: $M_{yi} = 2 \Rightarrow M_{yi}^2/b^2 = 25$

Prescribed outer wall temperature: $\theta_o = 2.0$

Using Correlation Figure 4.4.2:

$\therefore$ min $\theta_i' \approx 0.005$

- Minimum initial temperature gradient for solutions

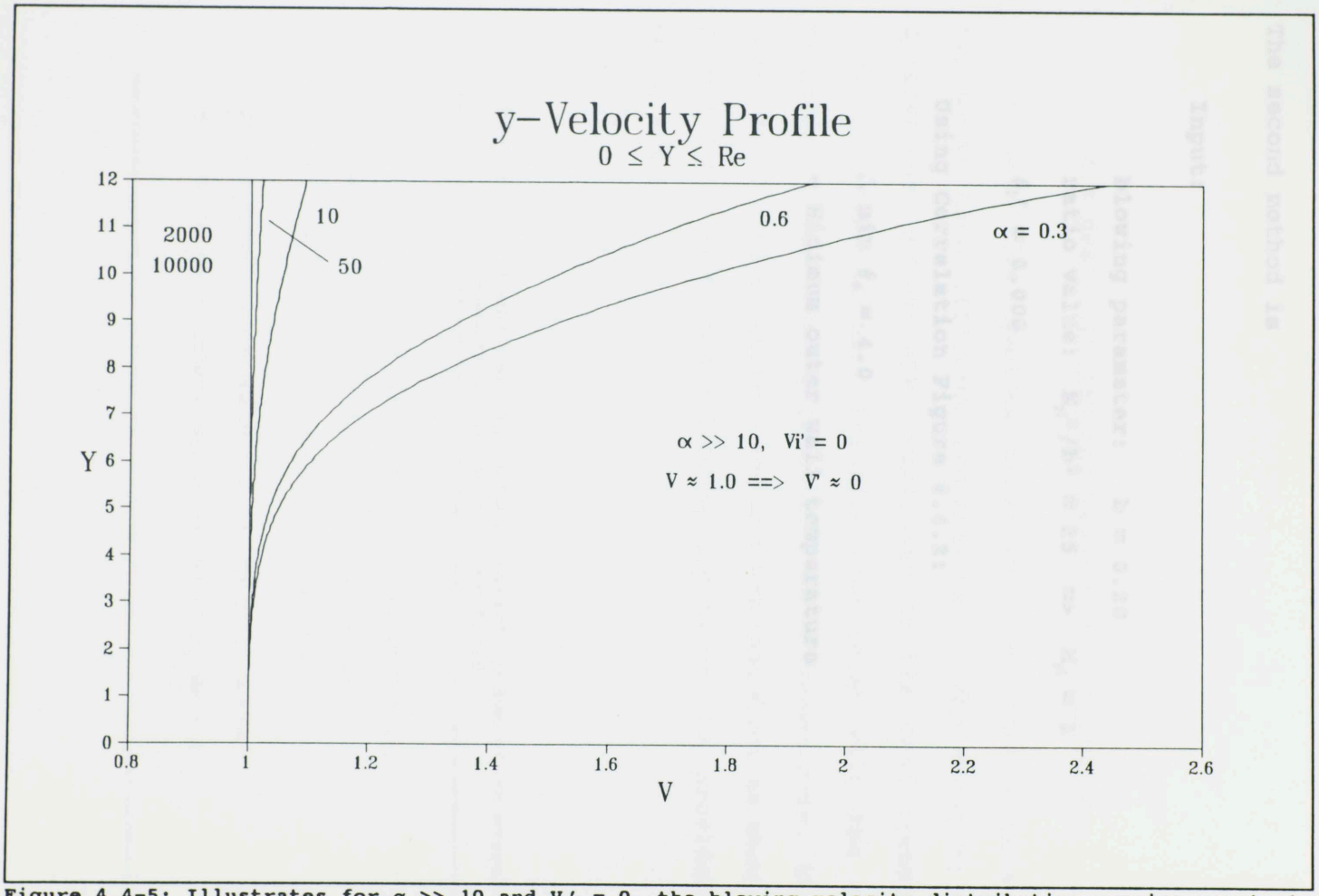

Figure 4.4-5: Illustrates for $\alpha >> 10$ and $V_1' = 0$, the blowing velocity distribution remains constant: i.e. $V \approx 0$; therefore, $V' \approx 0$.

The second method is

Input:

blowing parameter: $b = 0.20$

ratio value: $M_{yi}^2/b^2 = 25 \Rightarrow M_{yi} = 1$

$\theta_i' = 0.008$

Using Correlation Figure 4.4.2:

$\therefore$ **min** $\theta_o \approx 4.0$

- Minimum outer wall temperature

4.5 Heat transfer and Temperature Overshoot

Couette flow involves conductive heat transfer when the two walls have different temperatures. The shearing and dilatational motion also contribute to the heat transfer. Finally, there is heat transfer associated with the mass transfer of the blowing process. As a consequence, it is possible to have a sizeable temperature overshoot as shown in **Figure 4.5.1** using the following inputs for CO_2 provided in **Table 4.5-1:**

Table 4.5-1: Numerical inputs to illustrate temperature overshoot occurring within the flow field

$\gamma = 1.285$	$\omega = 0.867$	$Pr = 0.770$
$\alpha = 2000$	$b = 0.5$	$M_{y1} = 3.0$
$\theta_o = 2.0$	$Re = 14.0$	$V_1' = 0$

$U_1' = 0.000045$ <= Determined by the Shooting Method

$\theta_1' = 0.005703$ <= Determined by the Shooting Method

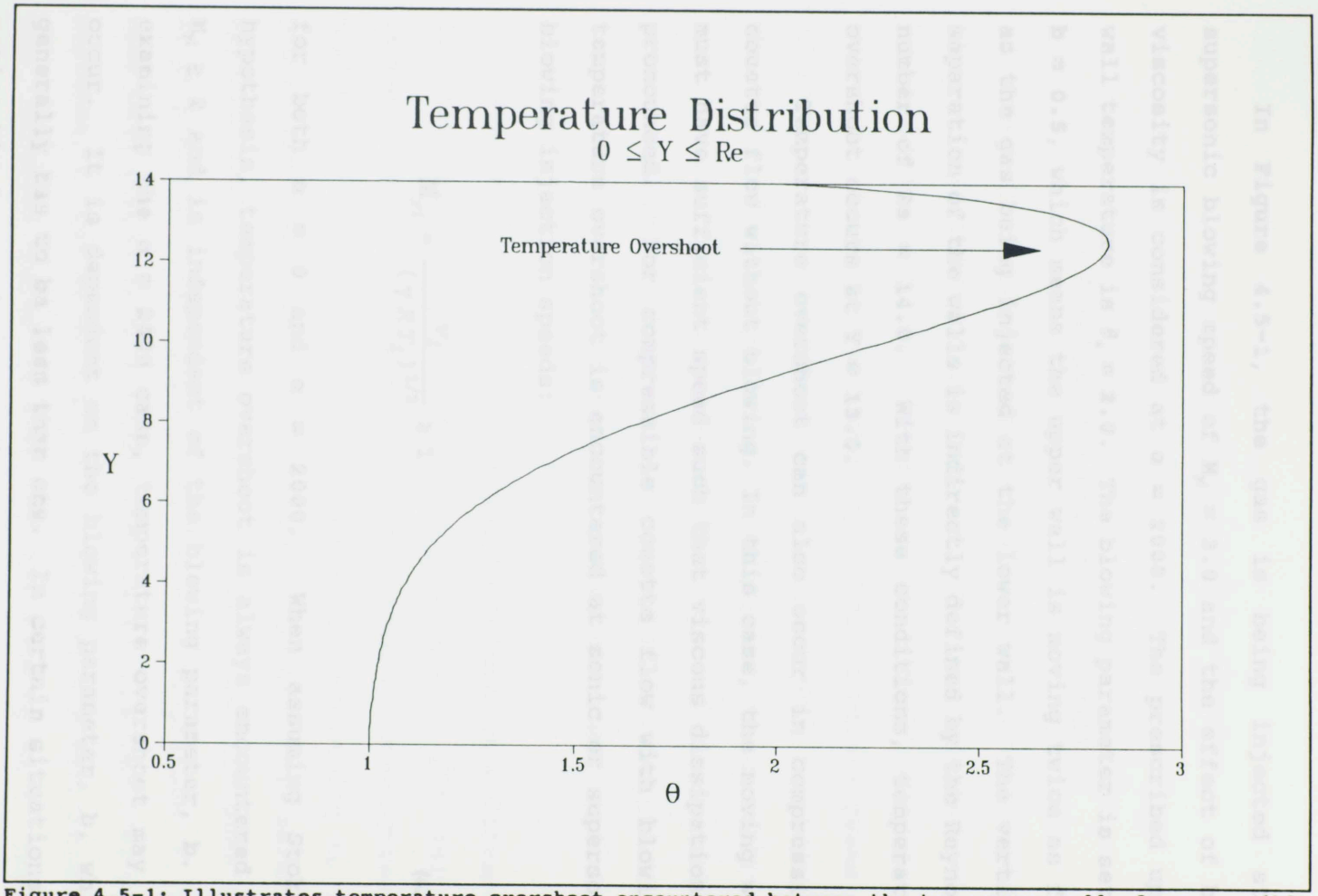

Figure 4.5-1: Illustrates temperature overshoot encountered between the two porous wall of compressible couette flow with blowing.

In **Figure 4.5-1**, the gas is being injected at a supersonic blowing speed of $M_{yi} = 3.0$ and the effect of bulk viscosity is considered at $\alpha = 2000$. The prescribed upper wall temperature is $\theta_0 = 2.0$. The blowing parameter is set at $b = 0.5$, which means the upper wall is moving twice as fast as the gas being injected at the lower wall. The vertical separation of the walls is indirectly defined by the Reynolds number of $Re = 14.0$. With these conditions, temperature overshoot occurs at $Y \approx 13.0$.

Temperature overshoot can also occur in compressible couette flow without blowing. In this case, the moving wall must have sufficient speed such that viscous dissipation is pronounced. For compressible couette flow with blowing, temperature overshoot is encountered at sonic or supersonic blowing injection speeds:

$$M_{yi} = \frac{v_i}{(\gamma R T_i)^{1/2}} \geq 1 \qquad (4.5\text{-}1)$$

for both $\alpha = 0$ and $\alpha = 2000$. When assuming Stokes' hypothesis, temperature overshoot is always encountered for $M_{yi} \geq 2$ and is independent of the blowing parameter, b. In examining the $\alpha = 2000$ case, temperature overshoot may not occur. It is dependent on the blowing parameter, b, which generally has to be less than one. In certain situations, a noticeable temperature overshoot occurs for subsonic blowing and when $b \leq 0.1$.

4.6 Subsonic and Supersonic Blowing

To analyze the influence of bulk viscosity, two separate blowing scenarios are investigated. The gas injected in the lower porous wall is introduced at either subsonic or supersonic blowing conditions, M_{yi}. These separate cases are analyzed by assuming either $\alpha = 0$ or $\alpha = 2000$. Depending on the injected speed of the gas, v_i, at the lower wall; the speed of the upper moving porous wall, u_o; and the prescribed outer temperature, T_o, which are embedded within the numerical input terms M_{yi}, b, and θ_o, temperature overshoot can occur within the flow.

The initial y-velocity gradient values is arbitrarily selected as $V_i' = 0$ and kept constant. The initial temperature and x-velocity gradient, θ_i' and U_i'; respectively, are solved using the shooting method by converging to the prescribed upper wall temperature, θ_o, and the selected Reynolds number, Re. The Reynolds number, defined when $U_o = 1$, is prescribed in order to keep the wall separation, ℓ, the same when comparing $\alpha = 0$ and 2000 cases. The vertical wall distance, ℓ, can be determined by combining the definition of the Reynolds number (2.3-1) and the blowing Mach number

(2.3-6) as follow:

$$\ell = \frac{Re\,\mu_i}{\rho_i\,(\gamma R T_i)^{1/2} M_{yi}} \qquad (4.6\text{-}2)$$

If the fluid properties are constant and the Reynolds number is fixed, the wall separation **(4.6-1)** is dependent only on M_{yi}, and subsonic flow will produce a larger wall separation than a supersonic flow. A fixed wall separation is useful for comparisons of different cases. For certain cases where the Reynolds number is prescribed, a solution may not exist for both α = 0 and 2000. When this situation occurs, a lower **Re** usually has to be used.

The first case (**Case I**) has the following inputs provided in **Table 4.6-1** below:

Table 4.6-1: Numerical inputs for Case I for constant wall temperatures

γ = 1.285	ω = 0.867	Pr = 0.770
α = 0, 2000	b = 0.6	M_{yi} = 0.1, 0.5, 1, 2
θ_o = 1.0	Re = 11.0	V_i' = 0

U_i' = Determined by the Shooting Method for each case

θ_i' = Determined by the Shooting Method for each case

The second case (**Case II**) has the following inputs provided in

Table 4.6-2 below:

Table 4.6-2: Numerical inputs for Case II for variation of wall temperatures

$\gamma = 1.285$	$\omega = 0.867$	$Pr = 0.770$
$\alpha = 0,\ 2000$	$b = 1.0$	$M_{y1} = 0.5,\ 1,\ 1.5$
$\theta_0 = 2.0$	$Re = 12.0$	$V_1' = 0$

U_1' = Determined by the Shooting Method for each case

θ_1' = Determined by the Shooting Method for each case

For **Case I**, the Reynolds number is set at **Re = 11.0**. The upper wall temperature is kept at the same temperature as the lower wall. The upper wall is moving at a speed which is approximately one and a half times faster than the speed of the gas being injected. Subsonic, sonic and supersonic blowing speeds are examined with and without a bulk viscosity effect for the same Reynolds number. For **Case II**, the Reynolds number is set at **Re = 12.0** and the upper wall temperature is twice as hot as the lower wall, i.e., $\theta_0 = 2.0$. The speed for the moving upper wall and the gas being injected at the lower wall are kept the same. Three blowing speed are selected to compare the influence of bulk viscosity.

For **Cases I** and **II**, **Table 4.6-I, 4.6-II** and graphical profiles are provided in **Appendix C**. These results are generated when the upper wall conditions are satisfied for U_o = **1** based on the Reynolds number selected. The maximum temperature, θ_{max}, encountered between the two porous wall and the initial temperature and **x**-velocity gradients, θ_i' and U_i', determined by the shooting method are provided in the tables. The **x**-velocity distributions for the flow parallel to the walls are shown in **Figures 4.6I-1a** through **4.6I-1d** for **Case I** and **Figures 4.6II-1a** through **4.6II-1c** for **Case II**. The blowing velocity distribution associated with the gas being injected at either supersonic or subsonic conditions are presented in **Figures 4.6I-2a** through **4.6I-2d** for **Case I** and **Figures 4.6II-2a** through **4.6II-2c** for **Case II**.

In **Case I** for α = **0** and **2000**, the **U** profile in **Figures 4.6I-1a - 4.6I-1d** for blowing Mach numbers M_{yi} = **0.1, 0.5, 1** and **2** produce approximately the same numerical result. For **Case II**, provided by **Figures 4.6II-1a -4.6II-1c** with M_{yi} = **0.5, 1** and **1.5**, the distribution profiles are approximately equal; except for **Figure 4.6II-1c.**

In **Cases I** and **II** shown in **Figures 4.6I-2a** through **4.6II-2c**, the **V** profiles involving α = **2000** at both subsonic and supersonic blowing remain virtually constant, as would be the case for incompressible flow. While for α = **0** the blowing profile do show compressible flow characteristics, except at

an extremely low blowing speed of $M_{yi} \leq 0.1$. The vertical speed V_o for $\alpha = 0$ increases as the injected blowing velocity increases and is visible noticeable for supersonic blowing conditions. When $\alpha >> 10$, the α effect induced on the flow field is governed by the energy equation **(2.5-10)**, since the **y**-momentum equations **(2.5-9b)** is virtually negligible, as discussed in section 4.4.

The temperature distributions for **Cases I** and **II** are shown in **Figures 4.6I-3a** through **4.6I-3d** and **Figures 4.6II-3a** through **4.6II-3c**, respectively. For **Case I**, the influence of the bulk viscosity, $\alpha = 2000$, at subsonic or sonic blowing produces sightly higher temperatures in the flow field as compared to $\alpha = 0$. For a low blowing speed of $M_{yi} = 0.1$ the temperature distribution remains virtually constant, i.e, $\theta \approx 1.0$. At a supersonic blowing speed of $M_{yi} = 2.0$ **(Figure 4.6I-3d)**, a noticeable temperature overshoot occurs. **Case II** produces practically the same effects as in **Case I**, except when $M_{yi} = 1.5$ the $\alpha = 0$ case which has temperature overshoot.

From the auxiliary equations discussed in section 2.6, the density and pressure ratio distribution profile for **Cases I** and **II** are shown in **Figures 4.6I-4a** through **4.6I-5d** and **Figures 4.6II-4a** through **4.6II-5c**, respectively. These distributions investigate compressibility effects. The density ratio distribution for both **Cases I** and **II**, displays incompressible flow behavior for $\alpha = 2000$ at subsonic and

supersonic blowing speeds, while demonstrating compressible flow behavior for $\alpha = 0$. The compressibility characteristics for $\alpha = 0$ is visible as the blowing speed increases from subsonic to supersonic conditions.

For the pressure ratio distribution represented for **Cases I and II**, the flow field shows compressible flow behavior for $\alpha = 2000$ at subsonic and supersonic blowing speeds, while illustrating incompressible flow behavior for $\alpha = 0$ at small M_{yi}. This is noticeable as the blowing speed increases to supersonic conditions. In **Case I** where $M_{yi} = 0.1$ **(Figure 4.6I-5a)**, the pressure ratio for both $\alpha = 0$ and 2000 remains constant throughout the flow field. A similar situation is seen for **Case I** at $\alpha = 0$ where $M_{yi} = 0.5$ as shown in **Figure 4.6II-5a.**

The Mach number distribution profile encountered between the walls for **Cases I** and **II** are shown in **Figures 4.6I-6a** through **4.6I-6d** and **Figures 4.6II-6a** through **4.6II-6c**, respectively. For **Case I**, the Mach number distribution for $\alpha = 0$ and 2000 increases relative to increasing M_{yi} conditions as shown in **Figures 4.6I-6a** through **4.6I-6d.** For M_{yi} of 0.1, 0.5 and 1 at $\alpha = 0$ and 2000, the Mach number distribution is virtually the same, but for $M_{yi} = 2$ the Mach numbers produced within the flow field are larger for $\alpha = 0$ as compared to $\alpha = 2000$. For **Case II**, the Mach number distribution for $\alpha = 0$ increases as M_{yi} increases, while for $\alpha = 2000$ the flow

experiences a minimum Mach number, as shown in **Figure 4.6II-6a** through **4.6II-6c.**

The normalized viscous dissipation and the rate of entropy production distribution profile examined for **Cases I** and **II** are shown in **Figures 4.6I-7a** through **4.6I-8d** and **Figures 4.6II-7a** through **4.6II-8c**, respectively. These quantities depend on the heat transfer and the viscous stresses associated with the shearing and dilatational motion of the fluid. **Case I** with M_{yi} = **0.1, 0.5, 1** experiences virtually the same viscous dissipation distribution for both α = **0** and **2000** as shown in **Figures 4.6I-7a** through **4,6I-7c**, but for M_{yi} = **2.0** the normalized viscous profile for α = **0** is greater than for α = **2000**. For **Case II**, a different scenario is noted for $\hat{\Phi}$ which generates twice as much viscous dissipation for α = **0** as compared to α = **2000** for subsonic and sonic blowing speeds, as shown in **Figures 4.6II-7a** and **4.6II-7b**. The M_{yi} = **1.5** case produces almost six times as much viscous dissipation for α = **0** as compared to α = **2000**, as shown in **Figure 4.6II-7c.**

For **Case I**, the rate of entropy production is essentially the same for α = **0** and α = **2000**, as illustrated in **Figures 4.6I-8d and 4.6II-8c.** For **Case II** there is a significant difference between α = **0** and α = **2000**, as shown in **Figures 4.6II-8a** and **4.6II-8b.**

The Stanton number **St** and the skin friction coefficient C_f for the lower and upper walls are provide in **Tables 4.6-I and 4.6-II** for **Case I** and **II**, respectively. For **Case I**, St_o is negative due to temperature overshoot, which changes it's temperature gradient in order to conform to the outer wall temperature. For **Case II**, St_o is negative only for $\alpha = 0$ at supersonic blowing $M_{yi} = 1.5$. For **Case I** and **II**, Cf_i is nearly zero, as expected. On the other hand, Cf_o is quite large because **U** has an appreciable gradient at the upper wall.

CHAPTER V

CONCLUSIONS AND SUMMARY

The effect of bulk viscosity associated with a gas such as CO_2 can significantly influence a flow field. This is shown theoretically by studying compressible couette flow with blowing. The large differences seen between the same $\alpha = 0$ and $\alpha = 2000$ cases suggest that a rotating cylinder experiment might be a viable way of measuring α and thus μ_b.

The influence of a large α value tends to reduce the significance of the transverse momentum equation causing the vertically oriented blowing distribution to remain virtually constant. This is seen no matter what the injected gas speed is. For large α values, the energy equation is numerically determined without the influence of the transverse momentum equation. For Stokes' hypothesis ($\alpha = 0$), the transverse momentum equation does influence the transverse blowing distribution and as the injected speed increased this is more noticeable by producing a faster exiting blowing speed.

By allowing the transverse momentum equation to influence the flow, the temperature distribution for $\alpha = 0$ at supersonic blowing conditions produces slightly higher temperatures than

for large α values. The opposite scenario is seen when the blowing speed are at subsonic or sonic conditions, the temperature distributions are slightly higher for $\alpha = 2000$ than for $\alpha = 0$. The temperature distribution for $\alpha = 0$ at supersonic blowing conditions of $M_{yi} \geq 2$ virtually always encounters temperature overshoot, while for $\alpha = 2000$ this may not be the case.

Due to the derivation of the four first-order ODE's and the numerical scheme, larger values for the Reynolds number, **Re**, can not be specified to produce existing numerical solutions. There are several reasons for this constraint. One is that for large **Re** values the temperature encountered in the flow exceeds the temperature limits of $\theta \geq 10$, which causes the perfect gas assumption to become invalid. Another reason is that the numerical scheme would require an extremely small step size, which would cause the computation time to be extremely large, but even this may not be suitable to obtain larger **Re** values. A physical explanation, why lager **Re** in the order of 10^2 or greater are not possible to produce numerically, is that there are viscous and thermal boundary layers on the upper wall. This posses extreme difficulty for a numerical scheme to solve the equations for large **Re** values. Nevertheless, it would be useful to have large **Re** number solutions, since **Re** determines the walls separation distance, ℓ, as shown in equation (**4.5-2**).

NOMENCLATURE

b = blowing parameter

c_f = skin friction coefficient

C_{int} = specific heat of interest for the vibrational energy mode

C_p = specific heat for constant pressure

C_v = specific heat for constant volume

e = internal energy

f = Runge-Kutta formulas for ODE's

$\vec{F}^s$ = viscous stress

h = enthalpy

ℓ = vertical wall separation distance

M = Mach number

M_{yi} = blowing Mach number

p = pressure

Pr = Prandtl number

q = heat transfer, Fourier's Equation

R = specific gas constant

$\tilde{R}$ = universal gas constant

Re = Reynolds number

$\hat{s}_{irr}$ = rate of entropy production

St = Stanton number

t = Runge-Kutta step size

T = temperature

u = **x**-velocity component

U = dimensionless **x**-velocity distribution

U_i' = initial **x**-velocity gradient

v = transverse **y**-velocity component

V = dimensionless transverse **y**-velocity distribution

V_i' = initial **y**-velocity gradient

$\vec{W}$ = velocity vector

x = coordinate normal to the **yz**-plane

y = coordinate normal to the **xz**-plane

y = Runge-Kutta intermediate formulas

Y = dimensionless vertical wall separation distance

Greek Letters

α = bulk-shear viscosity ratio

γ = specific heat ratio

ϵ = specific minimum value

$\tilde{\epsilon}$ = strain rate tensor

θ = dimensionless temperature distribution

θ_i' = initial temperature gradient

Φ = viscous dissipation

$\hat{\Phi}$ = normalized viscous dissipation

κ = thermal conductivity

λ = second viscosity coefficient

μ = shear viscosity

μ_b = bulk viscosity

ρ = density

$\bar{\bar{\sigma}}$ = surface stress dyadic

τ = shear stress

ω = power law temperature exponent

$\hat{\omega}$ = normalized vorticity

Z = vibrational relaxation time

Special Symbols

d /dy = derivative with respect to y

d /dY = derivative with respect to dimensionless Y

D /Dt = substantial derivative

$\hat{e}_x$, $\hat{e}_y$ = Cartesian basis

∂ /∂y = partial derivative with respect to y

∇ = gradient

Subscripts

i = inner wall

o = outer wall

w = wall condition

x = **x**-coordinate system

y = **y**-coordinate system

REFERENCES

1. Dubrulle, B. and Zahn, J., "Nonlinear Instability of Viscous Plane Couette Flow, Part I. Analytical Approach to a Necessary Condition", J. Fluid Mech., Vol. 231, pp. 561-573 (April 1991).

2. Sadeghi, V. and Higgins, B., "Stability of Sliding Couette-Poiseuille Flow in an Annulus Subject to Axisymmetric and Asymmetric Disturbances", Phys. Fluids A, Vol. 3, No. 9, pp. 2092-2104 (September 1991).

3. Van Dyke, M., "Second-Order Compressible Boundary Layer Theory with Application to Bunt Bodies in Hypersonic Flow", Hypersonic Flow Research, edited by F. R. Riddell (Academic, New York, 1962), pp. 37-76.

4. Emanuel, G., "Effect of Bulk Viscosity on a Hypersonic Boundary Layer", Phys. Fluids A, Vol. 4, pp. 491-495 (March 1992).

5. Stokes, G. G., "XXII - On the Theories of the Internal Friction of Fluids in Motion, and of the Equilibrium and Motion of Elastic Solids", Cambridge Phil. Trans., 8, pp. 287-305 (1845).

6. Tisza, L., "Supersonic Absorption and Stokes' Viscosity Relation", Phys. Rev., Vol. 61, pp. 531 (1942).

7. Monchik, L., Yun, K. S., and Mason, E. A., "Formal Kinetic Theory of Transport Phenomena n Polyatomic Gas Mixtures", J. Chem. Phys., Vol. 39, pp. 654, (1963).

8. Emanuel, G., " Bulk Viscosity of a Dilute Polyatomic Gas", Phys. Fluids A, Vol. 2, pp. 2252-2254 (December 1990).

9. Truesdell, C., " Bulk Viscosity of a Dilute Polyatomic Gas", J. Rat. Mech, Anal. Vol 2, p. 643 (1953).

10. Kaufmann W. J. III, Universe, 3rd ed. Freeman, New York, 1990, p.158.

11. McRonald, A. D., and Randolph, J. E., "Hypersonic Maneuvering to Provide Planetary Gravity Assist", AIAA, Reprint No. 90-0539 (1990).

12. McRonald, A. D., and Randolph, J. E., "application of Aero-Gravity-Assist to High Energy Solar System Missions", AIAA, Reprint No. 90-2891 (1990).

13. Lewis, M. J. and McRonald, A. D., "The Design of Hypersonic Waveriders for Aero-Assisted Interplanetary Trajectories", AIAA, Reprint No. 91-0053 (1991).

14. Emanuel, G. and Jones, J. P., "Compressible Flow Through a Porous Plate", Int. J. Heat Mass Transfer, Vol. 11, pp. 827-836 (1968).

15. Emanuel, G., "Blowing from Porous cone or Wedge When the Contact Surface Is Straight", AIAA Journal, Vol. 5, No. 3, pp. 534-538 (March 1967).

16. Hornbeck, R., Numerical Methods, Prentice-Hall, Inc., Englewood Cliffs, New Jersey, 1975.

17. Emanuel, G., "Numerical Analysis of Stiff Equations", Aerospace Corporation, El Segundo, CA. Contract No. AF 04(695)-268 (January 1964).

18. Kays, W.M. and Moffat, R.J., "The Behavior of Transpired Turbulent Boundary Layers", Studies in Convection, Vol 1, Academic Press, New York, New York, pp. 223-319 (1975).

19. Owczarek, J., Introduction to Fluid Mechanics, International Textbook Company, Bethlehem, Pennsylvania, 1968.

20. Ozisik, M.N., Heat Transfer A Basic Approach, McGraw-Hill Book Company, New York, New York, 1985.

21. Pierce, A. D., Acoustics - An Introduction to Its Physical Principles and Applications. McGraw-Hill Book Company, New York, New York, 1981.

APPENDICES

APPENDIX A

DETAIL DERIVATION OF AUXILIARY EQUATIONS

Auxiliary Equations as functions of $0 \leq Y \leq Re$:

1. Pressure ratio (Perfect gas)

$$p = \rho R T$$

$$p = \frac{\rho_i}{V} R T_i \theta$$

$$p = (\rho_i R T_i) \frac{V}{\theta}$$

$$p = p_i \frac{V}{\theta}$$

$$\frac{p}{p_i} = \frac{\theta}{V}$$

2. Mach number:

$$M^2 = M_x^2 + M_y^2$$

$$M^2 = \frac{u^2 + v^2}{\gamma R T}$$

$$M^2 = \frac{(u_o U)^2 + (v_i V)^2}{\gamma R T_i \theta}$$

$$M^2 = \frac{v_i^2}{\gamma R T_i \theta}\left[\frac{u_o^2}{v_i^2} U^2 + V^2\right]$$

$$M^2 = M_{yi}^2 \frac{\frac{1}{b^2} U^2 + V^2}{\theta}$$

3. Normalized Vorticity:

$$\omega = \left| -\frac{du}{dy} \right|$$

$$\omega = \left(\frac{\rho v}{\mu}\right)_i u_o \frac{dU}{dY} = \left(\frac{\rho v}{\mu}\right)_i u_o U'$$

$$\hat{\omega} = \frac{\omega}{\left(\frac{\rho V}{\mu}\right)_i u_o}$$

$$\hat{\omega} = U'$$

4. Normalized Viscous Dissipation:

$$\Phi = \mu_i \theta^{\omega} \left(\frac{\rho V}{\mu}\right)_i^2 \left[u_o^2 (U')^2 + \left(\alpha + \frac{4}{3}\right) v_i^2 (V')^2 \right]$$

$$\Phi = \mu_i \theta^{\omega} \left(\frac{\rho^2 V^4}{\mu^2}\right)_i \left[\frac{u_o^2}{v_i^2} (U')^2 + \left(\alpha + \frac{4}{3}\right) (V')^2 \right]$$

$$\Phi = \theta^{\omega} \left(\frac{\rho^2 V^4}{\mu}\right)_i \left[\frac{1}{b^2} U'^2 + \left(\alpha + \frac{4}{3}\right) V'^2 \right]$$

$$\hat{\Phi} = \left(\frac{\mu}{\rho^2 V^4}\right)_i \Phi$$

$$\hat{\Phi} = \theta^{\omega} \left[\frac{1}{b^2} U'^2 + \left(\alpha + \frac{4}{3}\right) V'^2 \right]$$

5. Rate of Entropy Production:

$$\dot{s}_{irr} = \frac{1}{\rho T}\left[\Phi - \frac{1}{T}\,\vec{q}\cdot\nabla T\right]$$

$$\vec{q} = -\kappa\nabla T$$

$$\dot{s}_{irr} = \frac{1}{\rho T}\left[\Phi - \frac{1}{T}\,(-\kappa\nabla T)\cdot\nabla T\right]$$

$$\dot{s}_{irr} = \frac{1}{\rho T}\left[\Phi + \frac{\kappa}{T}\,(\nabla T)^2\right]$$

$$\nabla T = \left(\frac{\rho V}{\mu}\right)_i \frac{dT}{dY}$$

$$\nabla T = \left(\frac{\rho V}{\mu}\right)_i T_i \frac{d\theta}{dY}$$

$$\dot{s}_{irr} = \frac{1}{\frac{\rho_i}{V}\,T_i\,\theta}\left[\Phi + \frac{\kappa_i\,\theta^{\omega}}{T_i\,\theta}\left(\frac{\rho V}{\mu}\right)_i^2 T_i^2\left(\frac{d\theta}{dY}\right)^2\right]$$

$$\dot{s}_{irr} = \frac{V}{\rho_i T_i \theta}\left\{\left(\frac{\rho^2 V^4}{\mu}\right)_i \theta^{\omega}\left[\frac{1}{b^2}U'^2 + \left(\alpha + \frac{4}{3}\right)V'^2\right] + \kappa_i \theta^{\omega-1}\left(\frac{\rho V}{\mu}\right)_i^2 T_i\right.$$

$$\kappa_i = \frac{R\gamma\mu_i}{(\gamma - 1)Pr}$$

$$\dot{s}_{irr} = \frac{V}{\rho_i T_i \theta}\left\{\left(\frac{\rho^2 V^4}{\mu}\right)_i \hat{\Phi} + \frac{R\gamma\mu_i}{(\gamma - 1)Pr}\theta^{\omega-1}\left(\frac{\rho V}{\mu}\right)_i^2 T_i \theta'^2\right\}$$

$$\dot{s}_{irr} = \frac{V}{\rho_i T_i \theta}\left\{\left(\frac{\rho^2 V^4}{\mu}\right)_i \hat{\Phi} + \frac{\gamma R T_i \theta^{\omega 1}}{(\gamma - 1)Pr}\left(\frac{\rho^2 V^2}{\mu}\right)_i \theta'^2\right\}$$

$$\gamma R T_i = \frac{V_i^2}{M_i^2}$$

$$\dot{s}_{irr} = \frac{V}{\rho_i T_i \theta}\left\{\left(\frac{\rho^2 V^4}{\mu}\right)_i \hat{\Phi} + \frac{\theta^{\omega-1}}{(\gamma - 1)Pr M_{yi}^2}\left(\frac{\rho^2 V^4}{\mu}\right)_i \theta'^2\right\}$$

$$\dot{s}_{irr} = \frac{V}{\theta}\left(\frac{\rho V^4}{\mu T}\right)_i\left[\hat{\Phi} + \frac{\theta^{\omega-1}\theta'^2}{(\gamma - 1)Pr M_{yi}^2}\right]$$

$$\hat{\dot{s}}_{irr} = \left(\frac{\mu T}{\rho V^4}\right)_i \dot{s}_{irr}$$

$$\hat{\dot{s}}_{irr} = \frac{p_i}{p}\hat{\Phi} + \frac{V\theta^{\omega-1}\theta'^2}{(\gamma - 1)Pr M_{yi}^2}$$

6. Stanton Number

$$St = \frac{q}{\rho c_p u_o [T - T_t]}$$

$$T_t = Stagnation\ Temperature = T\left(1 + \frac{\gamma - 1}{2} M^2\right)$$

$$\vec{q} = - \kappa \nabla T$$

$$q = - \kappa \frac{dT}{dy} = - \kappa \theta^{\omega} T_i \left(\frac{\rho v}{\mu}\right)_i \frac{d\theta}{dY}$$

$$\kappa_i = \frac{C_p \mu_i}{Pr}$$

$$q = - \frac{C_p \mu_i}{Pr} \theta^{\omega} T_i \left(\frac{\rho v}{\mu}\right)_i \theta'^2$$

$$St = \frac{- \frac{C_p \mu_i}{Pr} \theta^{\omega} T_i \left(\frac{\rho v}{\mu}\right)_i \theta'^2}{\frac{\rho_i}{V} C_p u_o \left[T_i \theta - T_i \theta \left(1 + \frac{\gamma - 1}{2} M^2\right)\right]}$$

$$St = \frac{v_i}{u_o} \frac{V \theta^{\omega} \theta'}{Pr\, \theta \left(\frac{\gamma - 1}{2} M^2\right)}$$

$$St = \frac{2 b V \theta^{\omega - 1} \theta'}{Pr (\gamma - 1) M^2}$$

$$St = \frac{2}{\gamma - 1} \frac{b}{Pr} \frac{V \theta^{\omega - 1} \theta'}{M^2}$$

7. Skin Friction Coefficient

$$C_f = \frac{2\tau}{\rho u_o^2}$$

$$\tau = \mu \frac{du}{dy} = \mu_i \theta^{\omega} \left(\frac{\rho v}{\mu} \right)_i u_o \frac{dU}{dY} = \theta^{\omega} \rho_i v_i u_o U'$$

$$C_f = \frac{2 \theta^{\omega} \rho_i v_i u_o U'}{\frac{\rho_i}{V} u_o^2}$$

$$C_f = 2 \left(\frac{v_i}{u_o} \right) V \theta^{\omega} U'$$

$$C_f = 2 b V \theta^{\omega} U'$$

APPENDIX B

NUMERICAL CODE

```
      Program Boundary Value Couette Flow Problem
c
c  *******  Programmed by:  Hugo Gonzalez  *******
c
c  ************************************************************************
c  *  This program solves a steady, two dimensional couette flow of a     *
c  *  perfect gas.  The gas is assumed compressible and the bulk           *
c  *  viscosity term is introduces.  There is blowing and suction          *
c  *  occurring through the porous walls.  This problem is solved by       *
c  *  using the 4th-Order Runge-Kutta method with a variable step size     *
c  *  and the Shooting Method.                                             *
c  ************************************************************************
c
      integer i, i2, j, k, m, z
      real alpha, b, converg, gamma, i4, i3, Myi, N, n1, Ns, Nstep,
     +     Nstep1, Nstep2, Oi, O1ip, Ofmin, Opmin, Ore, O2ip, Pr,
     +     Pstep, psub1, psub2, psub3, R1(151), R3(151), ReC, Re,
     +     s1(151), s3(151), s3max, s3min, Ui, U1ip, U2ip, Vi, Vip,
     +     w, yes, yes2
      double precision Cf, dispc, deltaY, dYf, dYavg, dYmin, dYmax,
     +                 f(1:4,1:4), M1, M2, Ofpp(0:1000), Opp,
     +                 Rp, Rrho, sc, St, Up, Ufp(0:1000), Vfp(0:1000),
     +                 Vp, wc, y(1:4,1:4), Yd, yf(1:4,1:4,0:1000),
     +                 Ydt(0:1000), tal
c
c  **********  Questions asked for input values  *************
c
      write(*,100)
100   format(/,1x,'Do you want detailed print out of Runge-Kutta's ',
     +       'intermediate',/,2x,' formulas ?  Type (0) for YES or ',
     +       '(1) for NO.')
      read *, yes
      write(*,110)
110   format(1x,'Do you want detailed print out of U, Up, V, Vp,',
     +       ' Θ, Θ`, Θ" at',/,2x,'each step size interval ? ',
     +       'Type (0) for YES or (1) for NO.')
      read *, yes2
      write(*,140)
140   format(1x,'Input number of printed steps wanted for solution ?')
      read *, Nstep
      write(*,190)
190   format(1x,'Input specific heat ratio τ ≥ 1 for the gas ?')
      read *, gamma
      write(*,200)
200   format(1x,'Input power law temperature exponent w ≥ 0 for the ',
     +       'gas ?')
      read *, w
      write(*,210)
210   format(1x,'Input Prandtl number Pr > 0 for the gas ?')
      read *, Pr
      write(*,220)
220   format(1x,'Input bulk-shear viscosity ratio α ≥ 0 for the gas ?')
      read *, alpha
      write(*,230)
230   format(1x,'Input blowing parameter b > 0 ?')
      read *,  b
      write(*,240)
240   format(1x,'Input blowing Mach number Myi > 0 ?')
      read *, Myi
      write(*,250)
250   format(1x,'Input prescribed outer wall temperature 1 ≤ θo ≤ 5 ?')
      read *, n1
```

```
      write(*,255)
255   format(1x,'Input Reynolds number 10 ≤ Re ≤ 20 for Uo = 1 ',
     +       'condition ?')
      read *, ReC
c
c   *** The initial guess gradient values for Ui', Vi', θi'  ****
c
      U1ip = 0.00004
      U2ip = 0.00005
c
275   format(1x,'Input initial y-velocity gradient -0.001 ≤ Vi' ≤ ',
     +       ' 0.0001 ?')
      read *, Vip
      write(*,280)
c
      O1ip = 0
      O2ip = 0.1
c
c   **** The Four First-Order ODE Governing Equations ***************
c
c    y(m,1,i) = U     f(m,1,i) = U'     I.C. =>  U'(0) = Ui' = Shooting
c                                                              Method
c                                       I.C. =>  U(0) = Ui = 0
c                                       B.C. =>  U(N) = U/Uo = 1
c
c    y(m,2,i) = V     f(m,2,i) = V'     I.C. =>  V'(0) = Vi' = Input
c                                       I.C. =>  V(0) = 1
c
c    y(m,3,i) = θ̄     f(m,3,i) = θ̄'     I.C. =>  θ̄(0) = θi' = Shooting
c                                                              Method
c    y(m,4,i) = θ     f(m,4,i) = θ'     I.C. =>  θ(0) = 1
c
c   ******************************************************************
c
c   *******  The Shooting Method  *******
c
c   ******* The first two guess values Ui' to determine Re *****
c
      s1(1) = U1ip
      s1(2) = U2ip
c
      do 299 z = 1,150
c
         if (z.gt.2) then
          s1(z) = s1(z-1)-(R1(z-1)*(s1(z-1)-s1(z-2)))/(R1(z-1)-R1(z-2))
         end if
c
c   ******* The first two guess values for θi' to determine θo *****
c
      s3(1) = O1ip
      s3(2) = O2ip
      s3min = O1ip
      s3max = O2ip
c
      do 300 j = 1,150
305      call shoot (j, R3, s3, s3max, s3min)
c
         if (s3max.lt.0.00001.or.s3max.lt.s3min.or.s3min.gt.s3max.or.
     +       j.eq.150) then
            goto 600
         end if
c
```

```
          N = 1000000
c
c     **** The initial condition values ****
c
        Ui = 0
        Vi = 1
        Oi = 1
        y(1,1) = Ui
        yf(1,1,0) = Ui
        y(1,2) = Vi
        yf(1,2,0) = Vi
        y(1,3) = s3(j)
        yf(1,3,0) = s3(j)
        y(1,4)  = Oi
        yf(1,4,0) = Oi
        Yd = 0
        Ydt(0) = 0
        Nstep1 = 0.0
        Nstep2 = 0.0
        i2 = 1
        f(1,3) = 0.0
c
c     ************ Starts Fourth-Order Runge-Kutta Method ***********
c
         do 330 i = 0,N-1
c
           do 340 m = 1,4
c
              if (i.eq.0) then
                 Up = s1(z)
                 Vp = Vip
                 Ufp(0) = s1(z)
                 Vfp(0) = Vip
                 if (m.eq.1) then
                    Ofpp(0) = f(1,3)
                 end if
              end if
c
              f(m,1) = (y(m,1)+s1(z))/y(m,4)**w
              f(m,2) = (1.0/y(m,4)**w)*(Vip + (1.0/(alpha+4.0/3.0))
     +                  *(y(m,2)-1.0+(1.0/(gamma*Myi**2))*(y(m,4)/y(m,2)
     +                  -1.0)))
              f(m,3) = (Pr/y(m,4)**w)*(y(m,3)/gamma+((gamma-1.0)/gamma)
     +                  *(y(m,4)*f(m,2)/y(m,2)-(gamma*Myi**2)*y(m,4)**w
     +                 *((alpha+4.0/3.0)*f(m,2)**2+(1.0/b**2)*f(m,1)**2)))
     +                  - w*y(m,3)**2/y(m,4)
              f(m,4) = y(m,3)
c
c     ********* Adjust step size if equations are stiff **************
c
              if (m.eq.1) then
                 tal = y(m,2)*y(m,4)**w*(alpha+4.0/3.0)*(Myi**2)
                 Dymin = 0.00001
                 Dymax = 0.1
                 if (tal.lt.Dymin) then
                    deltaY = Dymin
                 elseif (tal.gt.Dymax) then
                    deltaY = Dymax
                 else
                    deltaY = tal
                 end if
                 Yd = deltaY + Yd
```

```
            end if
c
c     ***************************************************************
c
c
c     ************ Calls Subroutine for detail print out  **************
c
        psub1 = 1
        call psteps (i, Nstep, Nstep1, Yd, Ydt, i3, yes,
     +               m, y, f, i2, Nstep2, Ns, k, yf, Ufp, Up, Vfp,
     +               Vp, Ofpp, Opp, Dyf, i4, yes2, psub1, psub2,
     +               psub3, converg)
        psub1 = 0
c
c     ***************************************************************
c
                do 350 k = 1,4
c
                   if (m.eq.1) then
                      y(m+1,k) = y(1,k)+(deltaY/2.0)*f(m,k)
                   end if
                   if (m.eq.2) then
                      y(m+1,k) = y(1,k)+(deltaY/2.0)*f(m,k)
                   end if
                   if (m.eq.3) then
                      y(m+1,k) = y(1,k)+deltaY*f(m,k)
                   end if
                   if (m.eq.4) then
                      y(1,k) = y(1,k)+deltaY*(1.0/6.0)*(f(1,k)
     +                       +2.0*(f(2,k)+f(3,k))+f(4,k))
                   end if
c
c     *********  Checks temperature limits of 0.6 ≤ θ ≤ 10  **********
c
                   if (m.lt.4.and.y(m+1,4).lt.0.or.y(1,4).lt.0.6) then
                      if (m.lt.4) then
                         y(m+1,4) = 1.0
                      else
                         y(1,4) = 1.0
                      end if
                      print *, 'θ < 0 : Invalid Value determined ',
     +                         'based on Your Initial Inputs.'
                      if (s3(1).eq.s3min.and.s3(2).eq.O2ip) then
                         if (j.eq.1) then
                            s3(1) = s3min + 0.0001
                            s3min = s3(1)
                         else
                            s3(2) = 0.09999
                         end if
                      end if
                      goto 305
                   end if
c
                   if (y(1,4).gt.10) then
                      print *, 'θ = ',y(1,4)
                      print *, 'θ > 10 : Invalid Value determined ',
     +                         'based on Your Initial Inputs.'
                      if (s3(1).eq.s3min.and.s3(2).eq.O2ip) then
                         if (j.eq.1) then
                            s3(1) = s3min + 0.0001
                            s3min = s3(1)
                         else
```

```
                        s3(2) = 0.09999
                      end if
                    end if
                    goto 305
                  end if
c
c     ****************************************************************
                  if (m.eq.4) then
                    Up = (y(1,1)+s1(z))/y(1,4)**w
                    Vp = (1.0/y(1,4)**w)*(Vip + (1.0/(alpha+4.0/3.0))
     +                   *(y(1,2)-1.0+(1.0/(gamma*Myi**2))*(y(1,4)
     +                   /y(1,2)-1.0)))
                    Opp = (Pr/y(1,4)**w)*(y(1,3)/gamma+((gamma-1.0)
     +                    /gamma)*(y(1,4)*Vp/y(1,2)-(gamma*Myi**2)
     +                    *y(1,4)**w*((alpha+4.0/3.0)*Vp**2+(1.0/b**2)
     +                    *Up**2))) - w*y(1,3)**2/y(1,4)
c
                    psub2 = 1
                    call psteps (i, Nstep, Nstep1, Yd, Ydt, i3, yes,
     +                  m, y, f, i2, Nstep2, Ns, k, yf, Ufp, Up, Vfp,
     +                  Vp, Ofpp, Opp, Dyf, i4, yes2, psub1, psub2,
     +                  psub3, converg)
                    psub2 = 0
                    if (converg.eq.1) then
                      converg = 0
                      goto 400
                    end if
c
                  end if
c
350               continue
c
340             continue
c
          psub3 = 1
          call psteps (i, Nstep, Nstep1, Yd, Ydt, i3, yes,
     +                 m, y, f, i2, Nstep2, Ns, k, yf, Ufp, Up, Vfp,
     +                 Vp, Ofpp, Opp, Dyf, i4, yes2, psub1, psub2,
     +                psub3, converg)
          psub3 = 0
c
330       continue
c
400     Re = Ydt(I3)
        Pstep = I3
        Dyavg = Yd/(i+1)
c
        R3(j) = yf(1,4,Pstep) - n1
c
        if (j.eq.1) then
          Ore = Re
          Ofmin = yf(1,4,Pstep)
          Opmin = s3(j)
        elseif (yf(1,4,Pstep).lt.Ofmin) then
                Ore = Re
                Ofmin = yf(1,4,Pstep)
                Opmin = s3(j)
        end if
c
          if (abs(R3(j)).lt.0.000001) then
            goto 405
```

```
         end if
c
300    continue
c
405    R1(z) = Re - ReC
c
       if (abs(R1(z)).lt.0.000001) then
          goto 410
       end if
c
299    continue
c
c
c    ****  Print out of numerical solution for each method  *************
c
410    write(*,420)
420    format(/,/,' This Couette flow problem is solved for a steady, ',
     +       'two dimensional flow ',/,'of a compressible perfect gas.',
     +       'The effect of bulk viscosity is considered.',/,' There ',
     +       'is blowing and suction occurring in this Couette flow ',
     +       'problem through porous walls.',/,/)
c
       write(*,440) Nstep, i+1, Pstep, Re, deltaY, Dyavg, gamma, w, Pr,
     +              alpha, b, Myi, Ui, Vi, Oi
440    format(' These are the Input Parameters used for this Couette ',
     +       'Flow Problem:',/,/,4x,'Nstep = ',f10.5,2x,'i Convg = ',
     +       i10,2x,'Pstep = ',f10.5,/,7x,
     +       'Re = ',f10.5,2x,'delta Y = ',f10.5,2x,'dYavg = ',f10.5,
     +       /,4x,'gamma = ',f10.5,8x,'w = ',f10.5,5x,'Pr = ',f10.5,
     +       /,8x,'α = ',f10.5,8x,'b = ',f10.5,4x,'Myi = ',f10.5,
     +       /,7x,'Ui = ',f10.5,7x,'Vi = ',f10.5,5x,'θi = ',f10.5,/)
c
       write(*,450) Dyavg
450    format(' The following output is the Numerical solution of this',
     +       ' Couette flow determined ',/,' from using the 4th Order',
     +       ' Runge-Kutta Method for 0 ≤ Y ≤ Re, where: delta Yavg = ',
     +       f10.5,/)
c
       write(*,460) s1(z), Vip, s3(j)
460    format(' The derivative inputs for the Runge-Kutta Method are:',/,
     +      /,5x,'Ui` = ',f11.8,5x,'Vi` = ',f11.8,5x,'θi` = ',f11.8,/,
     +       79x,'  ',11x,'  ',/,7x,'Y',11x,'U',11x,'U``',10x,'V',11x,'V``',
     +       10x,'θ̄',11x,'θ̄',11x,'θ``',6x,'Rho/Rhoi',7x,'p/pi',9x,'M',11x,
     +       'w',12x,'Φ',12x,'s',12x,'St',11x,'Cf',/)
c
          do 490 i = 0,Pstep
c
             Yd = Ydt(i)
c
c    ***********   Auxiliary Equations with respect to Y   ************
c
             Rrho = 1.0/yf(1,2,i)
             Rp = yf(1,4,i)/yf(1,2,i)
             M2 = (Myi**2)*((yf(1,1,i)/b)**2+yf(1,2,i)**2)/yf(1,4,i)
             M1 = SQRT(M2)
             wc = Ufp(i)
             dispc = (yf(1,4,i)**w)*((Ufp(i)/b)**2+(alpha+4.0/3.0)
     +                *Vfp(i)**2)
             sc = dispc/Rp + yf(1,2,i)*yf(1,4,i)**(w-2)
     +            *yf(1,3,i)**2/((gamma-1.0)*(Myi**2)*Pr)
```

```
            St = 2*b*yf(1,2,i)*yf(1,4,i)**(w-1)*yf(1,3,i)/((gamma-1.0)
     +           *Pr*M2)
            Cf = 2*b*yf(1,4,i)**w*yf(1,2,i)*Ufp(i)
c
            write(*,495) Yd, yf(1,1,i), Ufp(i), yf(1,2,i), Vfp(i),
     +                   yf(1,4,i), yf(1,3,i), Ofpp(i), Rrho, Rp, M1,
     +                   wc, dispc, sc, St, Cf
495         format(1x,f10.5,11(2x,f10.5),4(2x,f11.5))
490       continue
c
          print *, ' '
          print *, ' '
          print *, '[redacted]'
          goto 605
600       print *, ' '
          print *, ' '
          print *, '[redacted] No Convergence [redacted]'
605       print *, ' '
          print *, 'Ui` = ',s1(z),'  Vi` = ',Vip
          print *, 'θ1i` = ',O1ip,'  θ2i` = ',O2ip
          print *, ' '
          print *, 'Bounded Limits:'
          print *, '  s3min = ',s3(1),'  s3max = ',s3(2)
          print *, ' '
          print *, 'Min:  θi` = ',Opmin,'    Re = ',Ore,'    θo = ',Ofmin
          print *, ' '
          print *, ' '
      stop
      end
c
c=======================================================================
```

```
      subroutine shoot (j, R3, s3, s3max, s3min)
c
c  ***********************************************************************
c  *  This subroutine uses the Shooting Method with a 4th-Order          *
c  *  Runge-Kutta method.  This method is used to solve the initial      *
c  *  temperature gradient to solve the upper wall temperature           *
c  *  condition.  Restriction are placed on the boundary limits when     *
c  *  using the shooting method to assure that no negative values        *
c  *  associated with the temperature are allowed.  This method is       *
c  *  also used to solve the initial x-velocity gradient based on        *
c  *  selected Reynolds number, Re.                                      *
c  ***********************************************************************
c
      integer j
      real R3(101), s3(101), s3max, s3min
c
c     ******  θi' Bounded Limits ******
c
         if(j.lt.3) then
            s3min = s3(1)
            s3max = s3(2)
         end if
c
         if (j.lt.3.and.s3max.ne.0.1.and.s3max.gt.s3min) then
            s3(j) = s3max*0.9
            s3max = s3(j)
         end if
c
c     **********************************
c
         if (j.gt.2) then
            if (j.eq.3) then
               s3min = s3(1)
               s3max = s3(2)
            end if
          s3(j) = s3(j-1)-(R3(j-1)*(s3(j-1)-s3(j-2)))/(R3(j-1)-R3(j-2))
c
            if (s3(j).gt.s3max.or.s3(j).lt.s3min) then
               s3(j) = s3max*0.9
               s3max = s3(j)
            end if
         end if
c
110   return
      end
c=======================================================================
```

```
      subroutine psteps (i, Nstep, Nstep1, Yd, Ydt, i3, yes,
     +                   m, y, f, i2, Nstep2, Ns, k, yf, Ufp, Up, Vfp,
     +                   Vp, Ofpp, Opp, Dyf, i4, yes2, psub1, psub2,
     +                   psub3, converg)
c
c  ***************************************************************************
c  *  This subroutine is used to print out the detailed information          *
c  *  for each variable step size increment.                                 *
c  ***************************************************************************
c
      integer i, i2, k, k2, m
      real i3, Nstep, Nstep1, Nstep2, yes, yes2, i4, Ns
      double precision f(1:4,1:4), Ofpp(0:1000), Opp, Up, Ufp(0:1000),
     +                 Vfp(0:1000), Vp, y(1:4,1:4), yf(1:4,1:4,0:1000),
     +                 Ydt(0:1000), Yd, Dyf
c

         if (i.eq.Nstep1.and.psub1.eq.1) then
            if (Nstep.eq.1) then
               Ydt(i+1) = Yd
            else
               if (i.ne.0) then
                   i3 = (Nstep1+1)/Nstep
                  Ydt(i3) = Yd
               end if
            end if
            if (yes.eq.0) then
               do 345 k = 1,4
                  write(*,347) m, k, i, y(m,k), m, k, i, f(m,k)
347                format(5x,'y(',I2,',',I2,',',I8,') = ',f10.5,
     +                   3x,'f(',I2,',',I2,',',I8,') = ',f20.5)
345            continue
            end if
            if (m.eq.4) then
               if (Nstep.eq.1) then
                  Nstep1 = Nstep*i2
               else
                  Nstep1 = Nstep*i2 - 1
               end if
            end if
         end if
c
         if (m.eq.4.and.psub2.eq.1) then
                     if (i.eq.Nstep2) then
                        Ns = 1
                        if (i.eq.0) then
                           yf(1,k,i+1) = y(1,k)
                           Ufp(i+1)  = Up
                           Vfp(i+1)  = Vp
                           Ofpp(i+1) = Opp
                        else
                           i3 = (Nstep2+1)/Nstep
                           yf(1,k,i3) = y(1,k)
                           Ufp(i3)  = Up
                           Vfp(i3)  = Vp
                           Ofpp(i3) = Opp
                        end if
                     end if
c
                     if (y(1,1).gt.1.and.k.eq.4) then
```

```
                        Dyf = (1-yf(1,1,i3-1))/(y(1,1)-yf(1,1,i3-1))
                        if (Ns.eq.1) then
                           i4 = i3
                        else
                           i4 = i3 + 1
                        end if
                        Ydt(i4) = Ydt(i3-1)+Dyf*(Yd-Ydt(i3-1))
                        do 355 k2 = 1,4
                           yf(1,k2,i4) = yf(1,k2,i3-1) +
     +                                    Dyf*(y(1,k2)-yf(1,k2,i3-1))
355                     continue
                        Ufp(i4)  = Ufp(i3-1)+Dyf*(Up-Ufp(i3-1))
                        Vfp(i4)  = Vfp(i3-1)+Dyf*(Vp-Vfp(i3-1))
                        Ofpp(i4)  = Ofpp(i3-1)+Dyf*(Opp-Ofpp(i3-1))
                        converg = 1.0
                     end if
         end if
c
         if (i.eq.Nstep2.and.psub3.eq.1) then
            if (yes2.eq.0) then
               write(*,380) i+1, y(1,1), i+1, Up,
     +                      i+1, y(1,2), i+1, Vp,
     +                      i+1, y(1,4), i+1, y(1,3),
     +                      i+1, Opp
380         format(5x,'U(',I6,') = ',f20.5,3x,'U`(',I6,') = ',f20.5,/,
     +          5x,'V(',I6,') = ',f20.5,3x,'V`(',I6,') = ',f20.5,/,
     +          5x,'θ(',I6,') = ',f20.5,3x,'θ`(',I6,') = ',f20.5,/,
     +          39x,'θ"(',I6,') = ',f20.5)
               print *, ' '
            end if
c
            if (Nstep.eq.1) then
                Nstep2 = Nstep*i2
            else
                Nstep2 = Nstep*i2 - 1
            end if
c
            i2 = i2+1
c
         end if
c
      return
      end
c
c=======================================================================
```

APPENDIX C

TABLES 4.6-I, 4.6-II AND GRAPHICAL PROFILES FOR CASES I AND II DISCUSSED IN SECTION 4.6

Table 4.6-I: Outer wall numerical results determined for Case I when the outer wall boundary condition is satisfied: $U_o = 1.0$

CO_2 $\gamma = 1.285$ $\omega = 0.867$ $Pr = 0.770$

$\alpha = 0, 2000$ $b = 0.6$ $M_{yi} = 0.1, 0.5, 1, 2$

$\theta_o = 1.0$ $Re = 11.0$ $V_i' = 0$

U_i' = Determined by the Shooting Method for each case

θ_i' = Determined by the Shooting Method for each case

α	M_{yi}	U_i'	θ_i'	ΔY_{avg}	Re	U_o	V_o	θ_o	θ_{max}	$(\rho/\rho_i)_o$
0	0.1	0.673E-05	4.000E-07	0.01334	11.00000	1.00000	1.00005	1.00000	1.00084	0.99995
2000	0.1	1.674E-05	1.660E-06	0.10000	11.00000	1.00000	1.00009	1.00000	1.00090	0.99991
0	0.5	1.740E-05	1.070E-05	0.10000	11.00000	1.00000	1.02043	1.00000	1.02001	0.97998
2000	0.5	1.763E-05	4.612E-05	0.10000	11.00000	1.00000	1.00010	1.00000	1.02270	0.99990
0	1.0	1.959E-05	5.616E-05	0.10000	11.00000	1.00000	1.15509	1.00000	1.07780	0.86573
2000	1.0	2.074E-05	2.038E-04	0.10000	11.00000	1.00000	1.00010	1.00000	1.09086	0.99990
0	2.0	4.257E-05	9.303E-04	0.10000	11.00000	1.00000	1.94764	1.00000	1.43032	0.51344
2000	2.0	3.916E-05	1.195E-03	0.10000	11.00000	1.00000	1.00010	1.00000	1.36292	0.99990

α	M_{yi}	$(p/p_i)_o$	$(p/pi)_{max}$	M_o	Φ_o	s_o	St_i	C_{fi}	St_o	C_{fo}
0	0.1	0.99995	1.00000	0.19437	2.77788	2.78223	0.00022	0.00002	-0.43994	1.20008
2000	0.1	0.99991	1.00083	0.19437	2.77787	2.78230	0.00091	0.00002	-0.43879	1.20013
0	0.5	0.97998	1.00002	0.97712	2.77919	2.93431	0.00023	0.00002	-0.42495	1.22454
2000	0.5	0.99990	1.02262	0.97185	2.77787	2.88381	0.00101	0.00002	-0.44085	1.20014
0	1.0	0.86573	1.00066	2.02781	2.77980	3.62625	0.00031	0.00002	-0.43148	1.38613
2000	1.0	0.99990	1.09077	1.94370	2.77789	3.20095	0.00111	0.00002	-0.44090	1.20014
0	2.0	0.51344	1.04955	5.12682	3.32369	11.14349	0.00127	0.00005	-0.58785	2.33726
2000	2.0	0.99990	1.36282	3.88739	2.77798	4.46886	0.00163	0.00005	-0.44083	1.20016

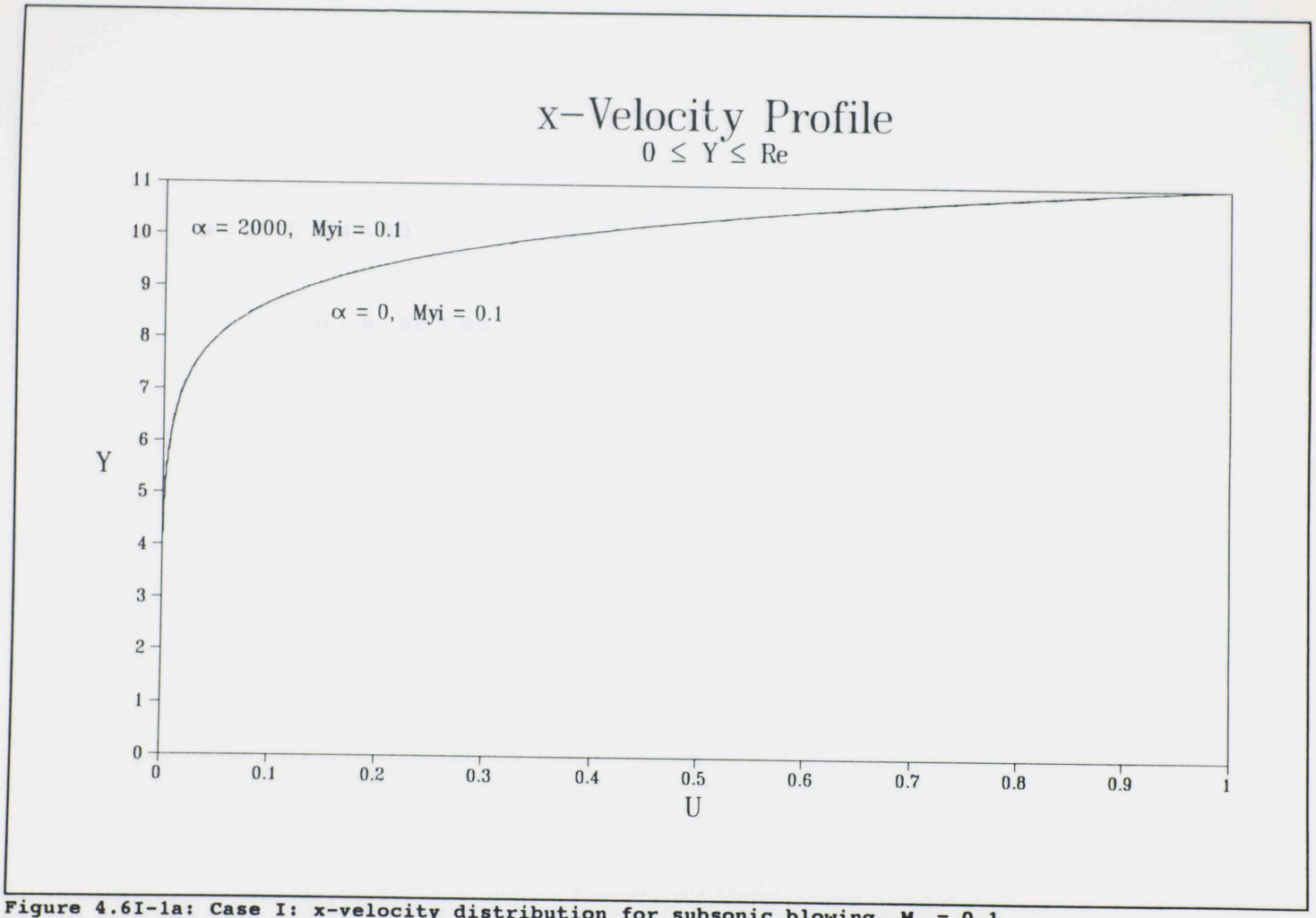

Figure 4.6I-1a: Case I: x-velocity distribution for subsonic blowing, $M_{yi} = 0.1$

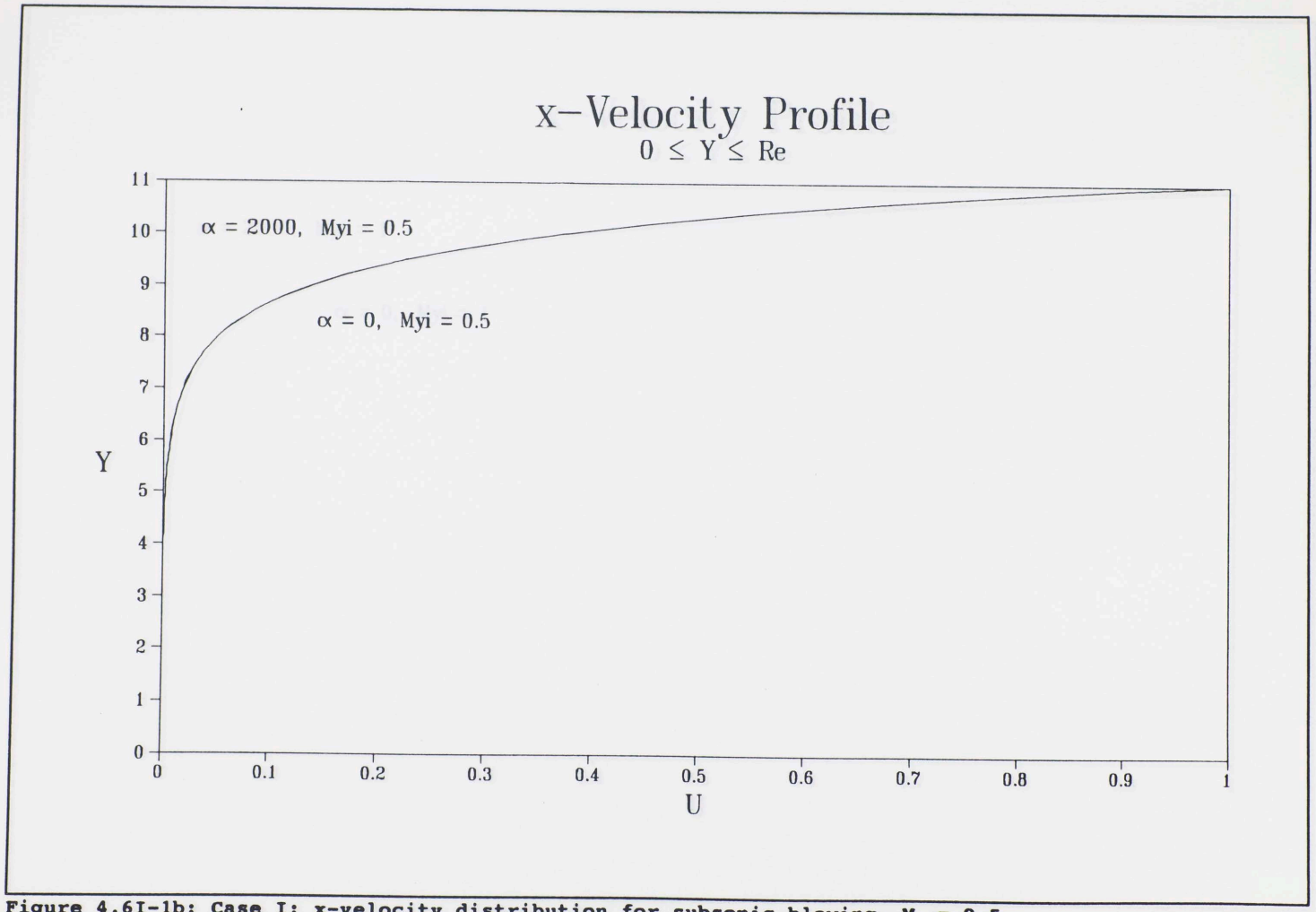

Figure 4.6I-1b: Case I: x-velocity distribution for subsonic blowing, M_{yi} = 0.5

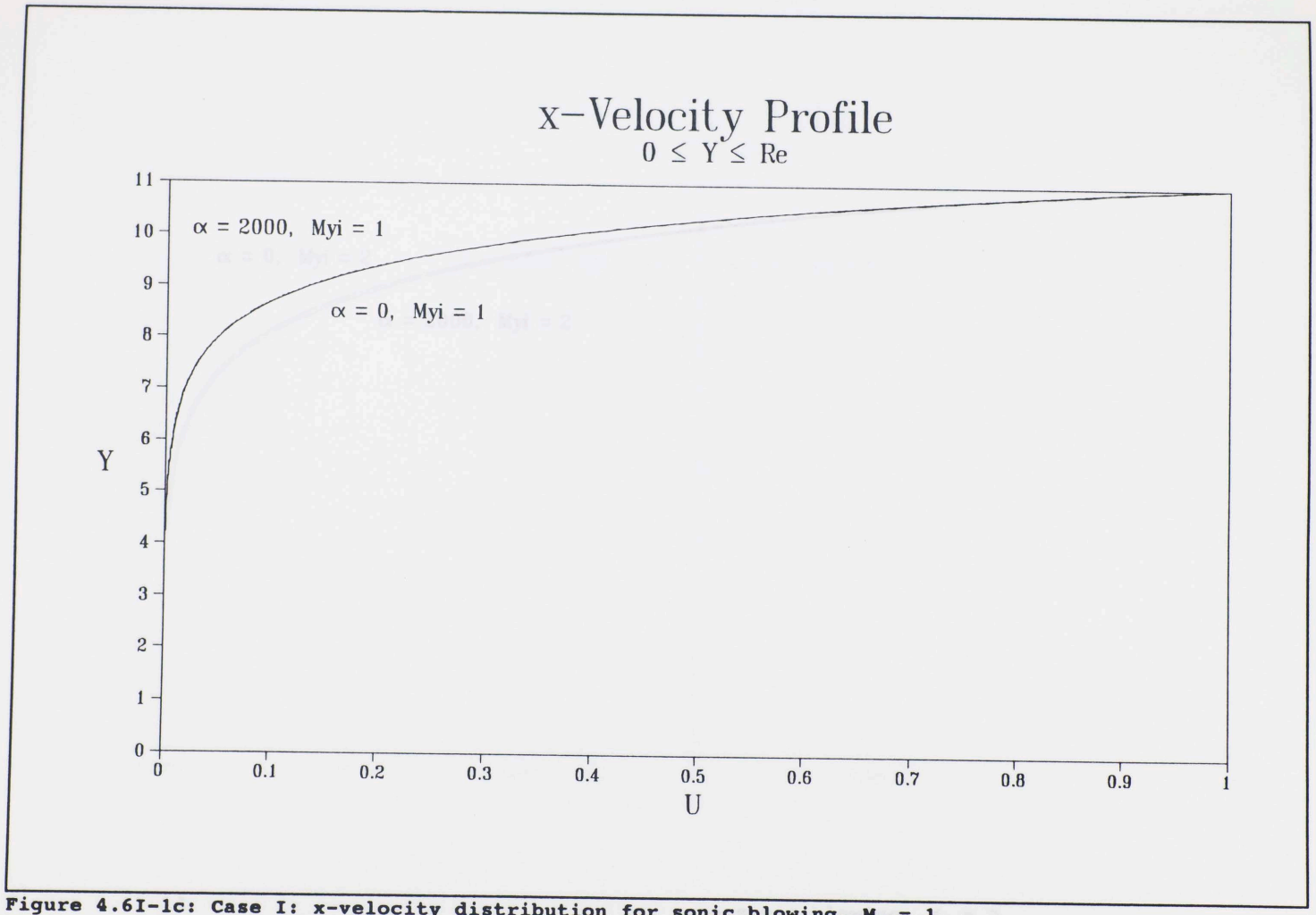

Figure 4.6I-1c: Case I: x-velocity distribution for sonic blowing, $M_{yi} = 1$

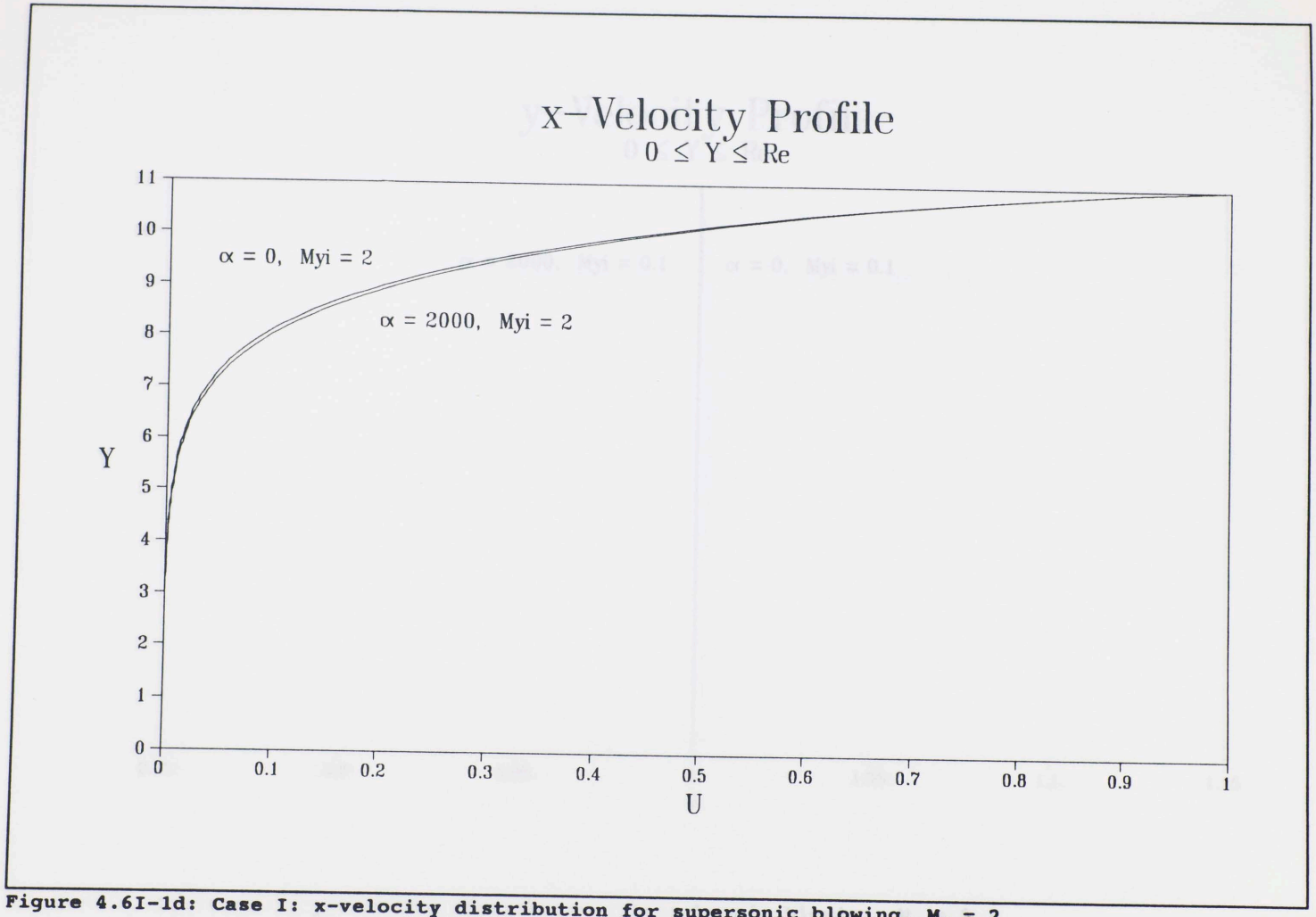

Figure 4.6I-1d: Case I: x-velocity distribution for supersonic blowing, $M_{yi} = 2$

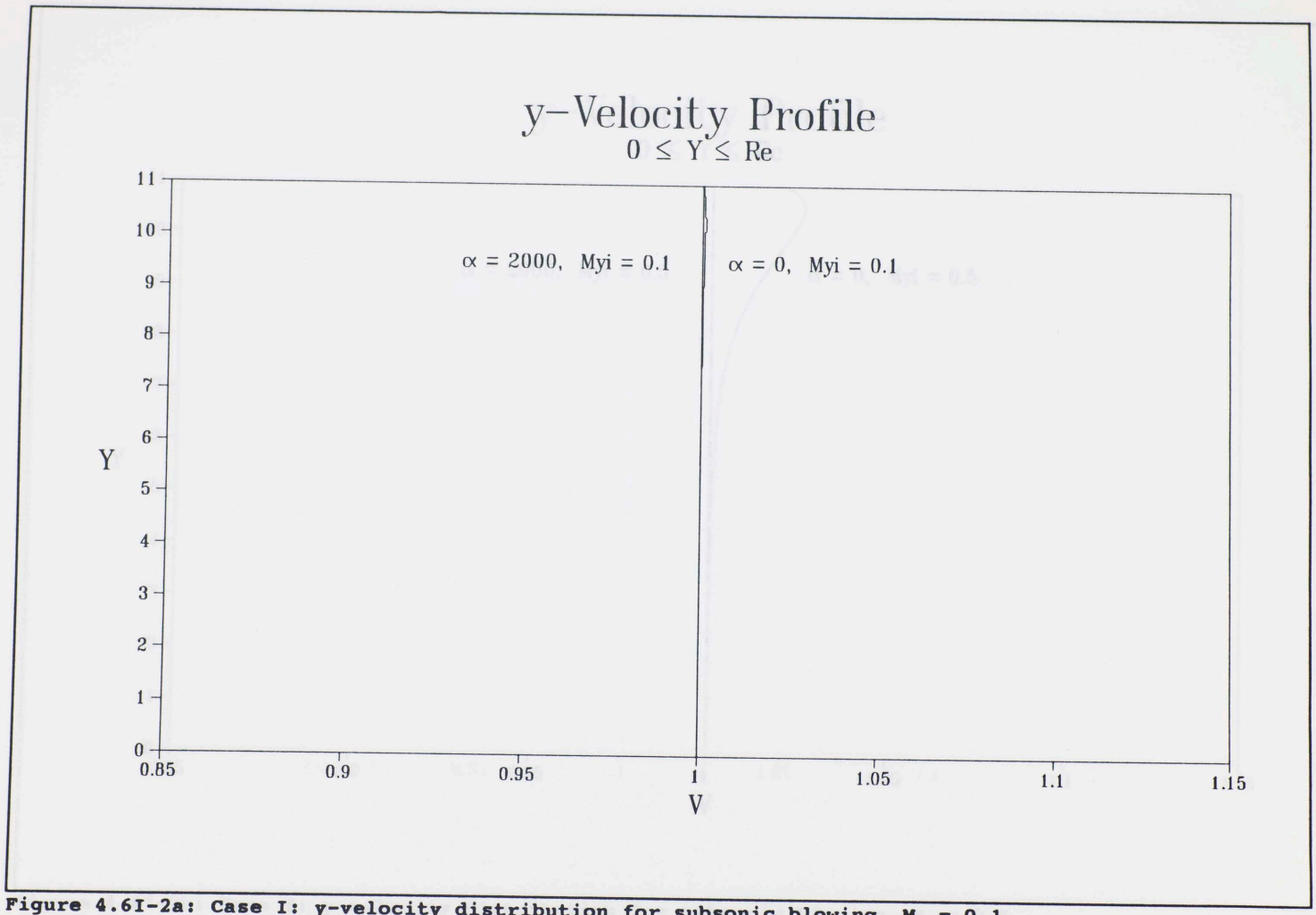

Figure 4.6I-2a: Case I: y-velocity distribution for subsonic blowing, $M_{yi} = 0.1$

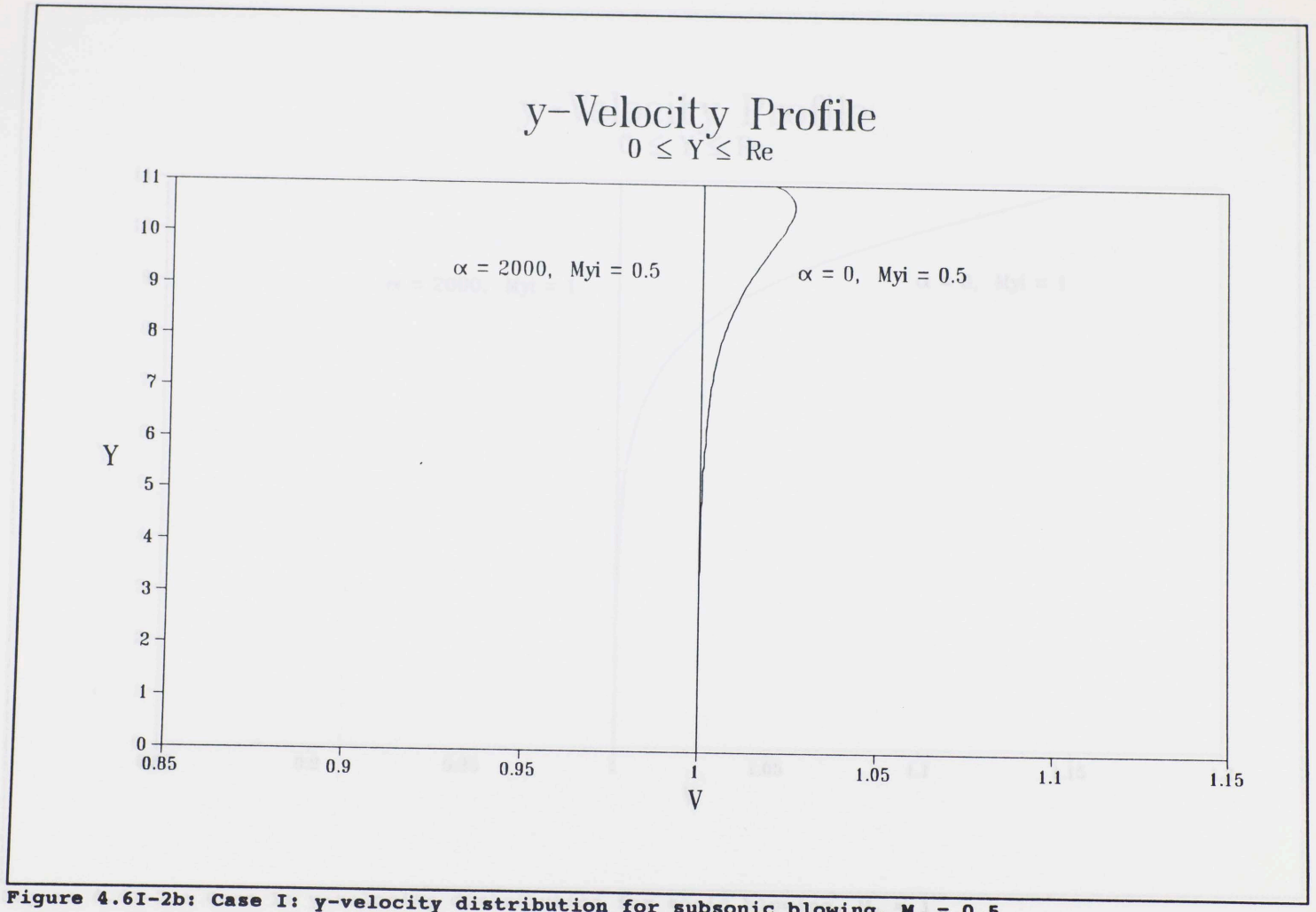

Figure 4.6I-2b: Case I: y-velocity distribution for subsonic blowing, M_{yi} = 0.5

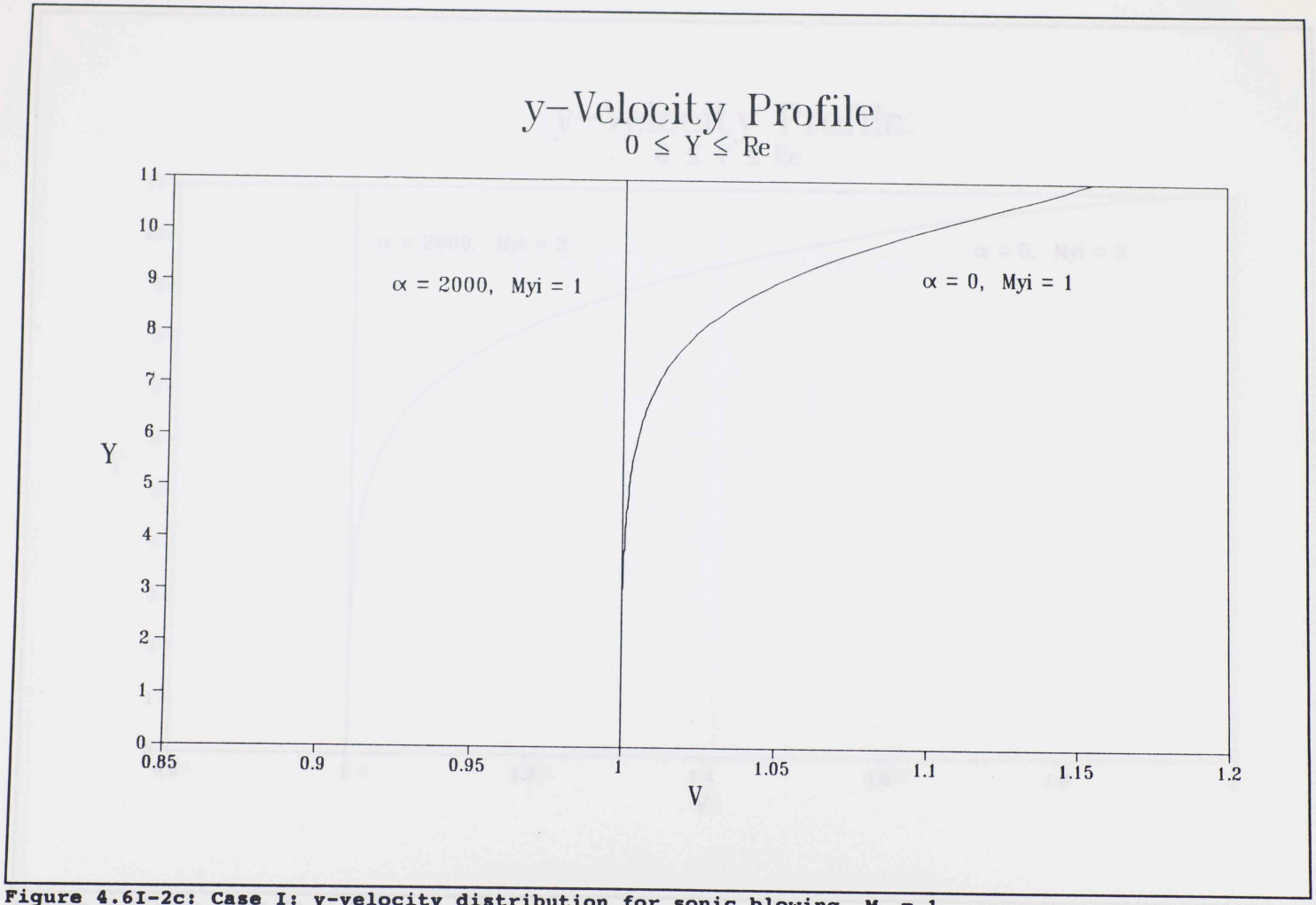

Figure 4.6I-2c: Case I: y-velocity distribution for sonic blowing, $M_{yi} = 1$

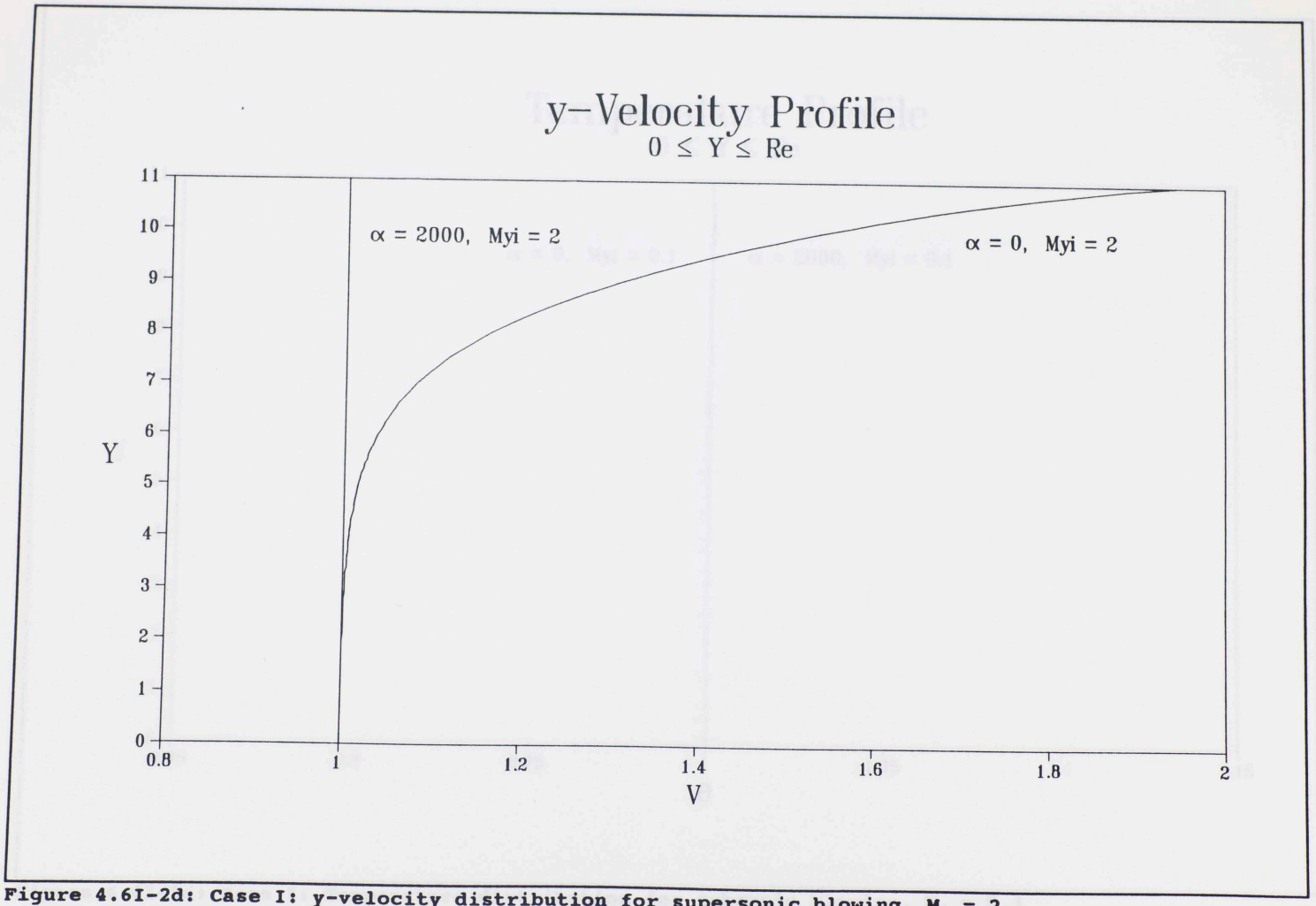

Figure 4.6I-2d: Case I: y-velocity distribution for supersonic blowing, $M_{yi} = 2$

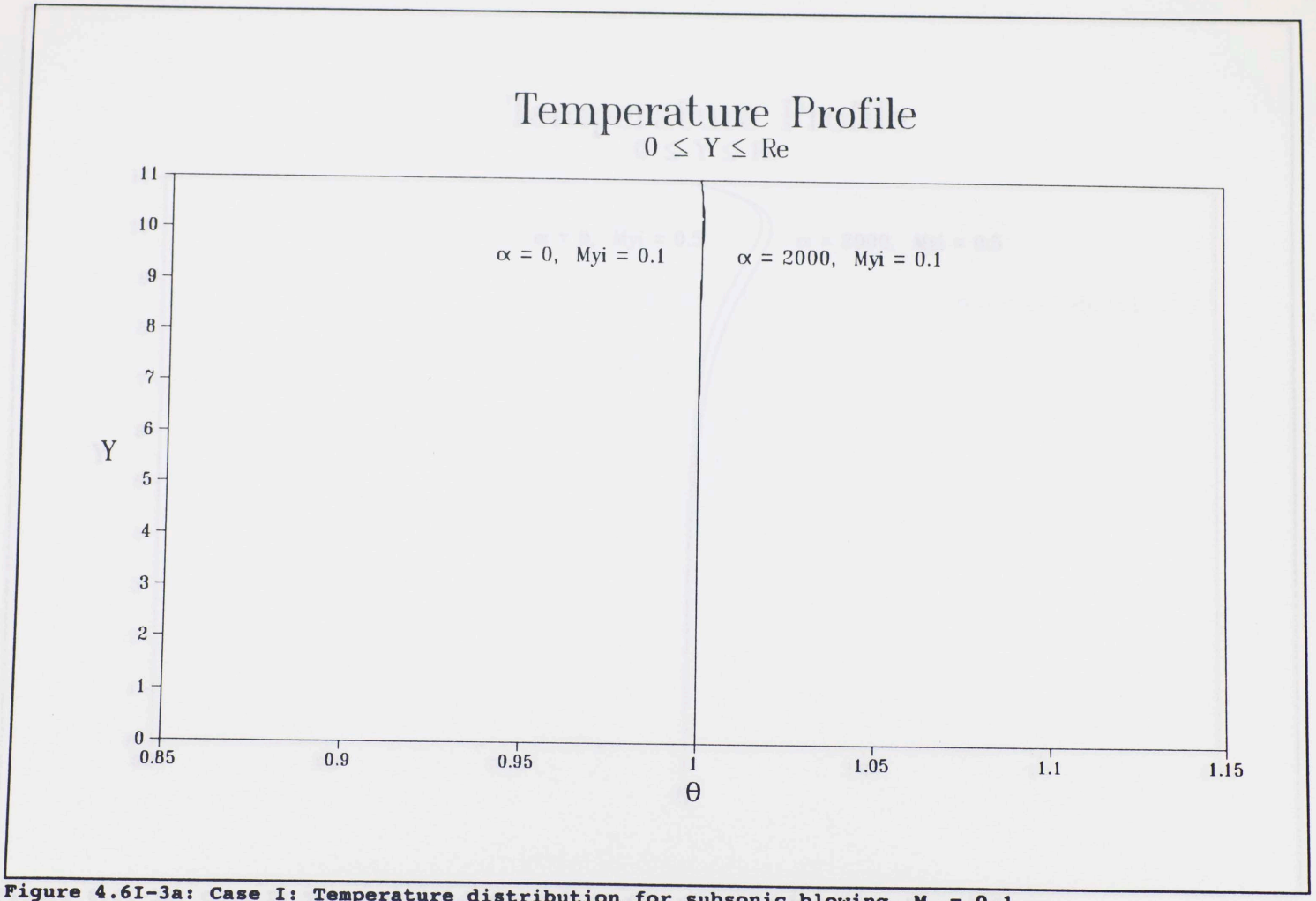

Figure 4.6I-3a: Case I: Temperature distribution for subsonic blowing, $M_{yi} = 0.1$

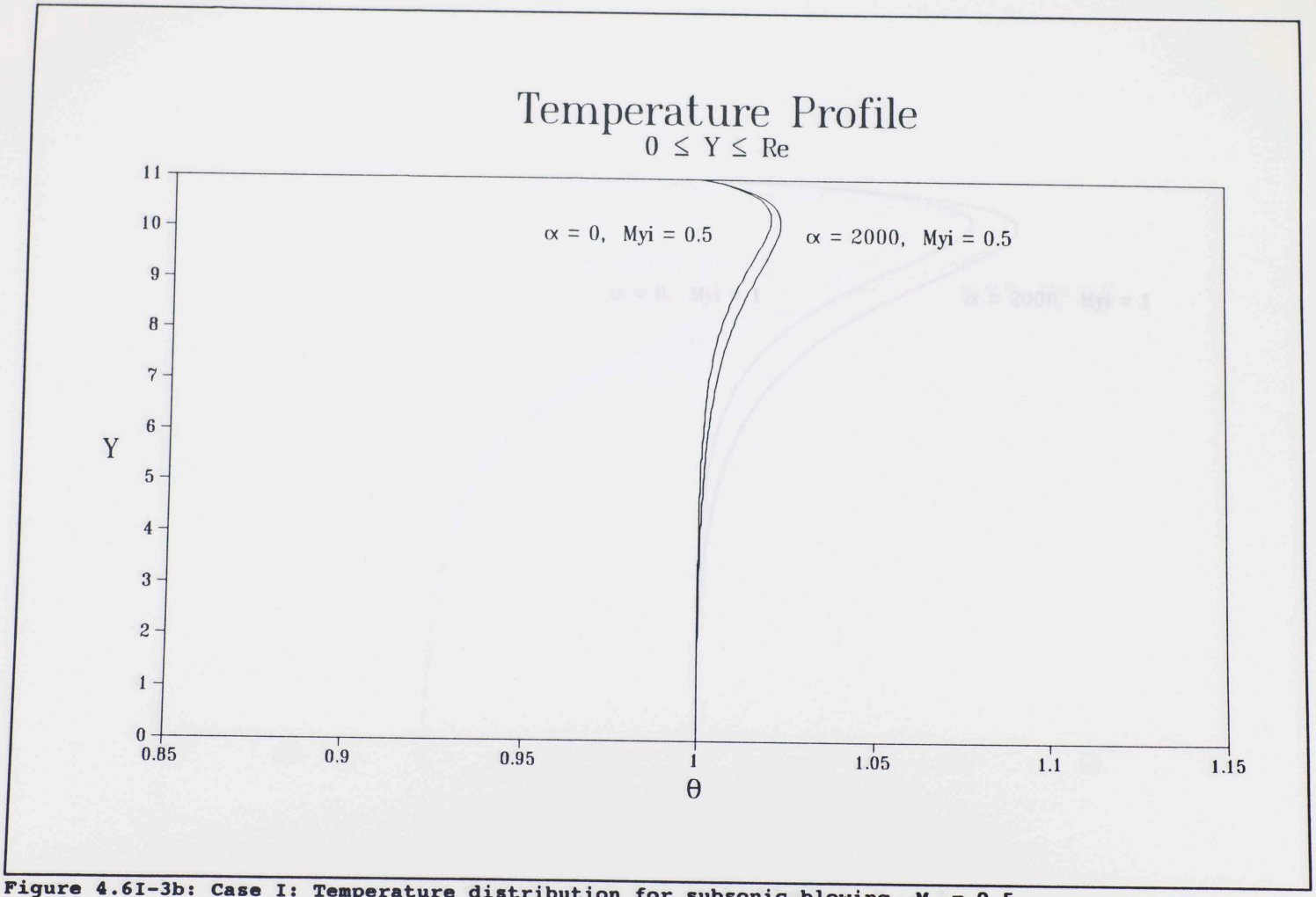

Figure 4.6I-3b: Case I: Temperature distribution for subsonic blowing, M_{yi} = 0.5

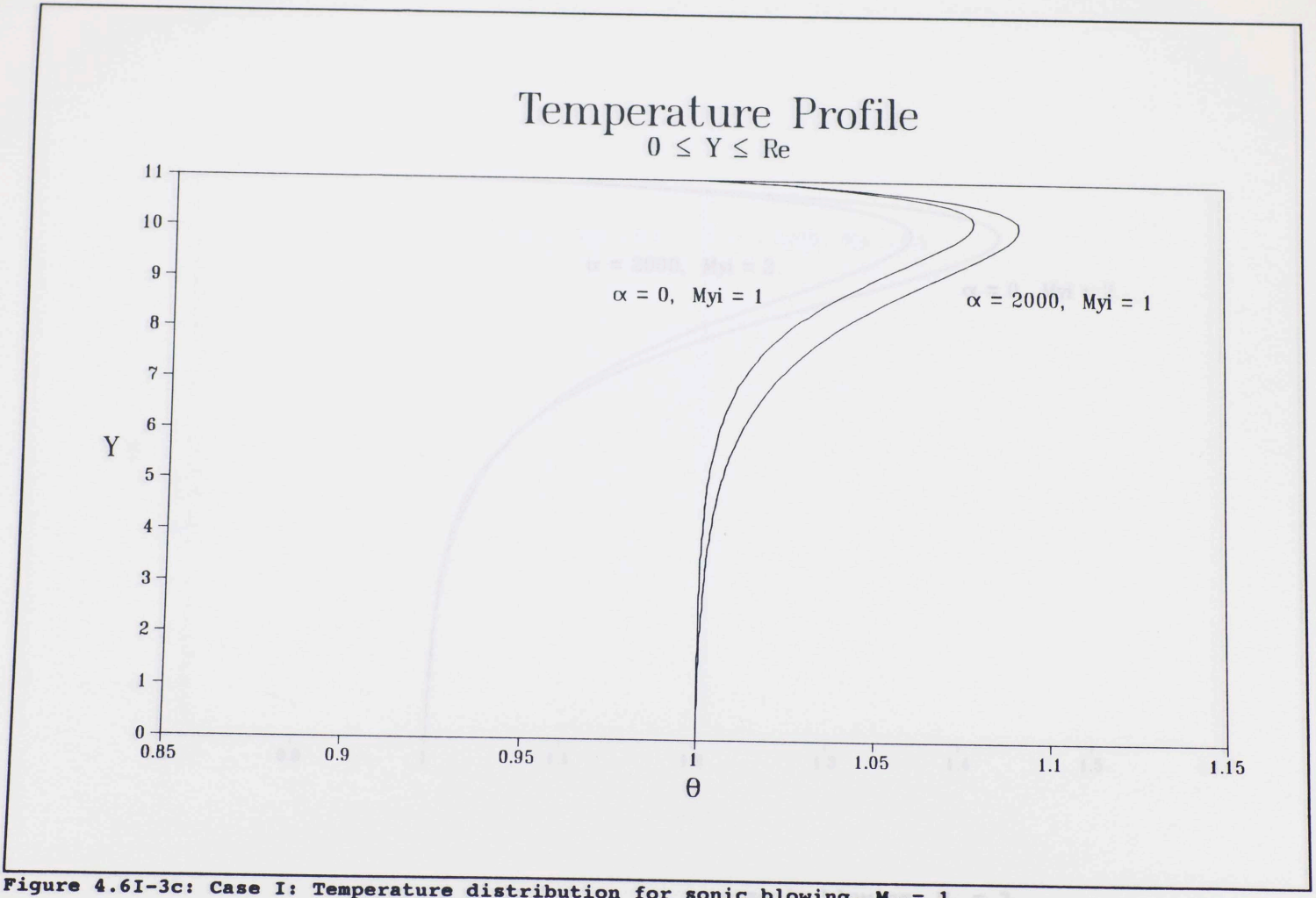

Figure 4.6I-3c: Case I: Temperature distribution for sonic blowing, $M_{yi} = 1$

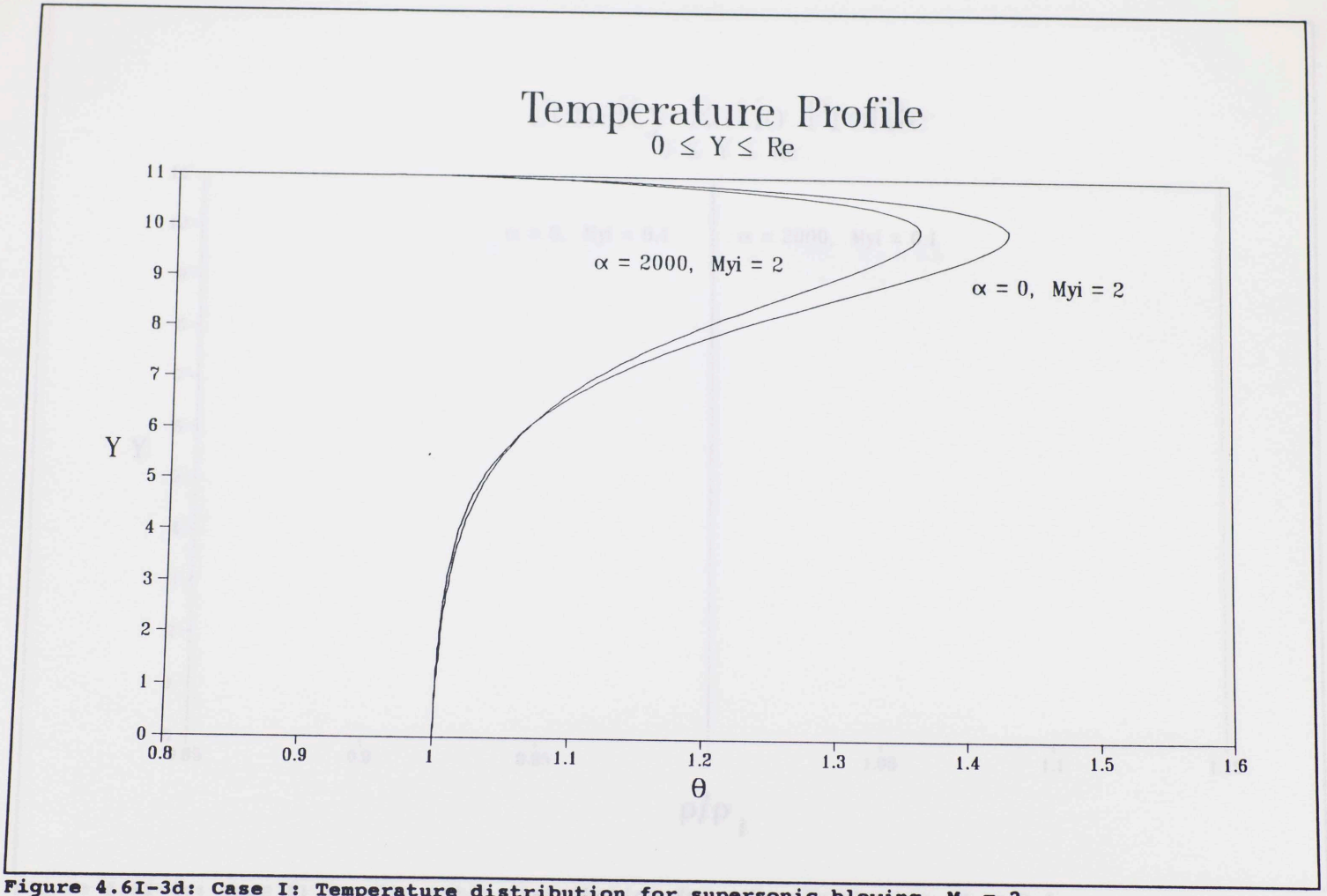

Figure 4.6I-3d: Case I: Temperature distribution for supersonic blowing, $M_{yi} = 2$

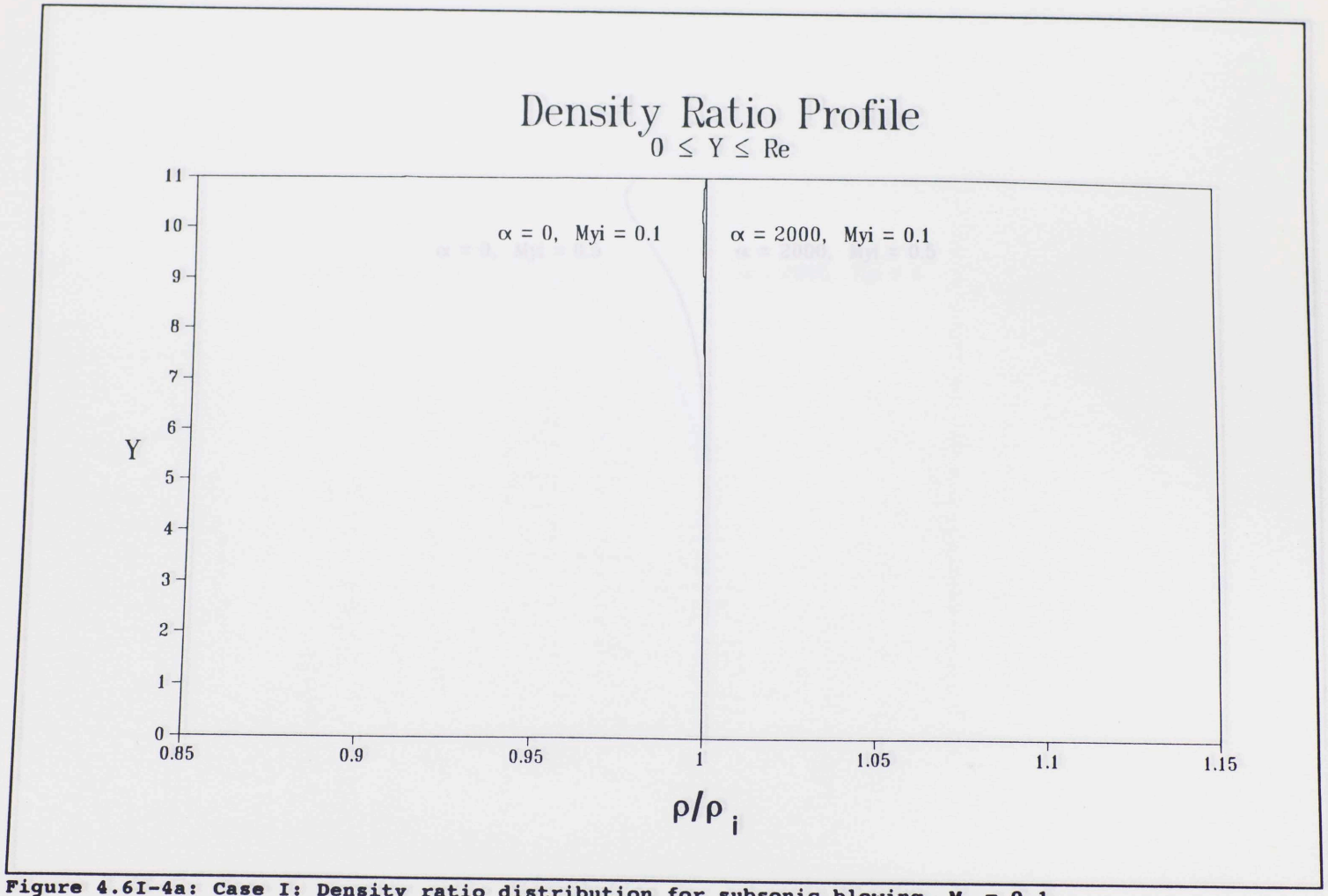

Figure 4.6I-4a: Case I: Density ratio distribution for subsonic blowing, M_{yi} = 0.1

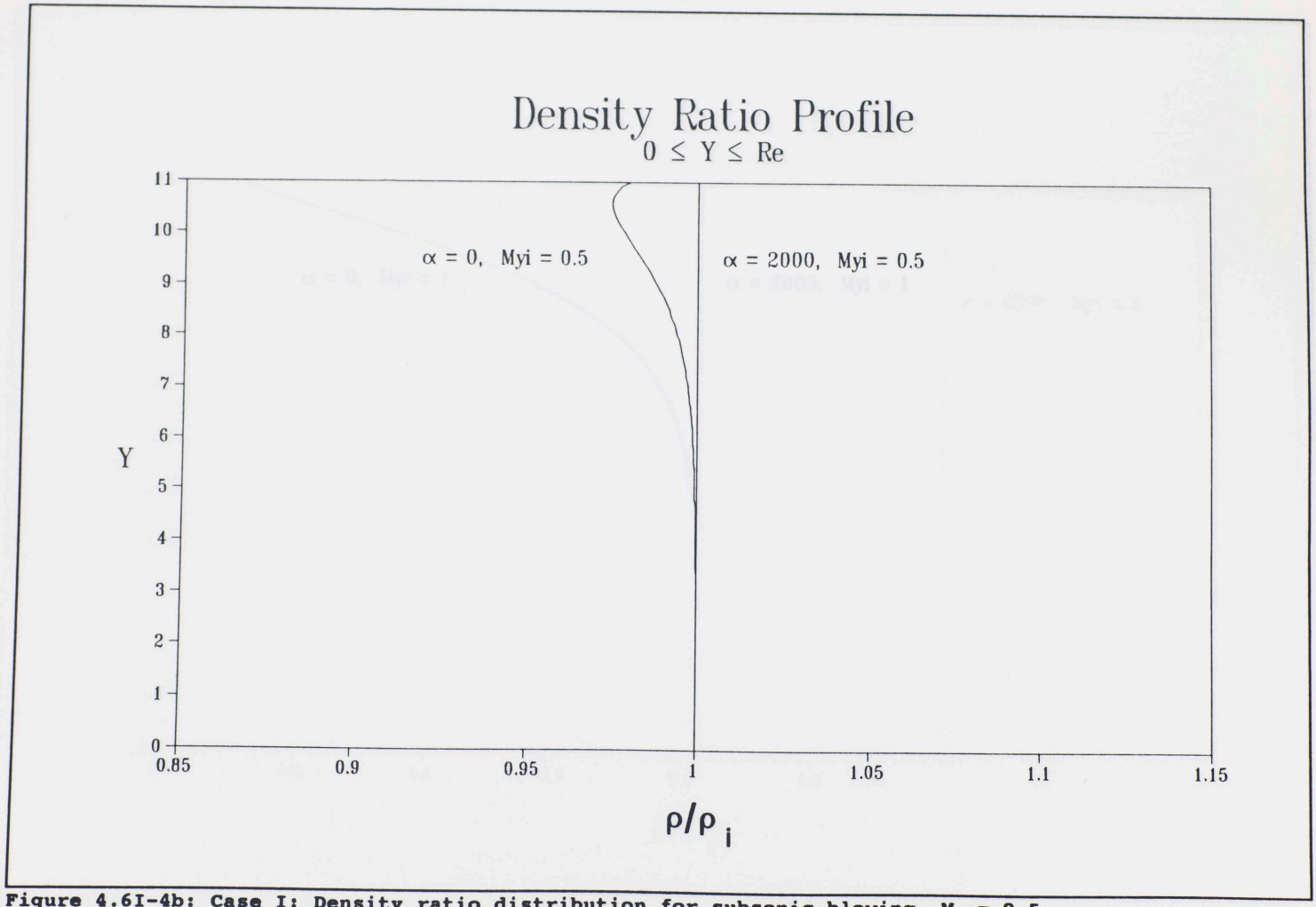

Figure 4.6I-4b: Case I: Density ratio distribution for subsonic blowing, M_{yi} = 0.5

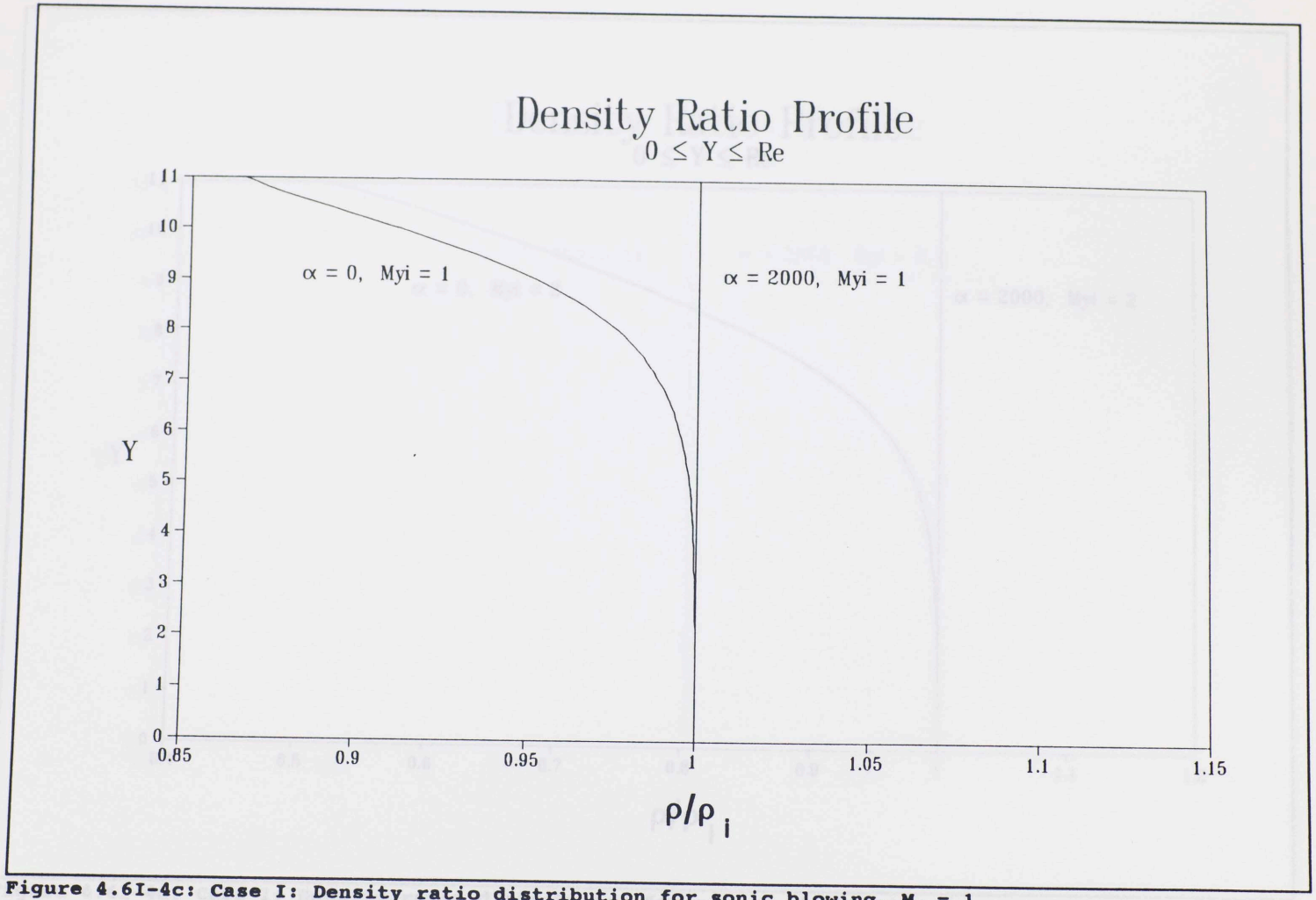

Figure 4.6I-4c: Case I: Density ratio distribution for sonic blowing, $M_{yi} = 1$

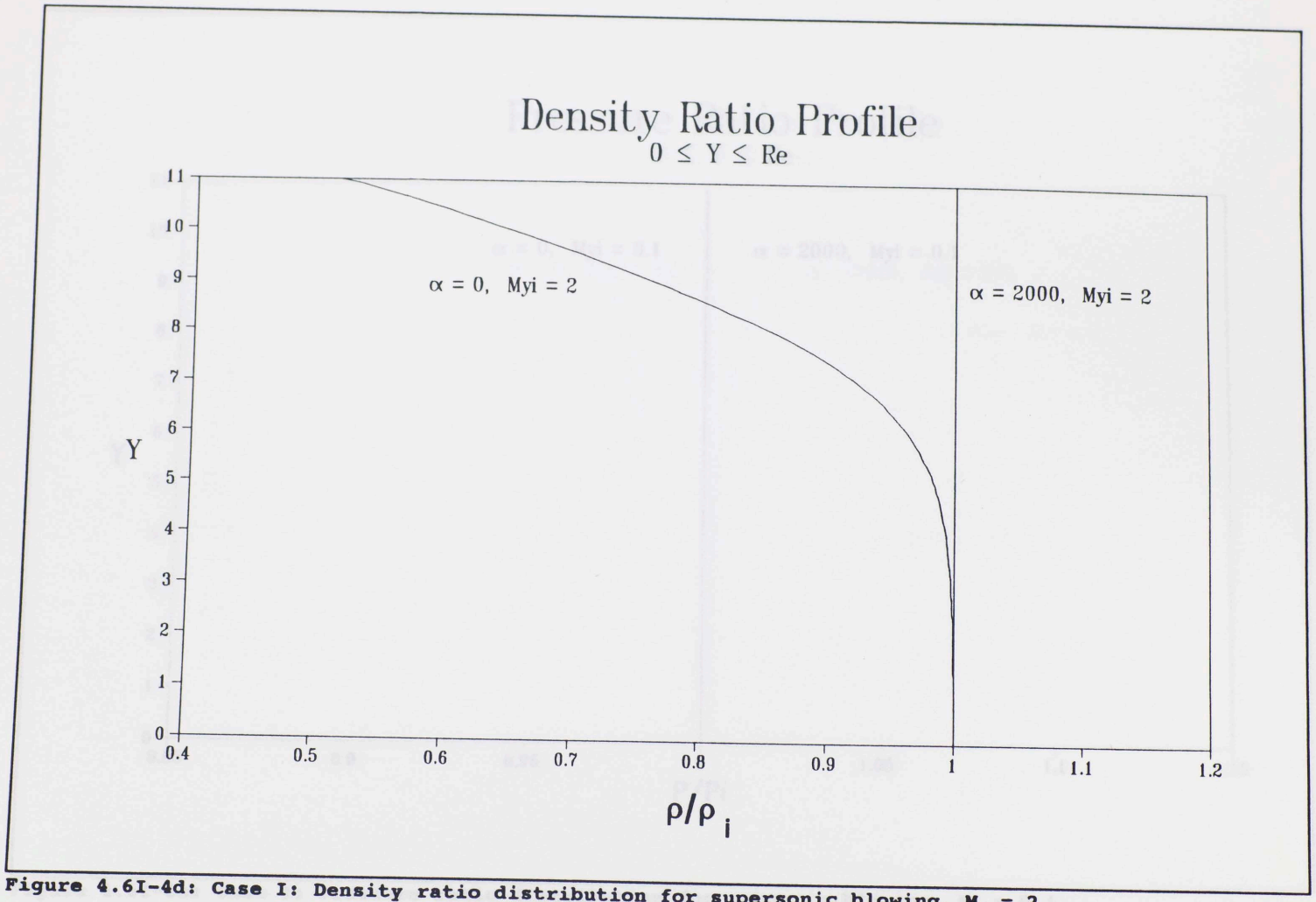

Figure 4.6I-4d: Case I: Density ratio distribution for supersonic blowing, $M_{yi} = 2$

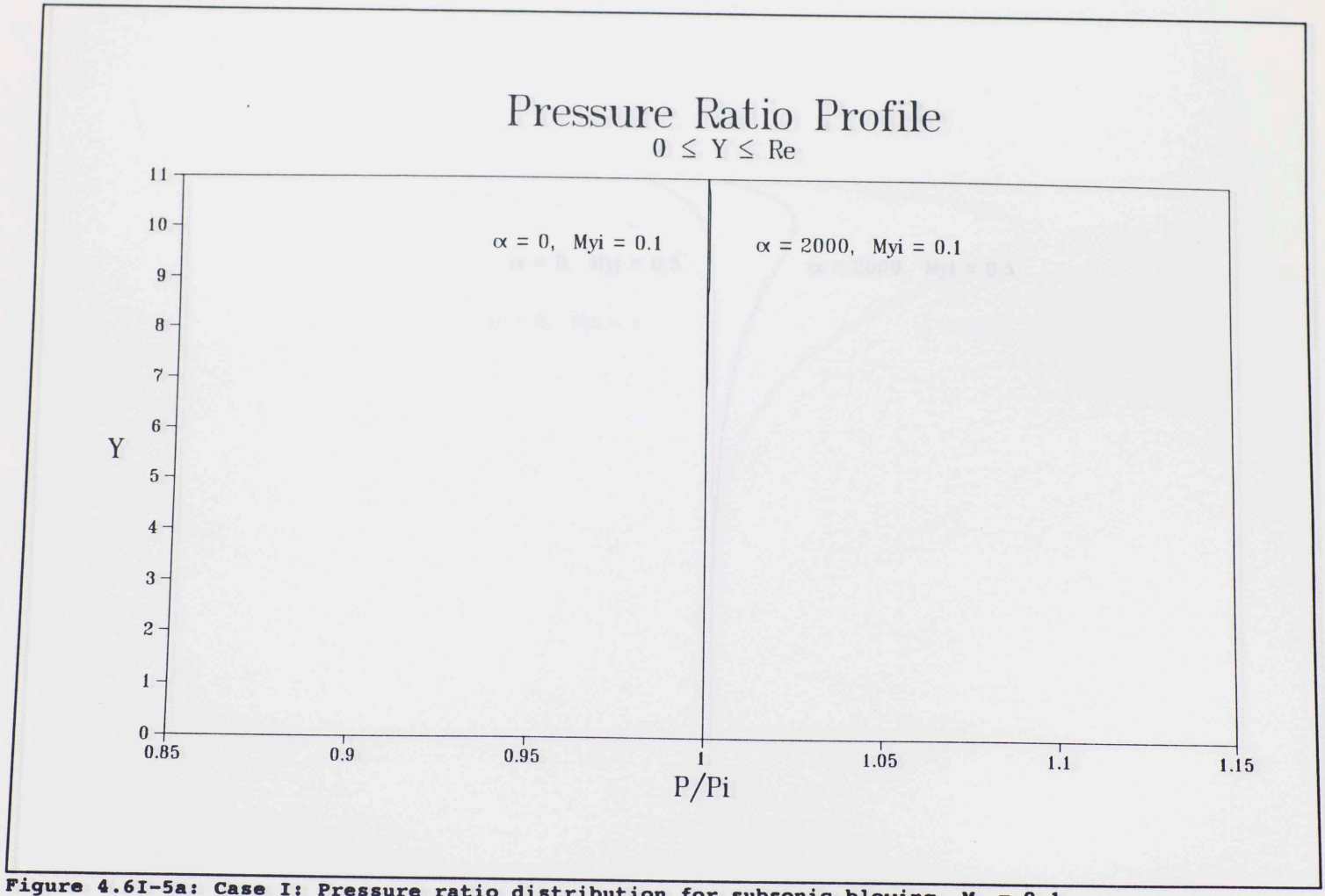

Figure 4.6I-5a: Case I: Pressure ratio distribution for subsonic blowing, M_{yi} = 0.1

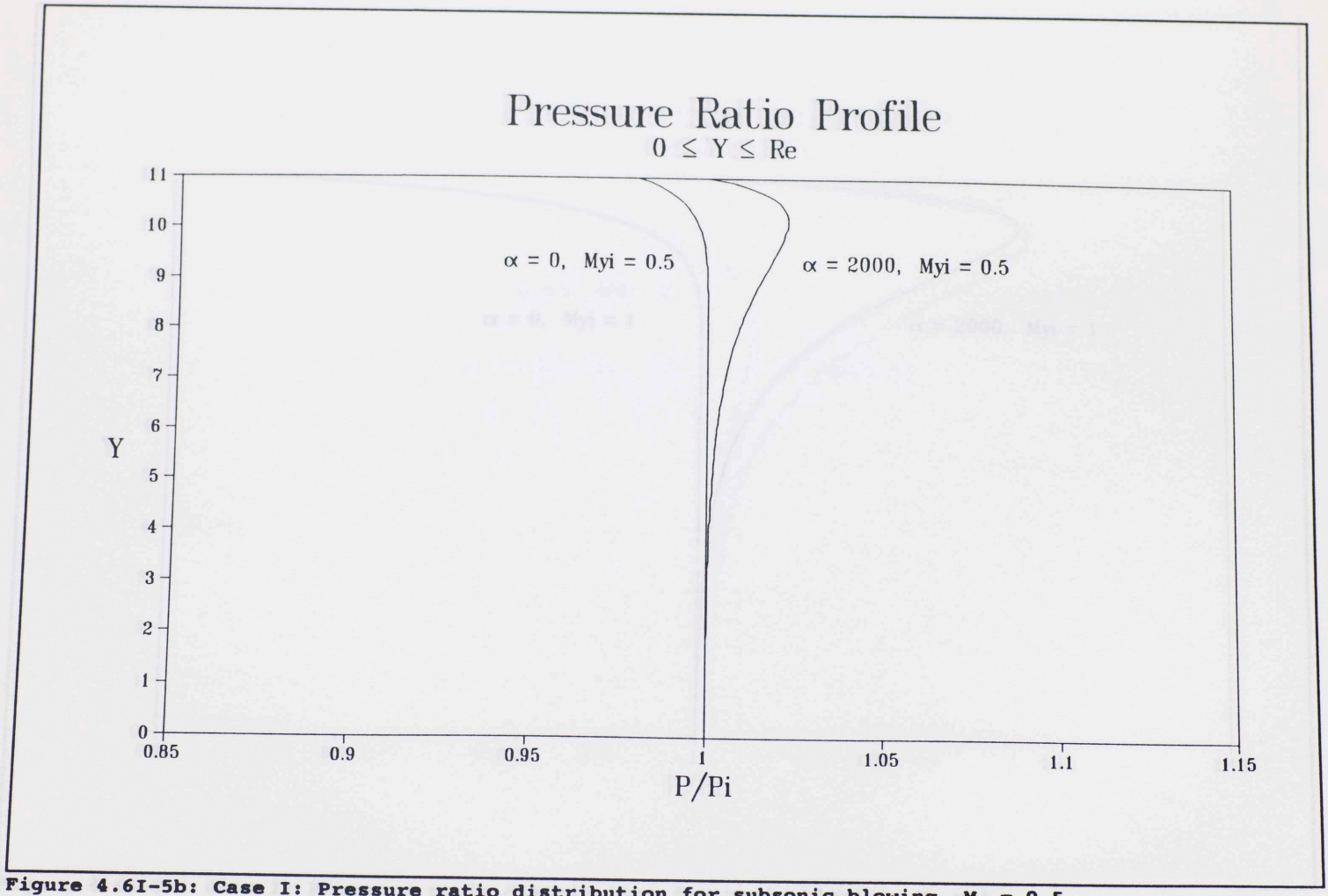

Figure 4.6I-5b: Case I: Pressure ratio distribution for subsonic blowing, M_{yi} = 0.5

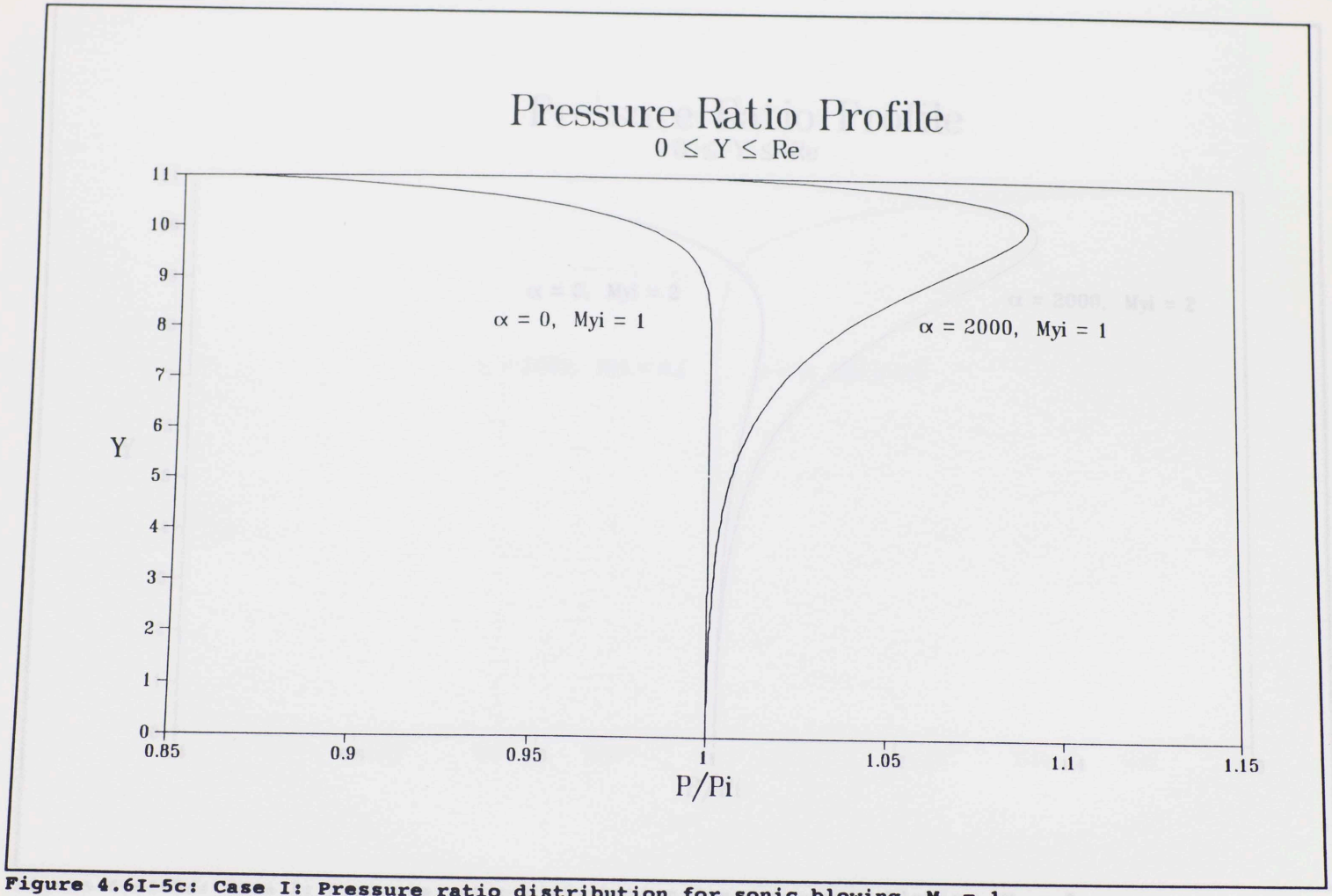

Figure 4.6I-5c: Case I: Pressure ratio distribution for sonic blowing, $M_{yi} = 1$

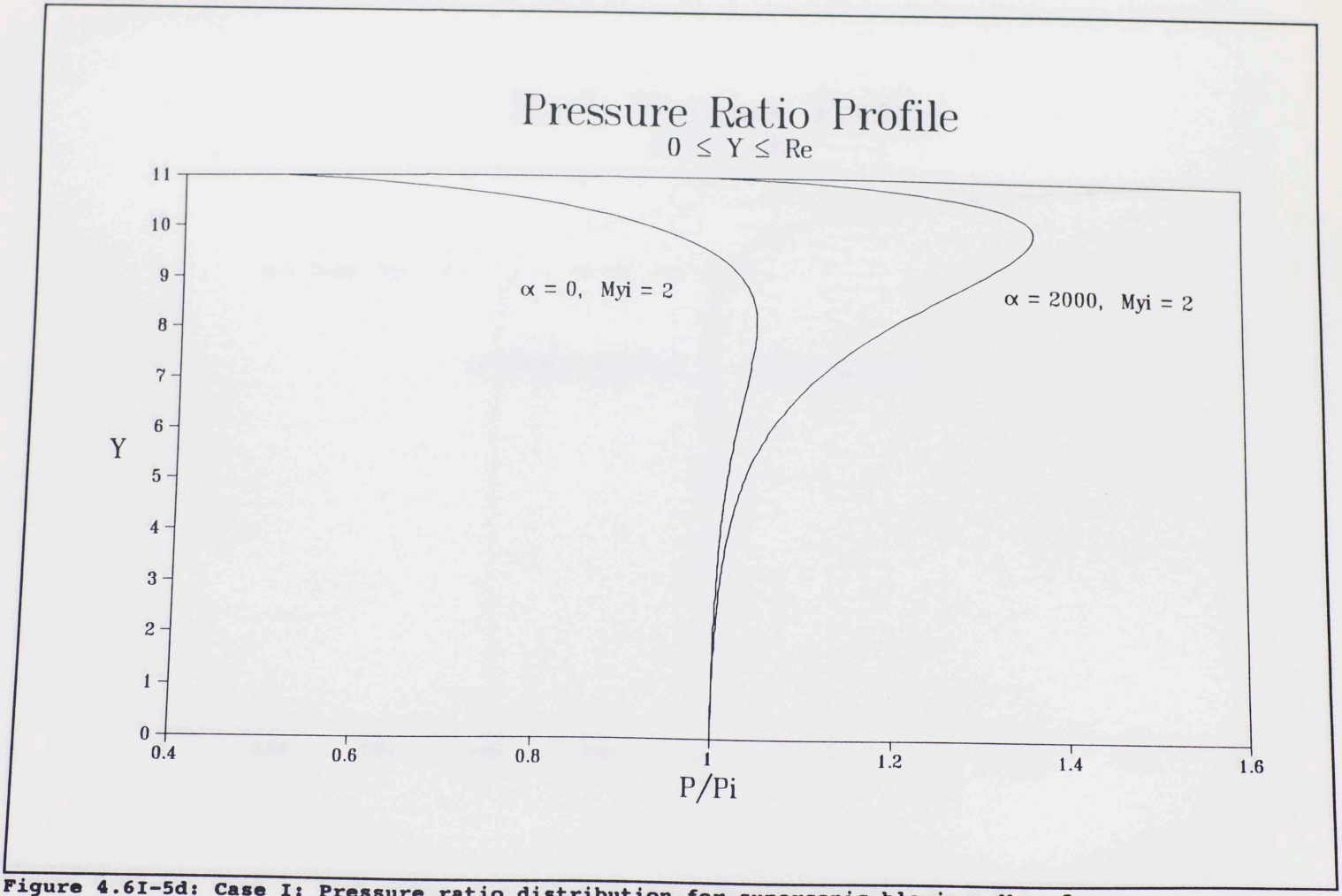

Figure 4.6I-5d: Case I: Pressure ratio distribution for supersonic blowing, $M_{yi} = 2$

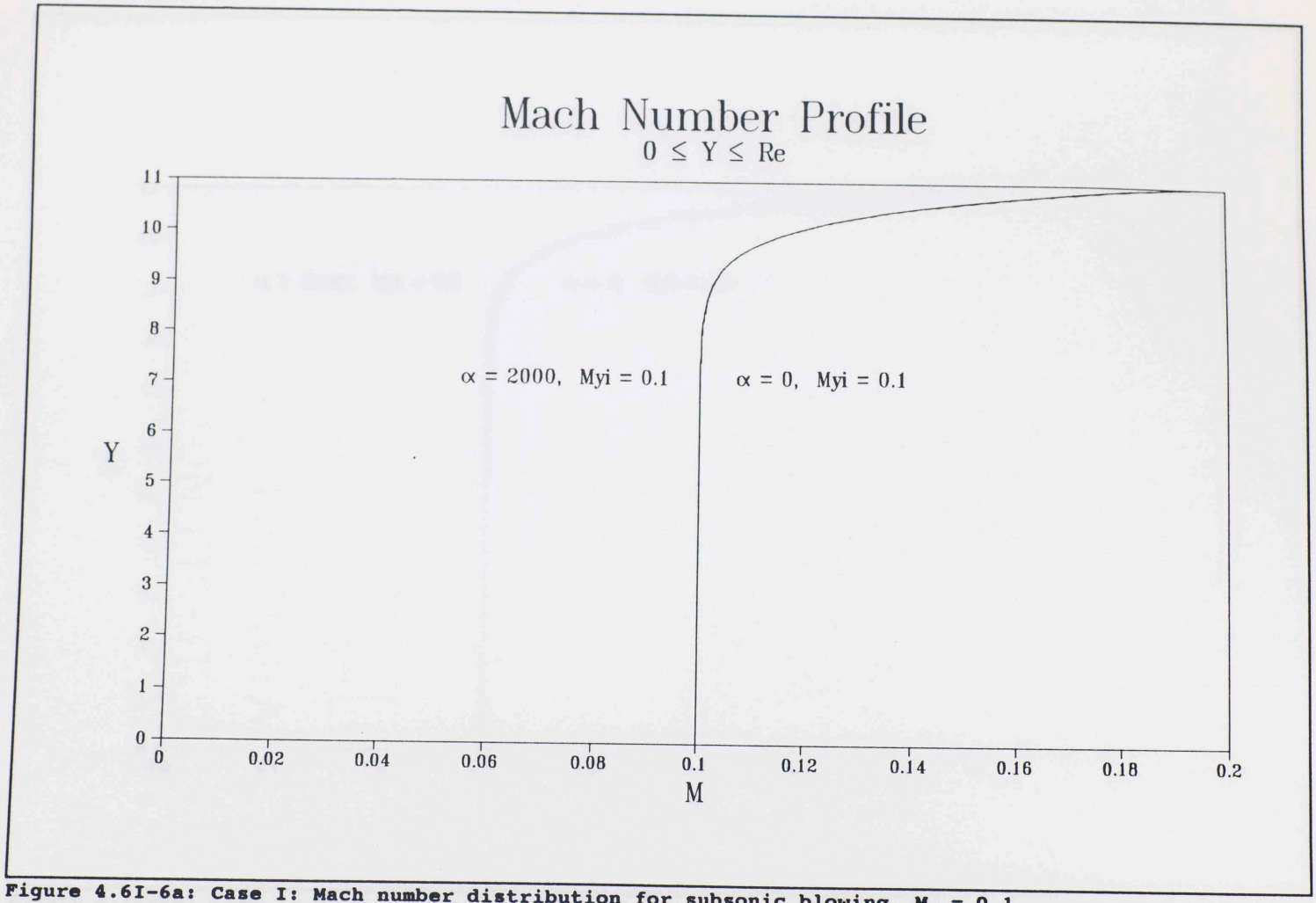

Figure 4.6I-6a: Case I: Mach number distribution for subsonic blowing, $M_{yi} = 0.1$

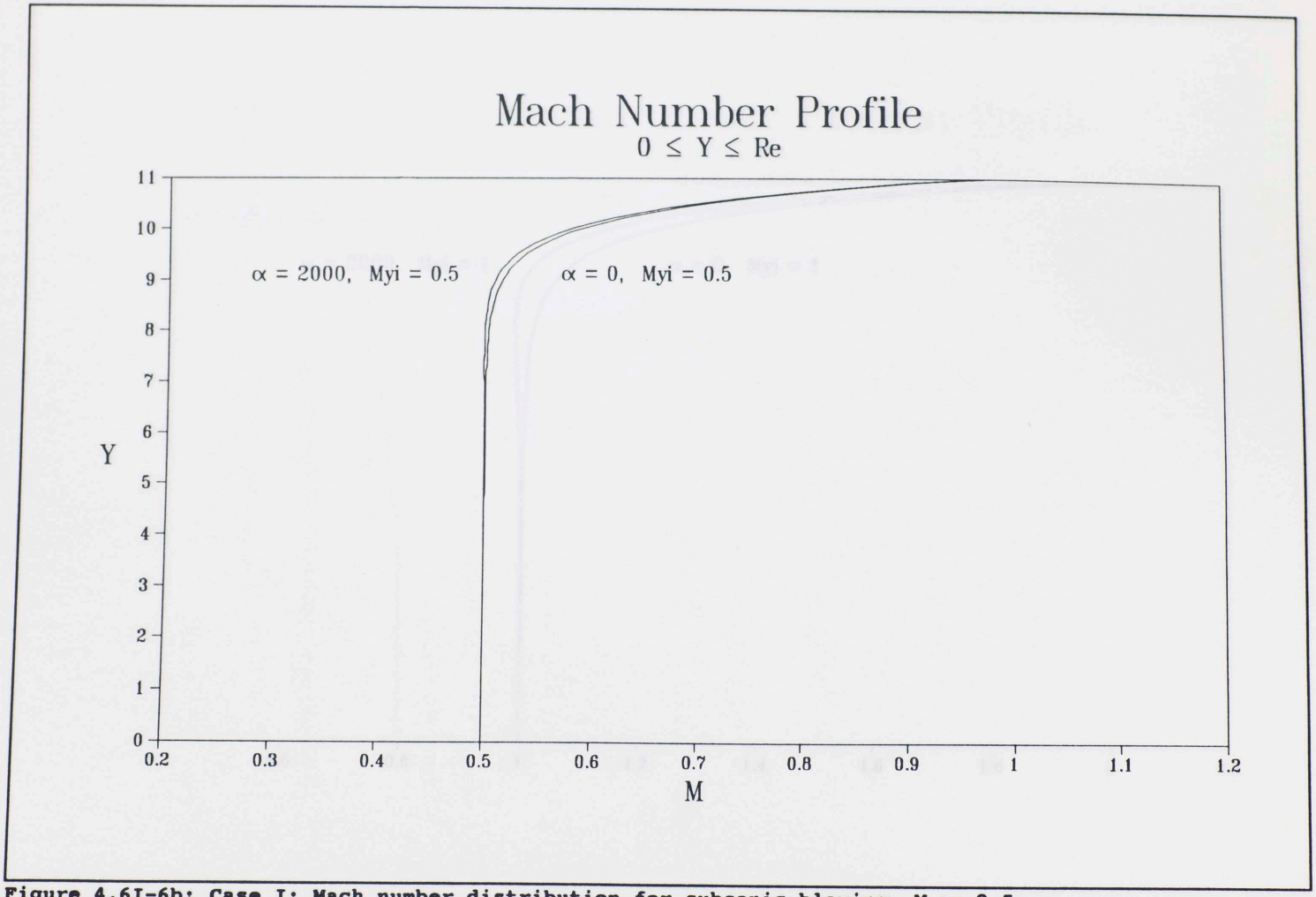

Figure 4.6I-6b: Case I: Mach number distribution for subsonic blowing, $M_{yi} = 0.5$

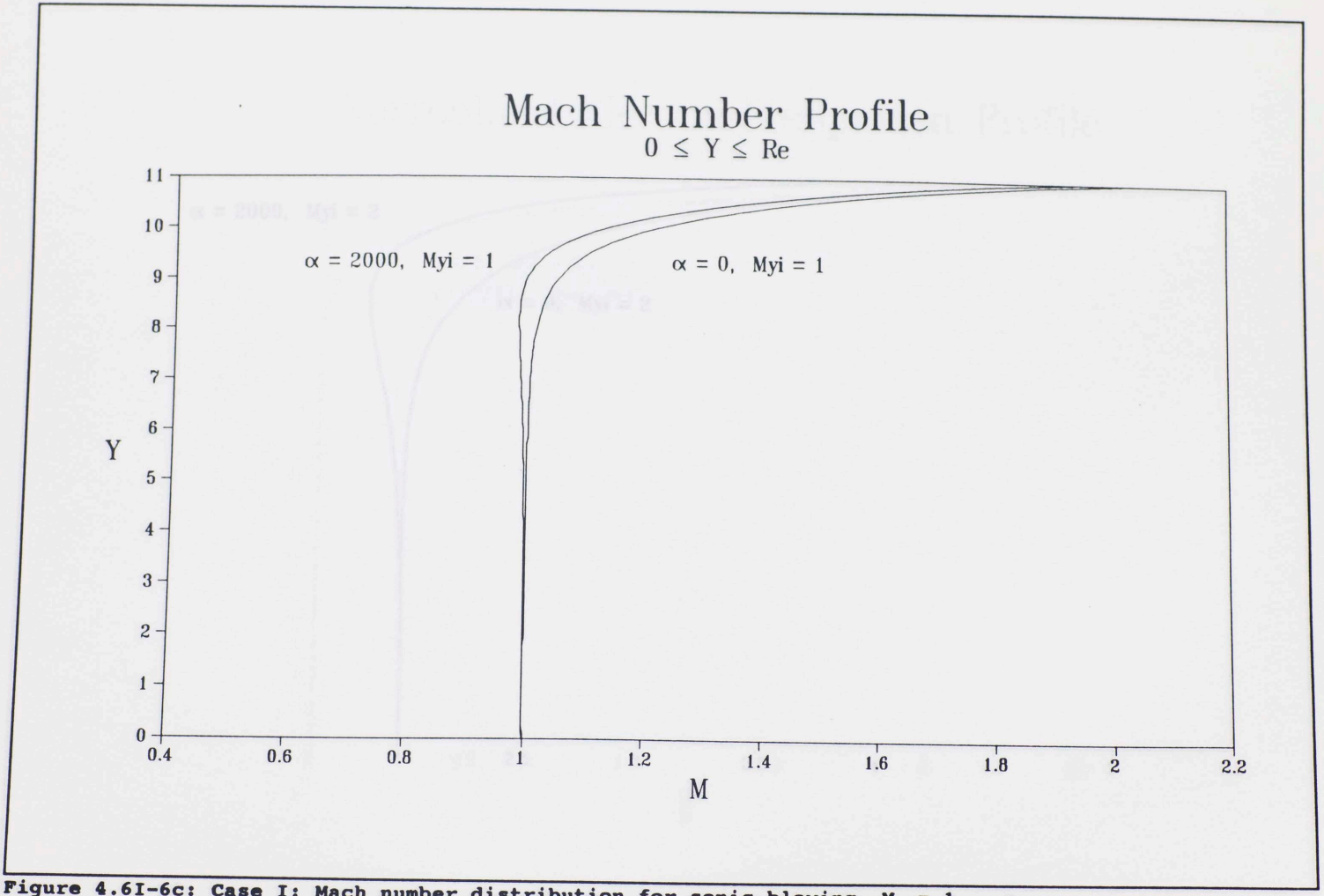

Figure 4.6I-6c: Case I: Mach number distribution for sonic blowing, $M_{yi} = 1$

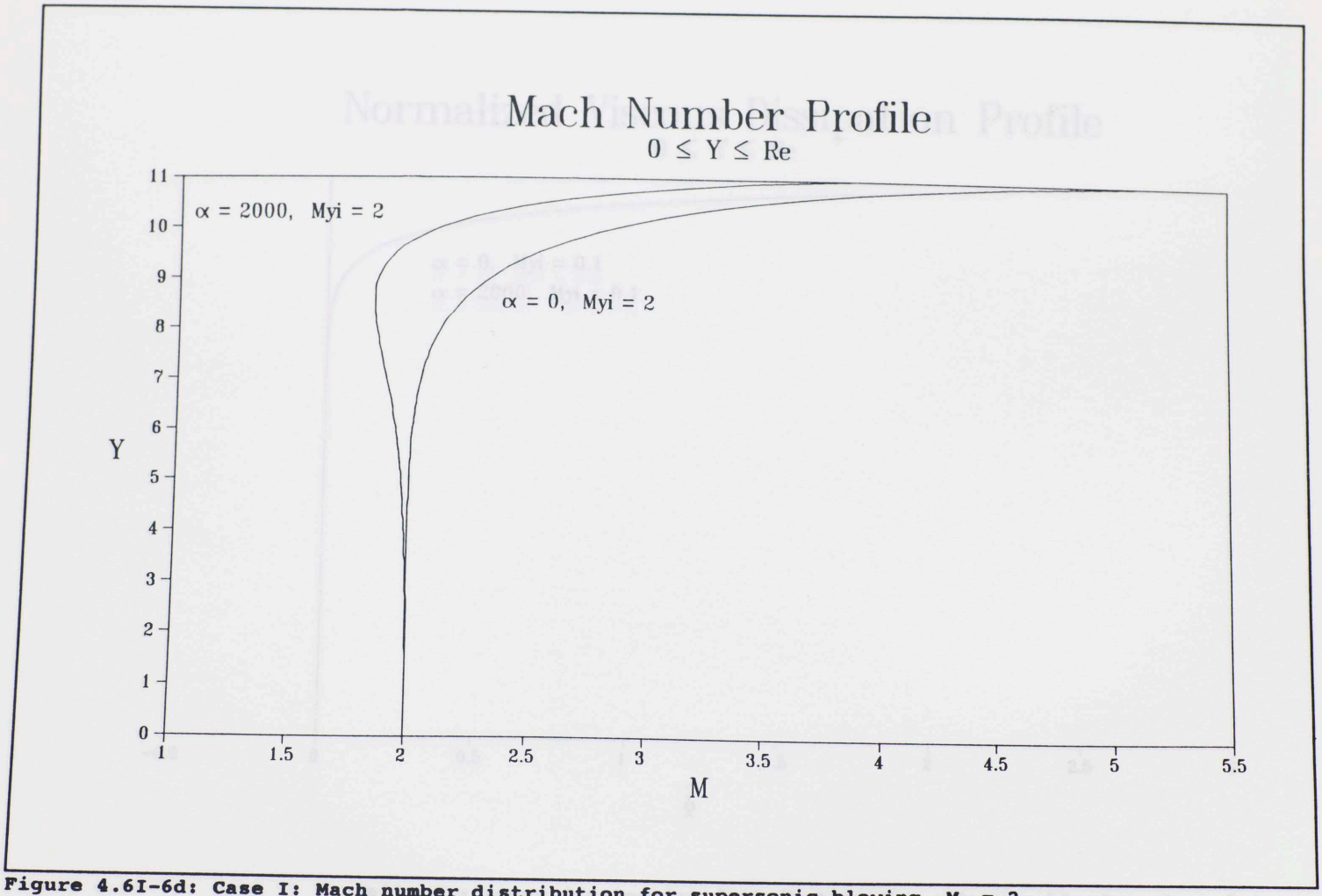

Figure 4.6I-6d: Case I: Mach number distribution for supersonic blowing, $M_{yi} = 2$

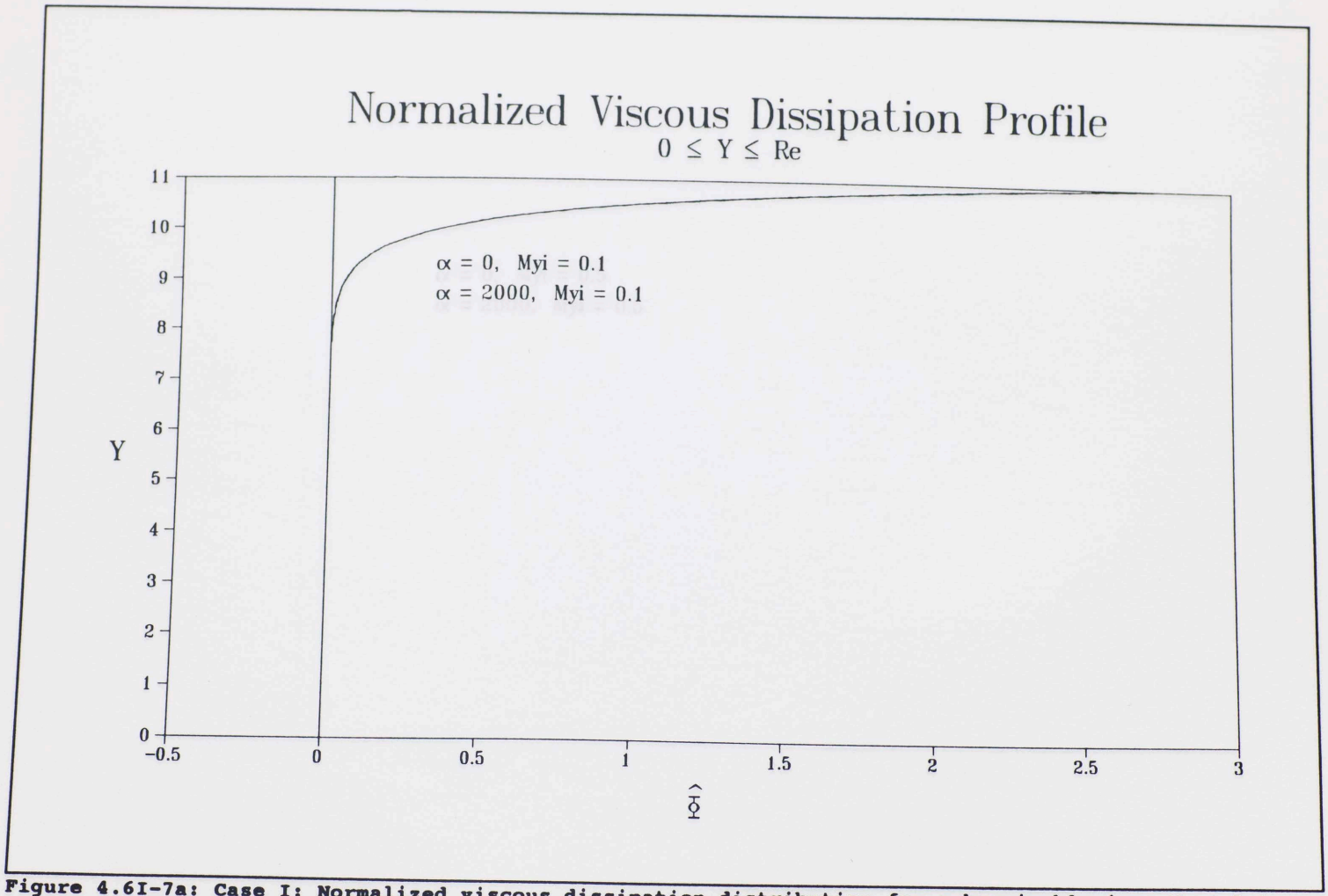

Figure 4.6I-7a: Case I: Normalized viscous dissipation distribution for subsonic blowing, $M_{yi} = 0.1$

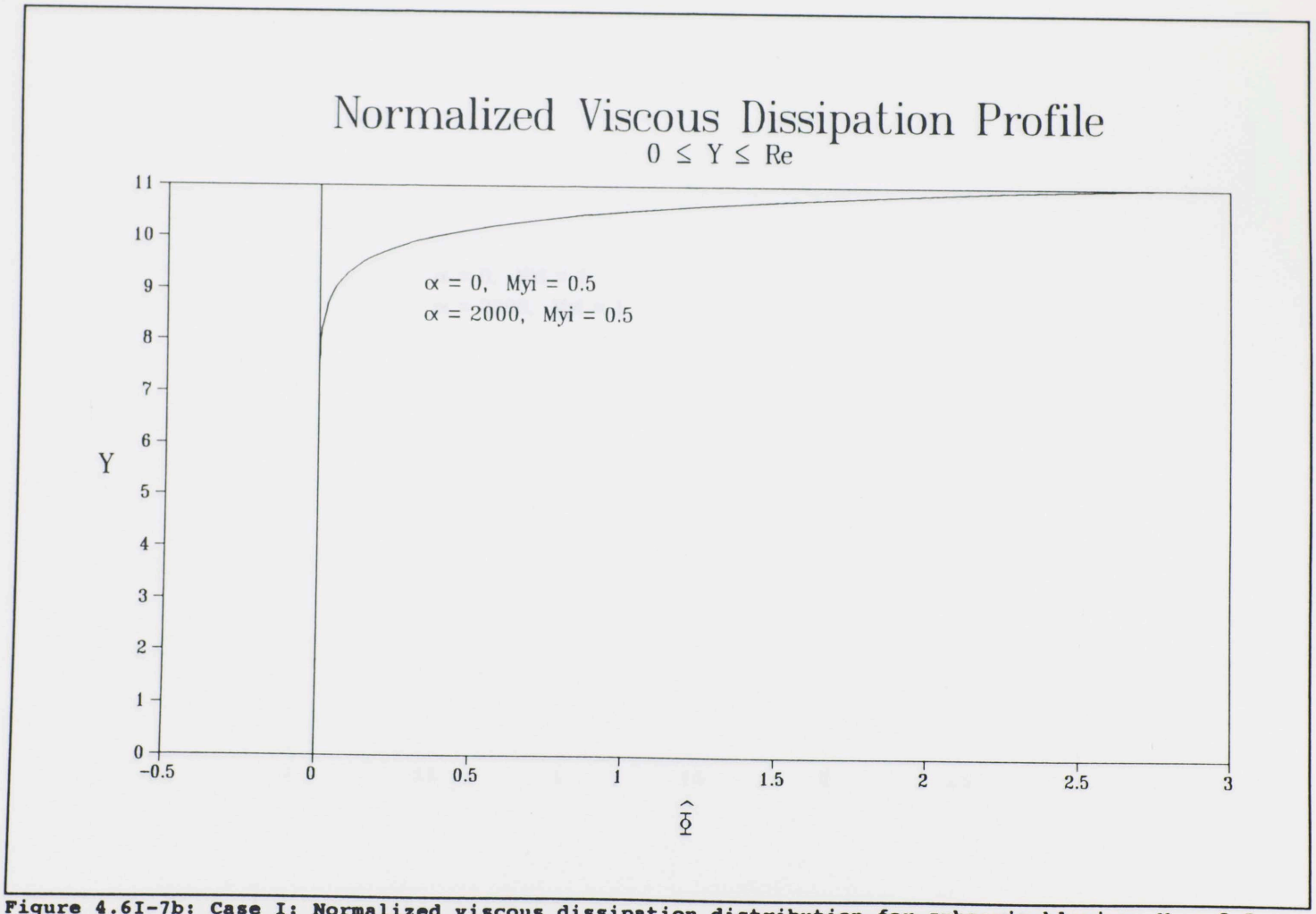

Figure 4.6I-7b: Case I: Normalized viscous dissipation distribution for subsonic blowing, M_{yi} = 0.5

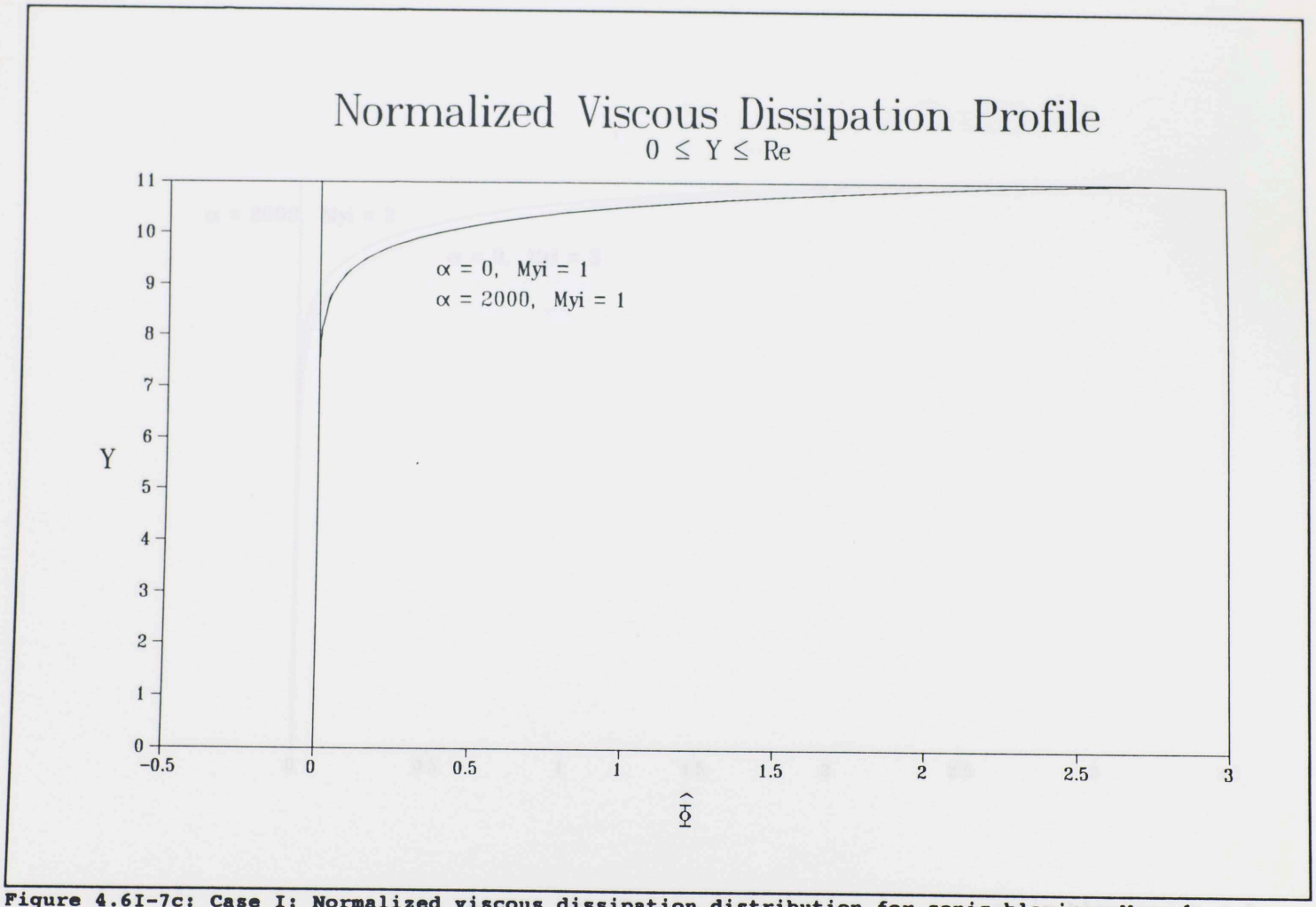

Figure 4.6I-7c: Case I: Normalized viscous dissipation distribution for sonic blowing, $M_{yi} = 1$

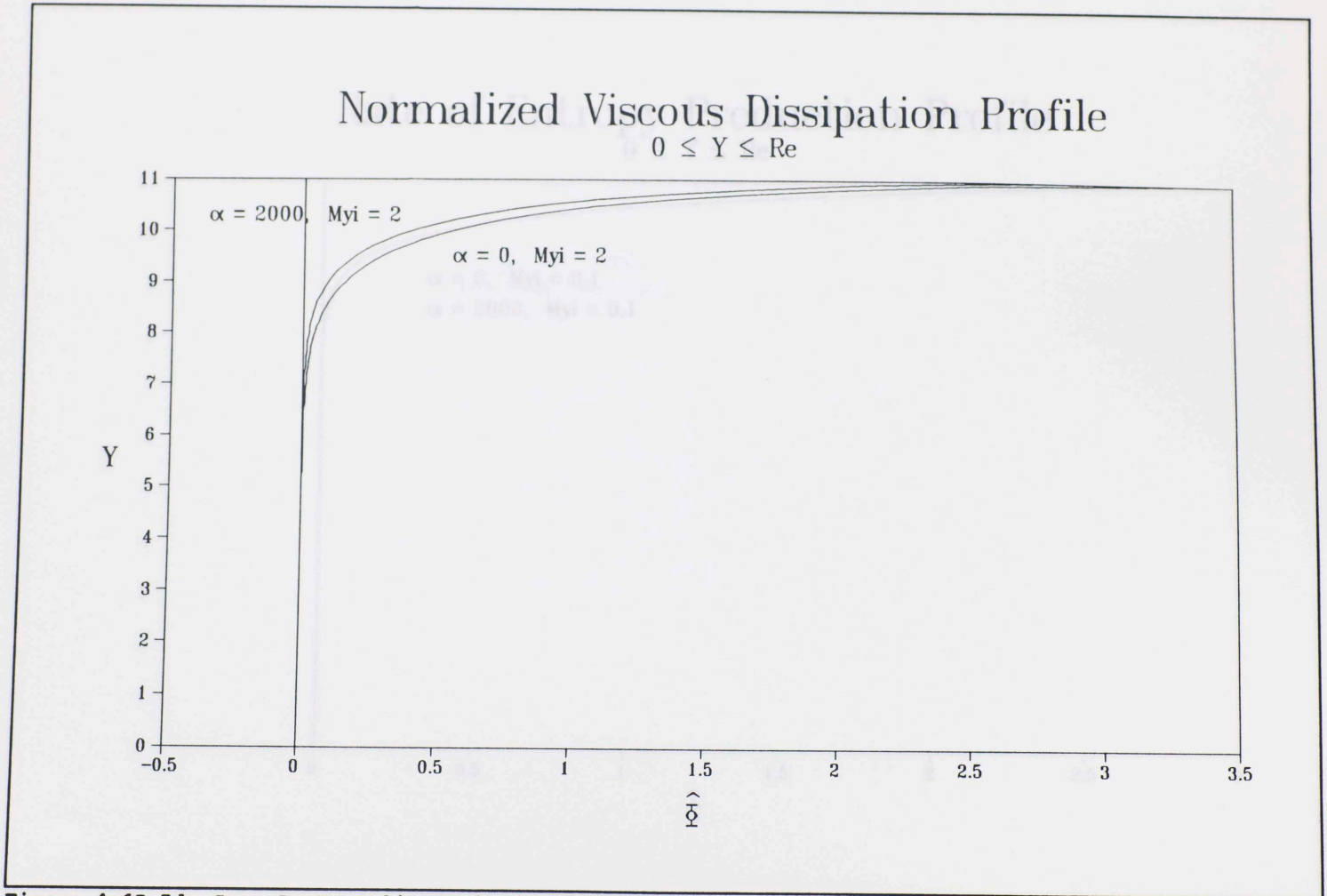

Figure 4.6I-7d: Case I: Normalized viscous dissipation distribution for supersonic blowing, M_{yi} = 2

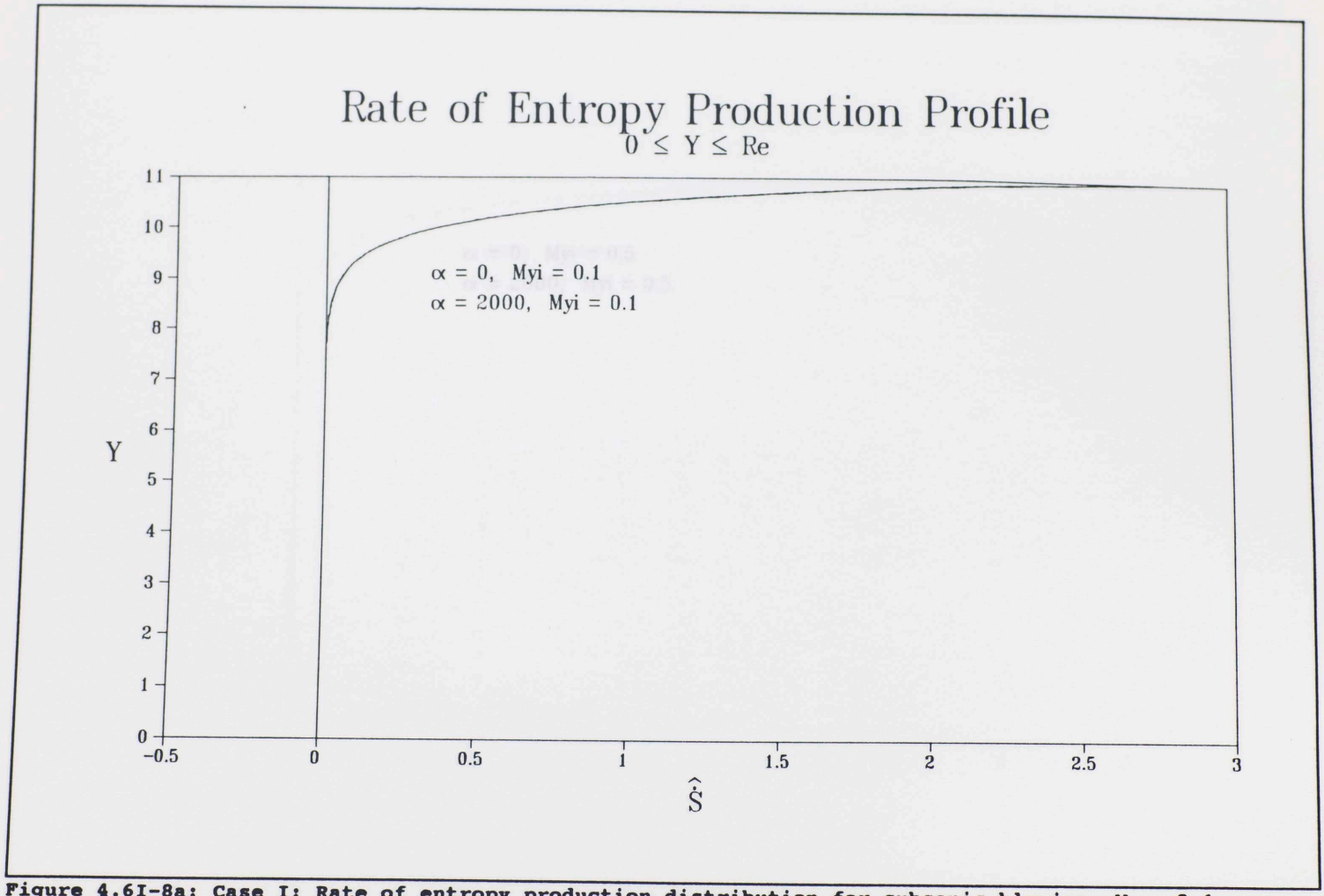

Figure 4.6I-8a: Case I: Rate of entropy production distribution for subsonic blowing, M_{yi} = 0.1

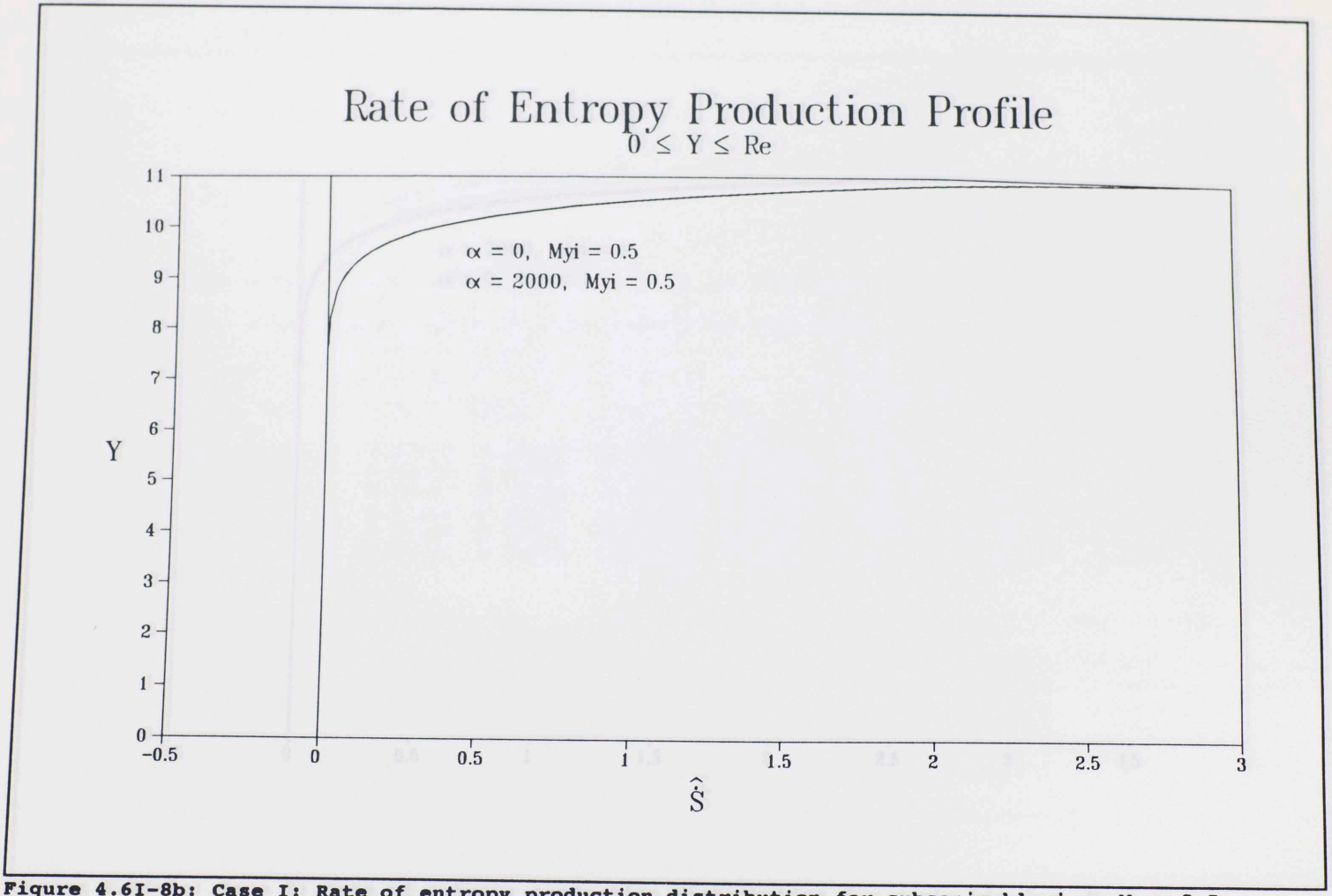

Figure 4.6I-8b: Case I: Rate of entropy production distribution for subsonic blowing, $M_{yi} = 0.5$

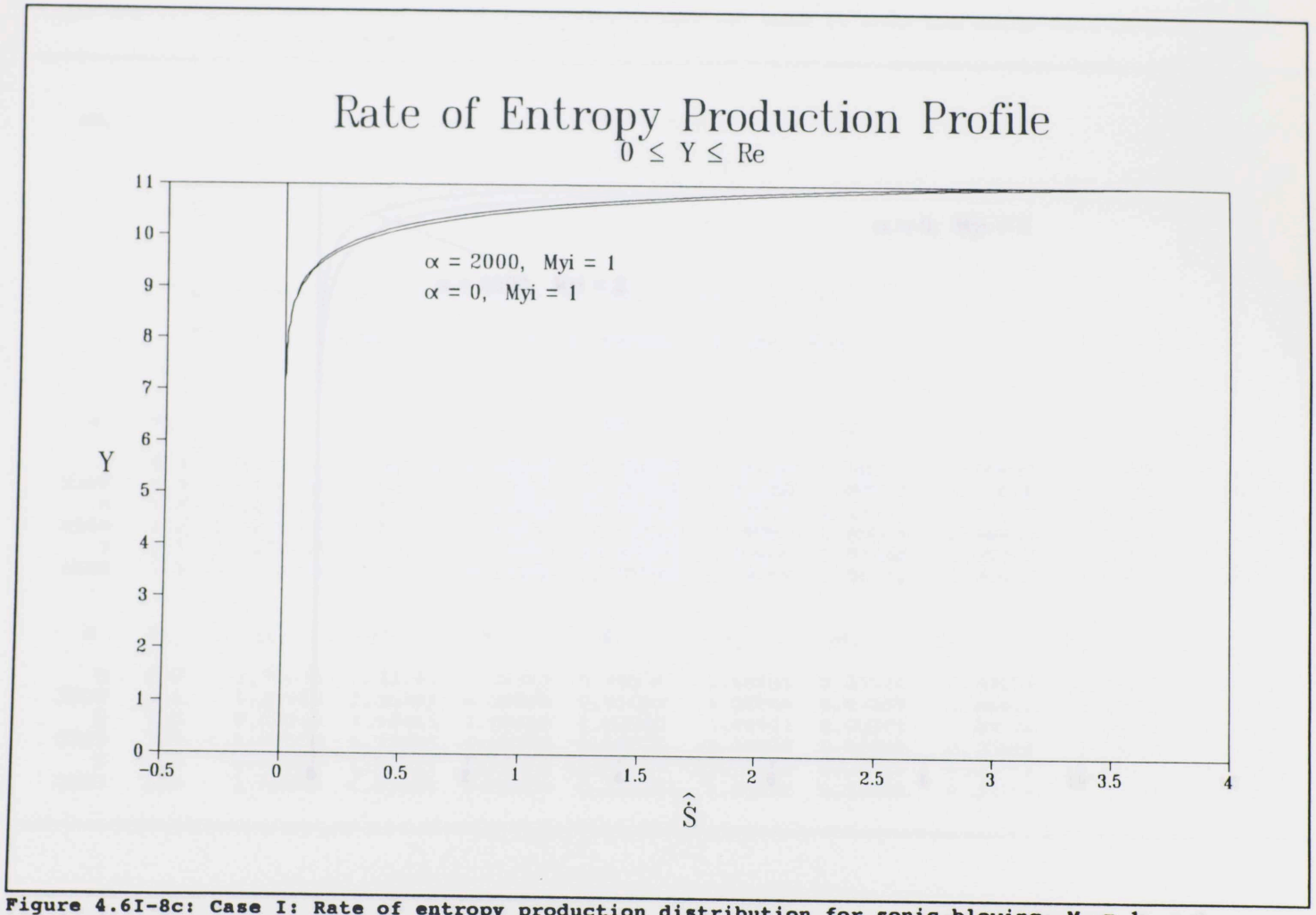

Figure 4.6I-8c: Case I: Rate of entropy production distribution for sonic blowing, $M_{yi} = 1$

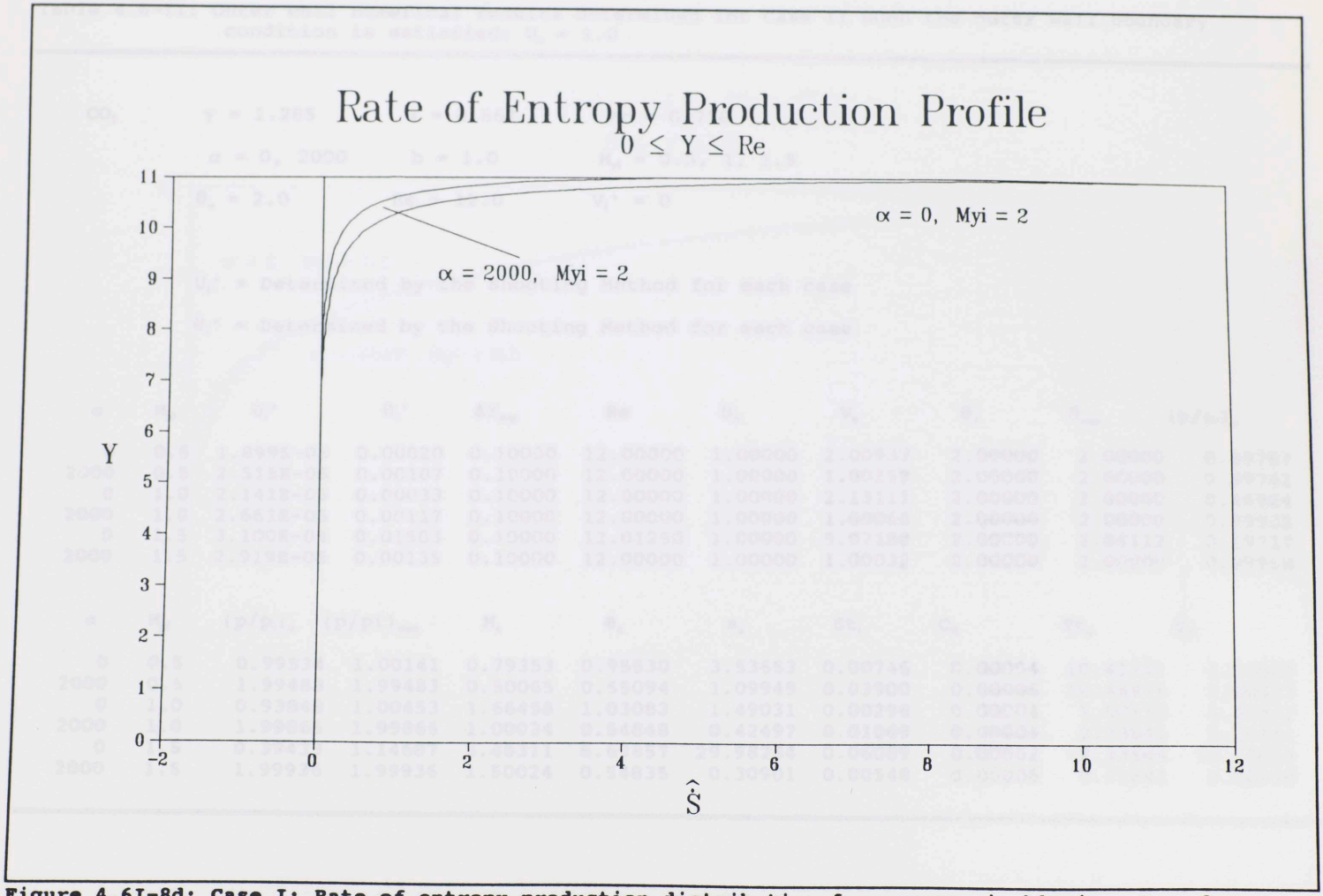

Figure 4.6I-8d: Case I: Rate of entropy production distribution for supersonic blowing, M_{y1} = 2

Table 4.6-II: Outer wall numerical results determined for Case II when the outer wall boundary condition is satisfied: $U_o = 1.0$

CO_2 $\quad \gamma = 1.285 \quad \omega = 0.867 \quad Pr = 0.770$

$\alpha = 0, 2000 \quad b = 1.0 \quad M_{yi} = 0.5, 1, 1.5$

$\theta_o = 2.0 \quad Re = 12.0 \quad V_i' = 0$

U_i' = Determined by the Shooting Method for each case

θ_i' = Determined by the Shooting Method for each case

α	M_{yi}	U_i'	θ_i'	ΔY_{avg}	Re	U_o	V_o	θ_o	θ_{max}	$(\rho/\rho_i)_o$
0	0.5	1.899E-05	0.00020	0.10000	12.00000	1.00000	2.00937	2.00000	2.00000	0.49767
2000	0.5	2.515E-05	0.00107	0.10000	12.00000	1.00000	1.00259	2.00000	2.00000	0.99741
0	1.0	2.141E-05	0.00033	0.10000	12.00000	1.00000	2.13111	2.00000	2.00000	0.46924
2000	1.0	2.661E-05	0.00117	0.10000	12.00000	1.00000	1.00068	2.00000	2.00000	0.99932
0	1.5	3.100E-04	0.01503	0.10000	12.01250	1.00000	5.07188	2.00000	2.84112	0.19717
2000	1.5	2.919E-05	0.00135	0.10000	12.00000	1.00000	1.00032	2.00000	2.00000	0.99968

α	M_{yi}	$(p/p_i)_o$	$(p/pi)_{max}$	M_o	Φ_o	s_o	St_i	C_{fi}	St_o	C_{fo}
0	0.5	0.99534	1.00141	0.79353	0.95530	3.53653	0.00746	0.00004	10.41751	4.01882
2000	0.5	1.99483	1.99483	0.50065	0.55094	1.09949	0.03900	0.00005	10.44976	2.00523
0	1.0	0.93848	1.00453	1.66458	1.03083	1.49031	0.00298	0.00004	1.90172	4.26232
2000	1.0	1.99865	1.99865	1.00034	0.54848	0.42497	0.01069	0.00005	2.23641	2.00141
0	1.5	0.39433	1.14687	5.48311	6.69857	29.98234	0.06089	0.00062	-2.33546	10.16006
2000	1.5	1.99936	1.99936	1.50024	0.54835	0.30901	0.00548	0.00006	0.71641	2.00070

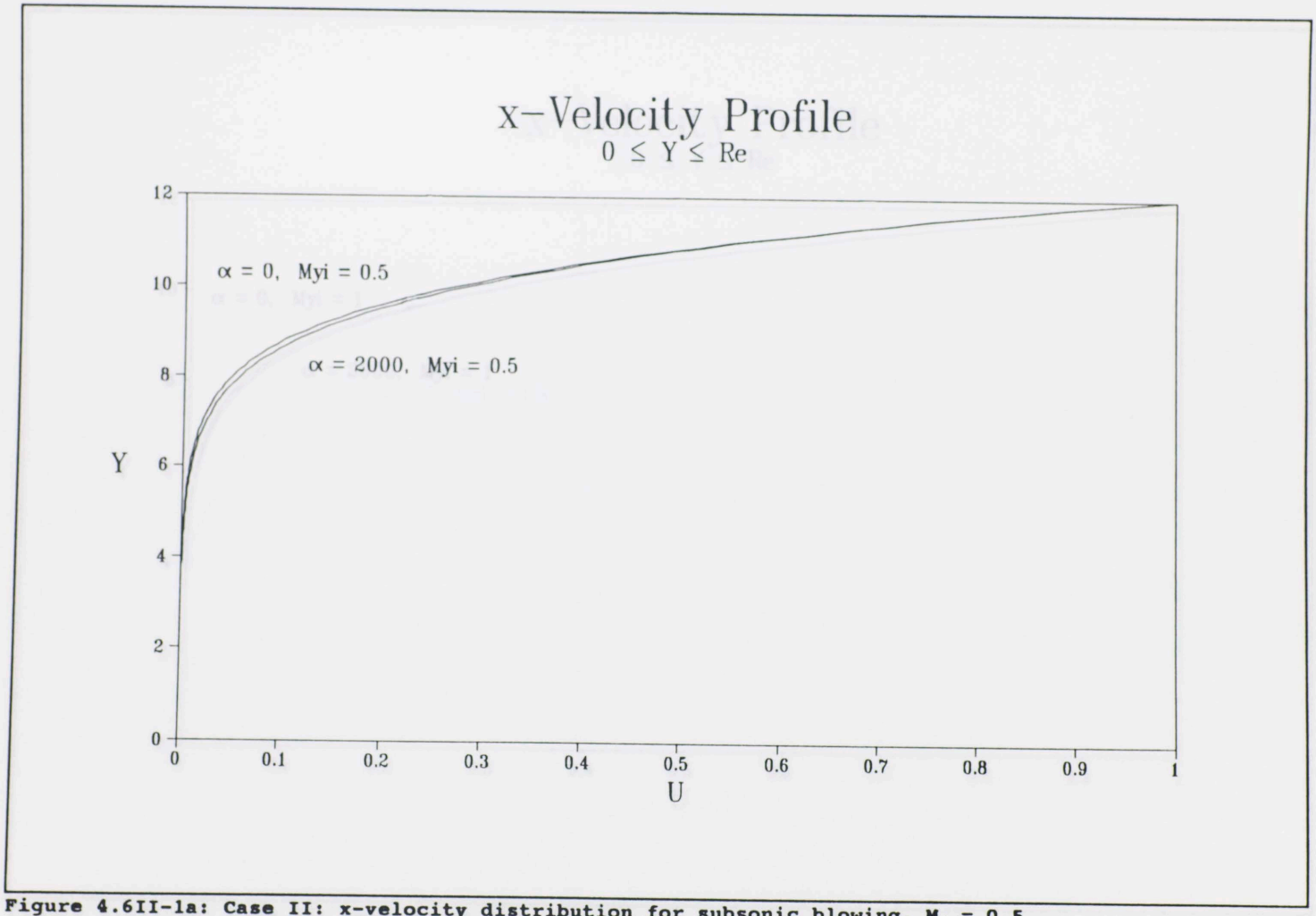

Figure 4.6II-1a: Case II: x-velocity distribution for subsonic blowing, M_{yi} = 0.5

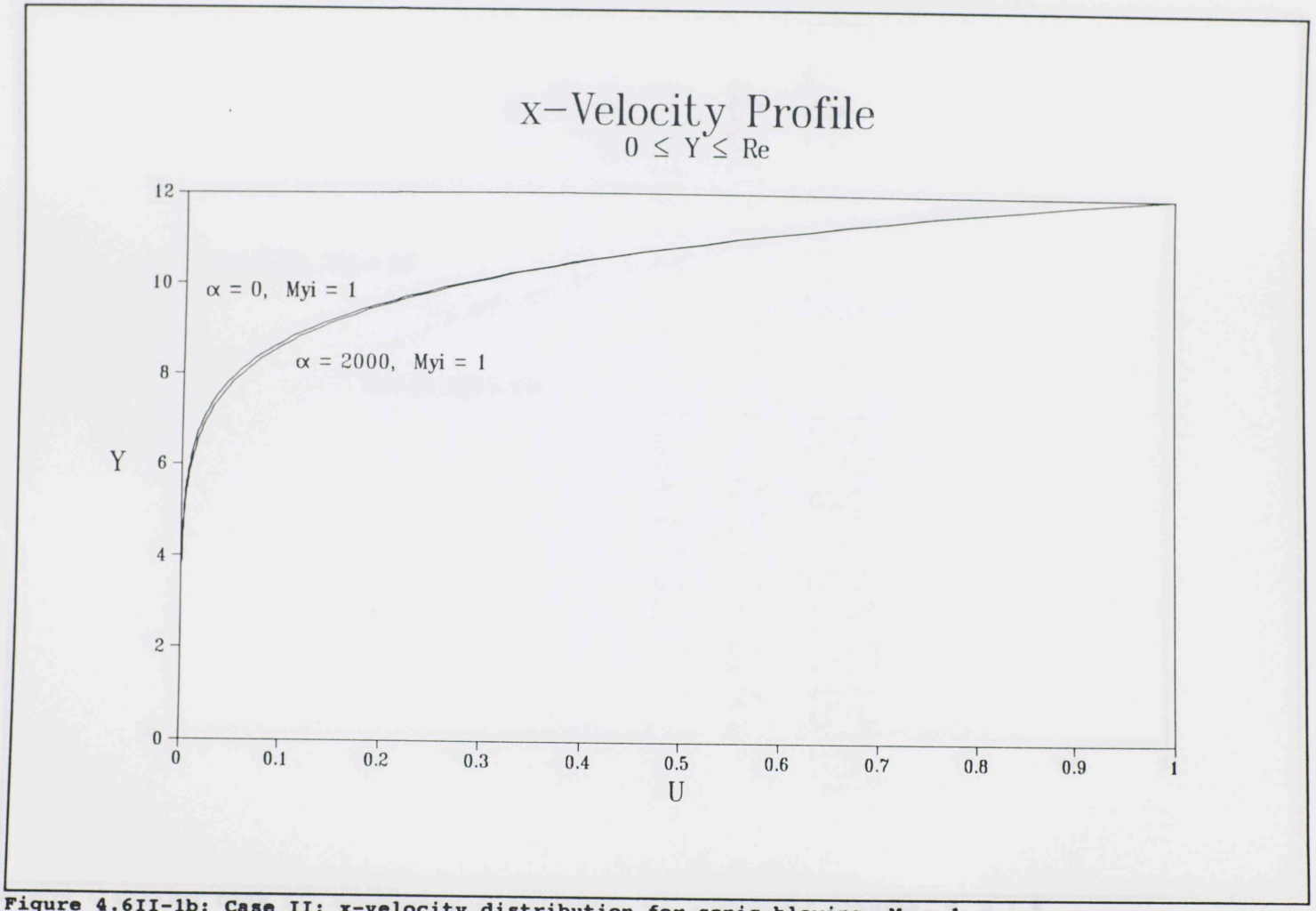

Figure 4.6II-1b: Case II: x-velocity distribution for sonic blowing, $M_{yi} = 1$

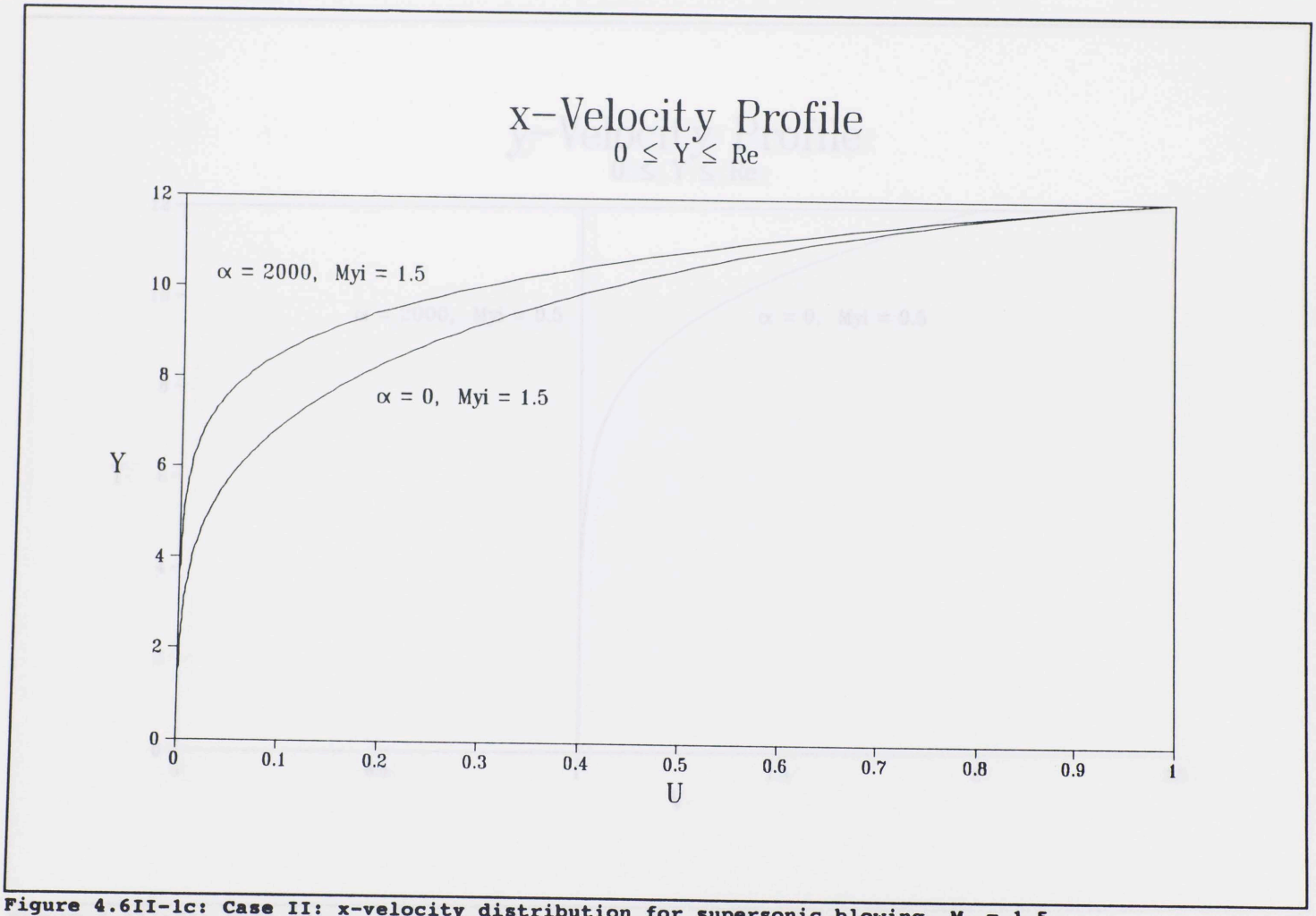

Figure 4.6II-1c: Case II: x-velocity distribution for supersonic blowing, M_{yi} = 1.5

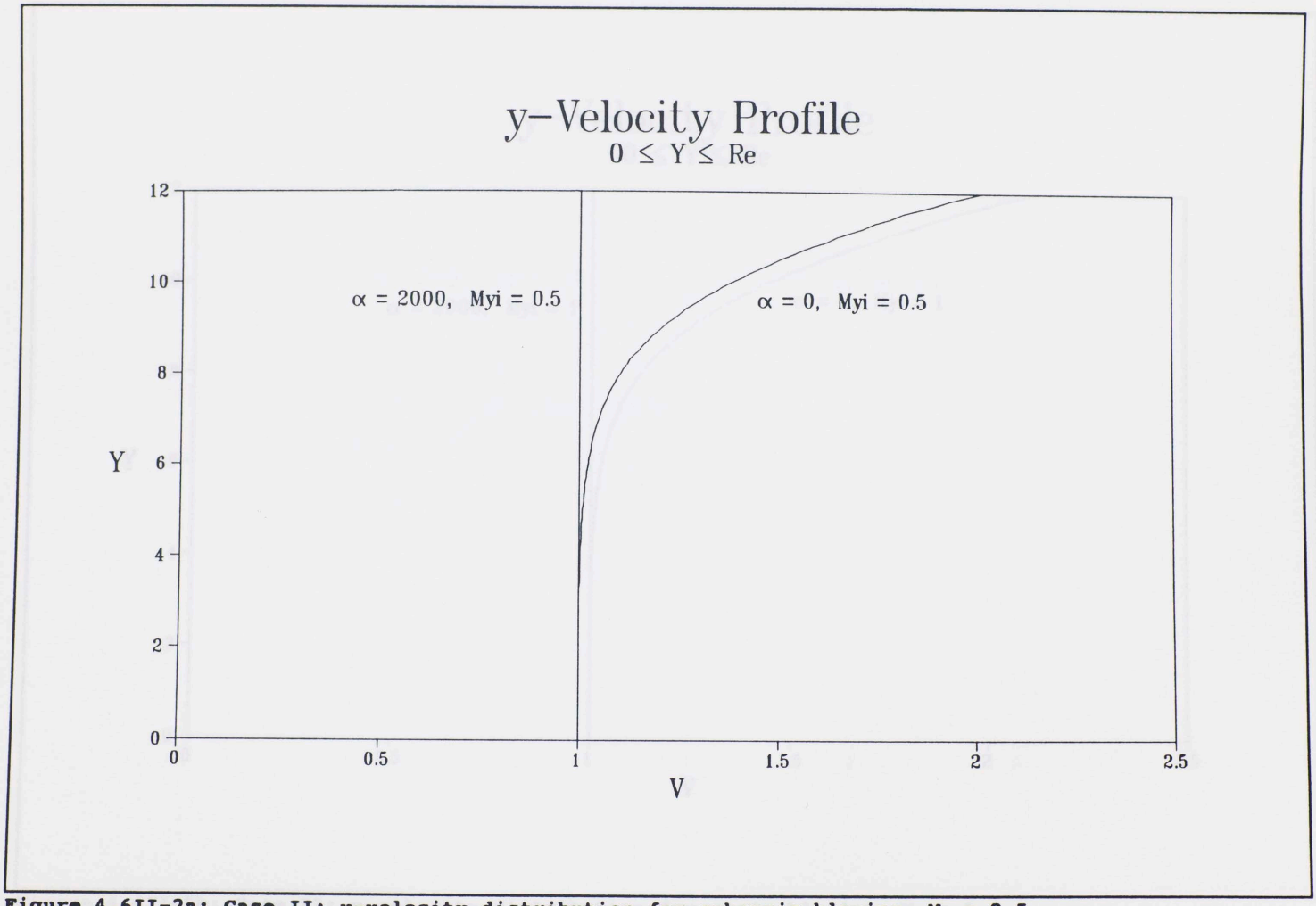

Figure 4.6II-2a: Case II: y-velocity distribution for subsonic blowing, M_{yi} = 0.5

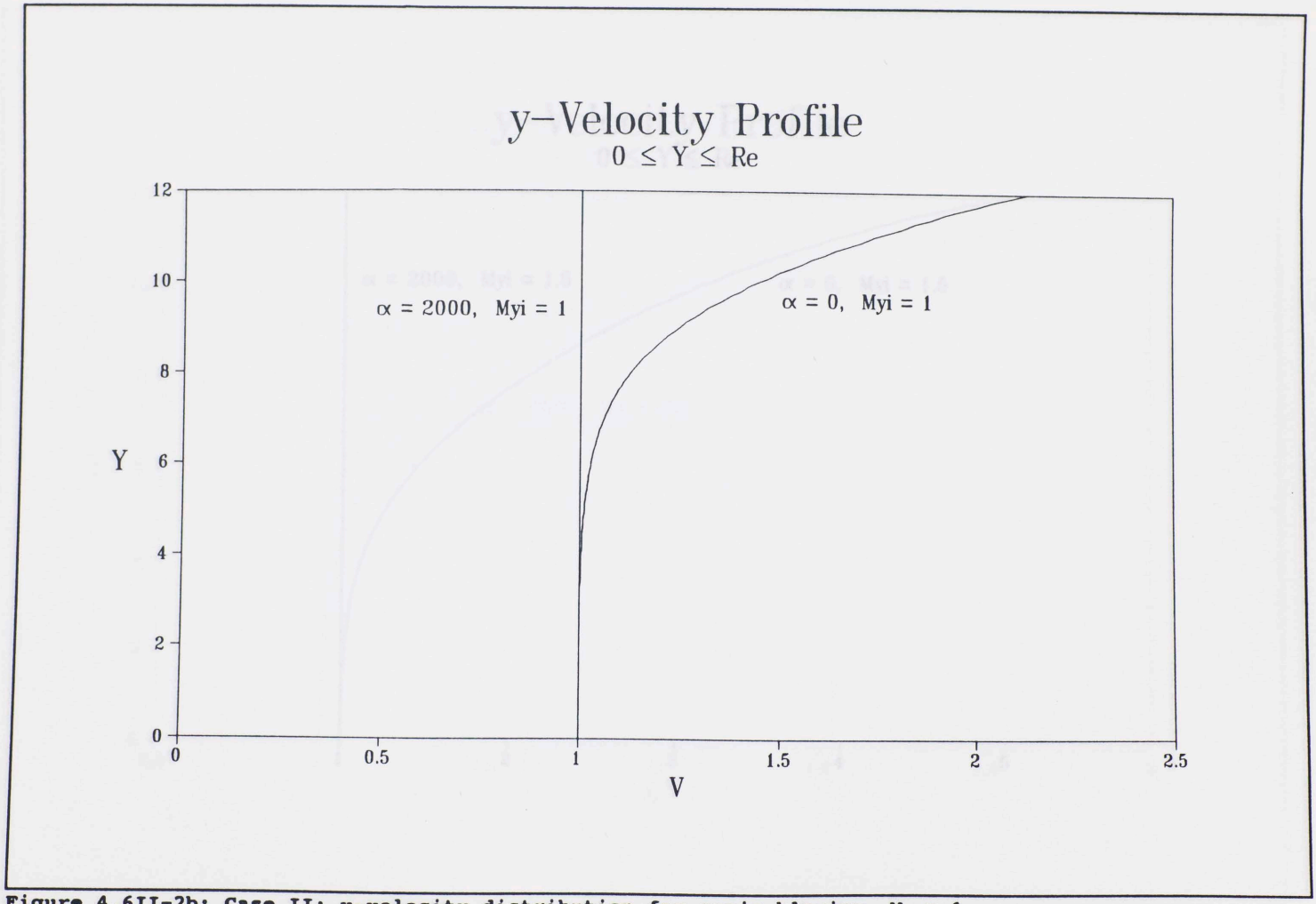

Figure 4.6II-2b: Case II: y-velocity distribution for sonic blowing, $M_{yi} = 1$

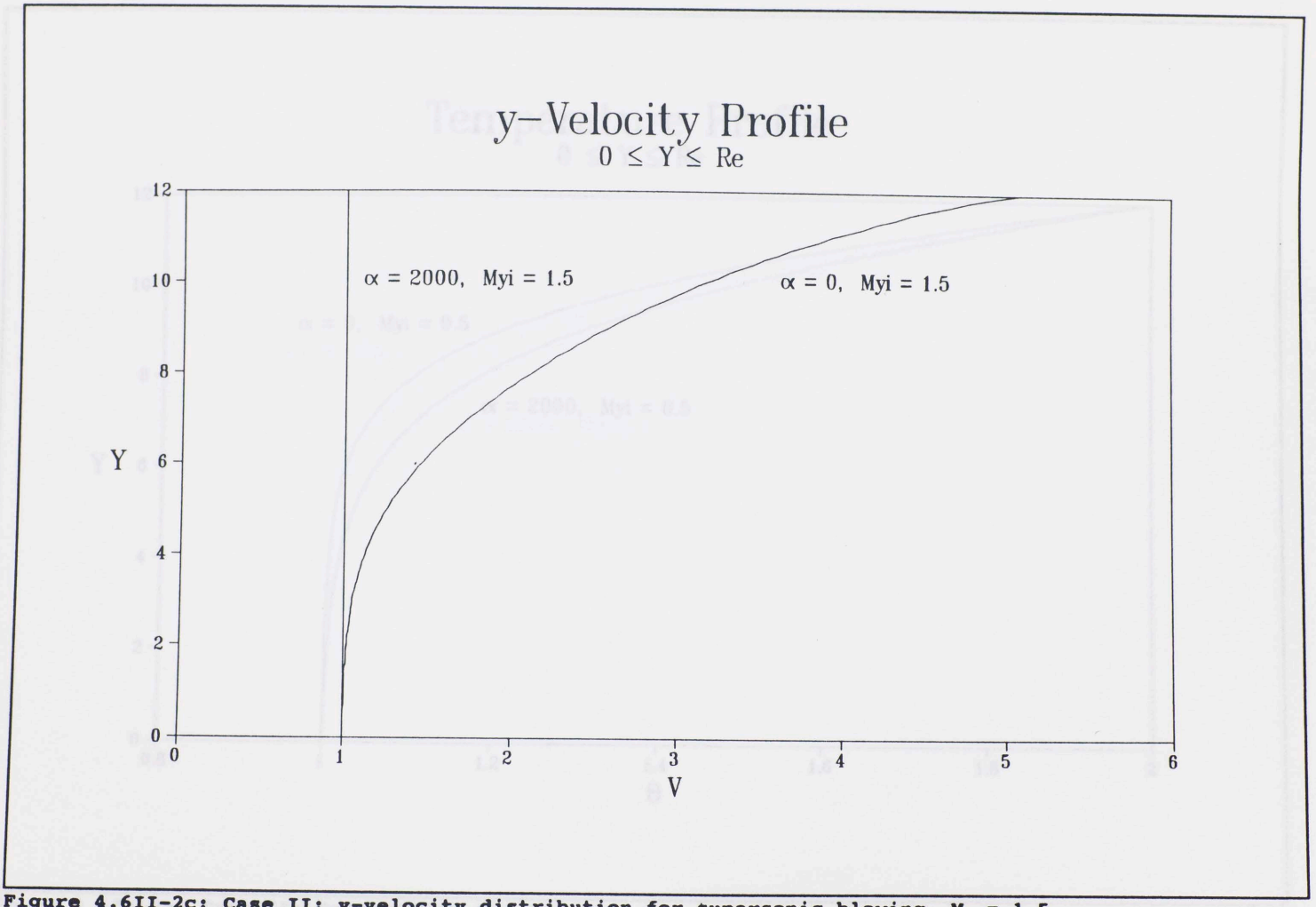

Figure 4.6II-2c: Case II: y-velocity distribution for supersonic blowing, M_{yi} = 1.5

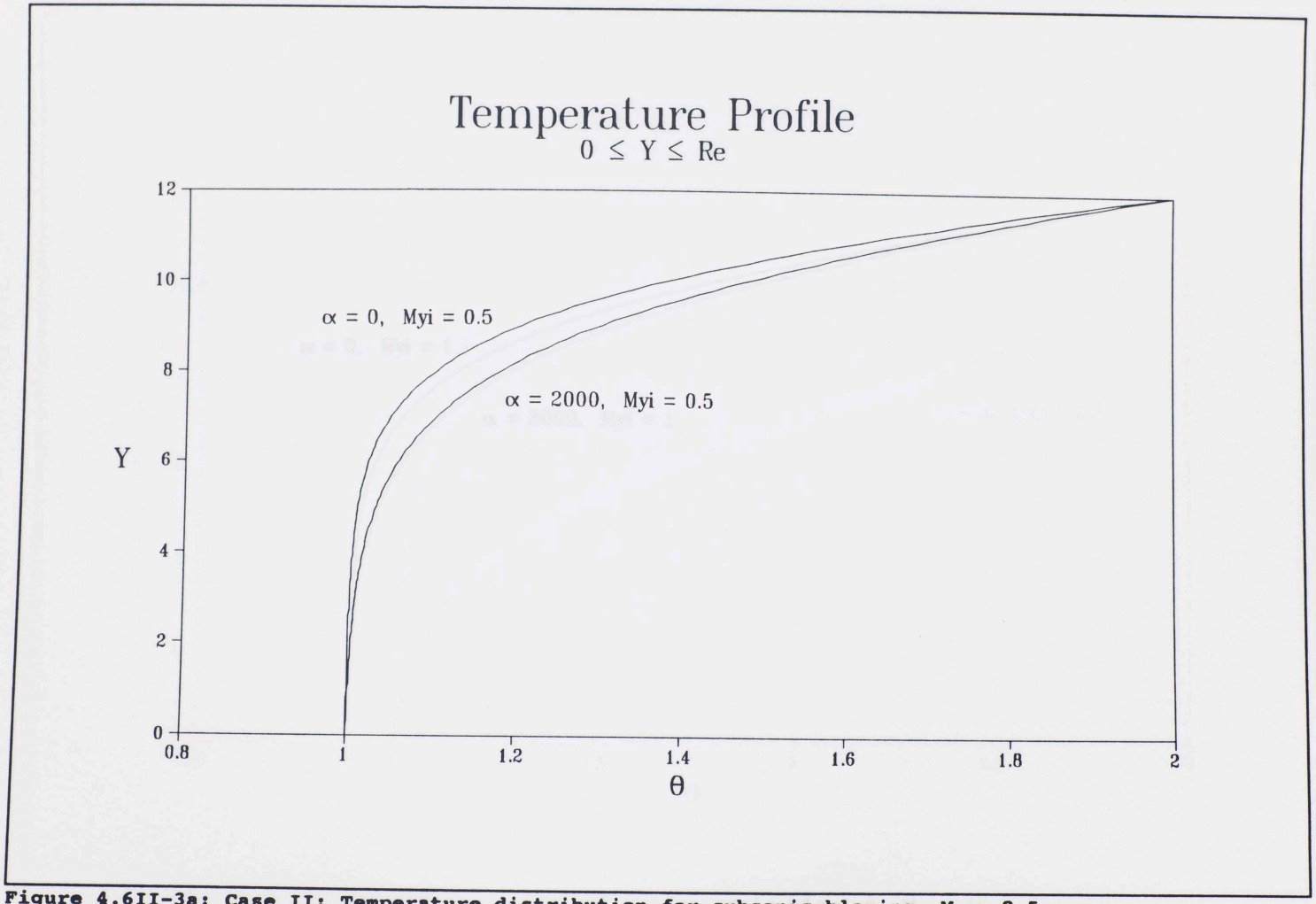

Figure 4.6II-3a: Case II: Temperature distribution for subsonic blowing, M_{yi} = 0.5

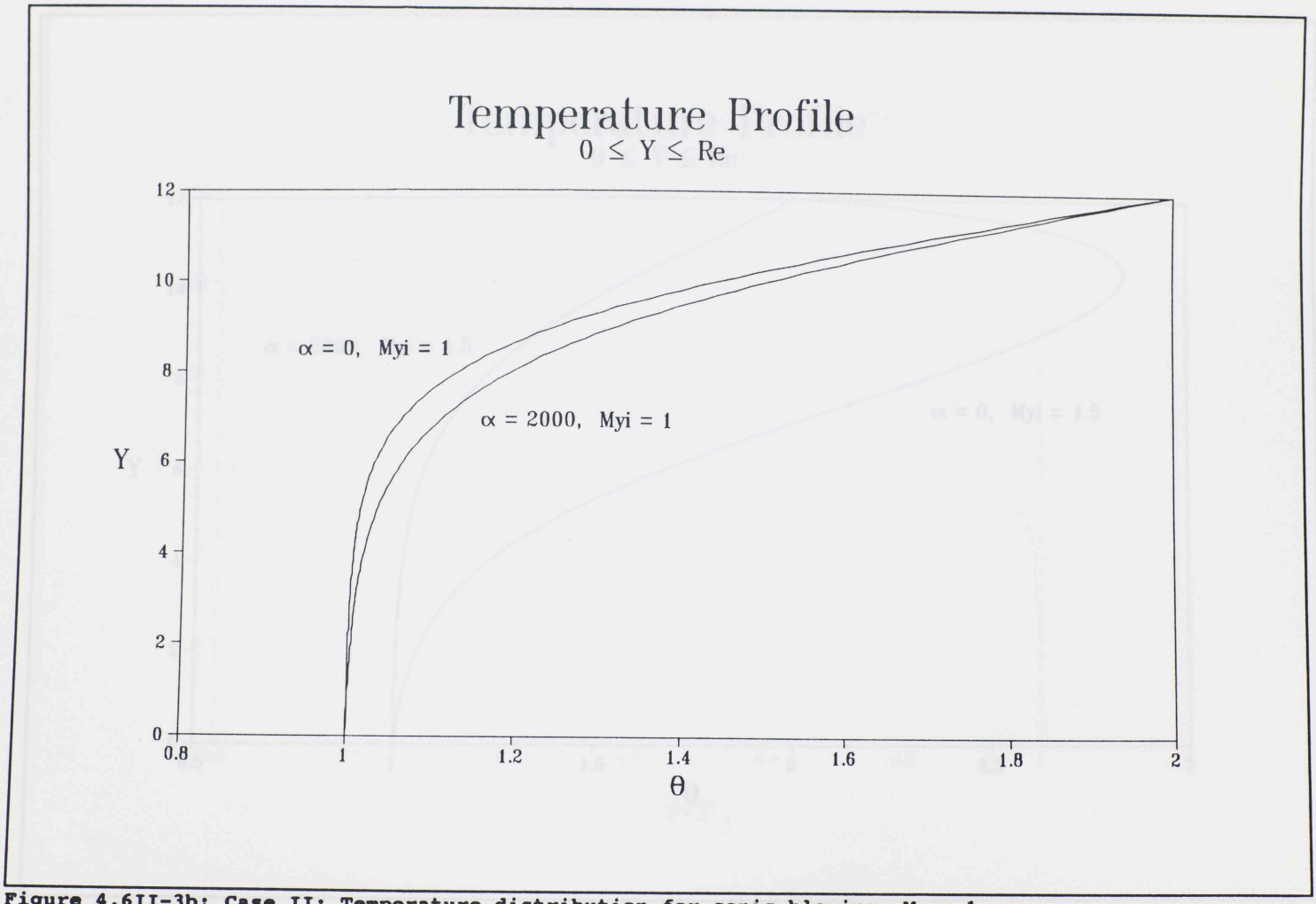

Figure 4.6II-3b: Case II: Temperature distribution for sonic blowing, $M_{yi} = 1$

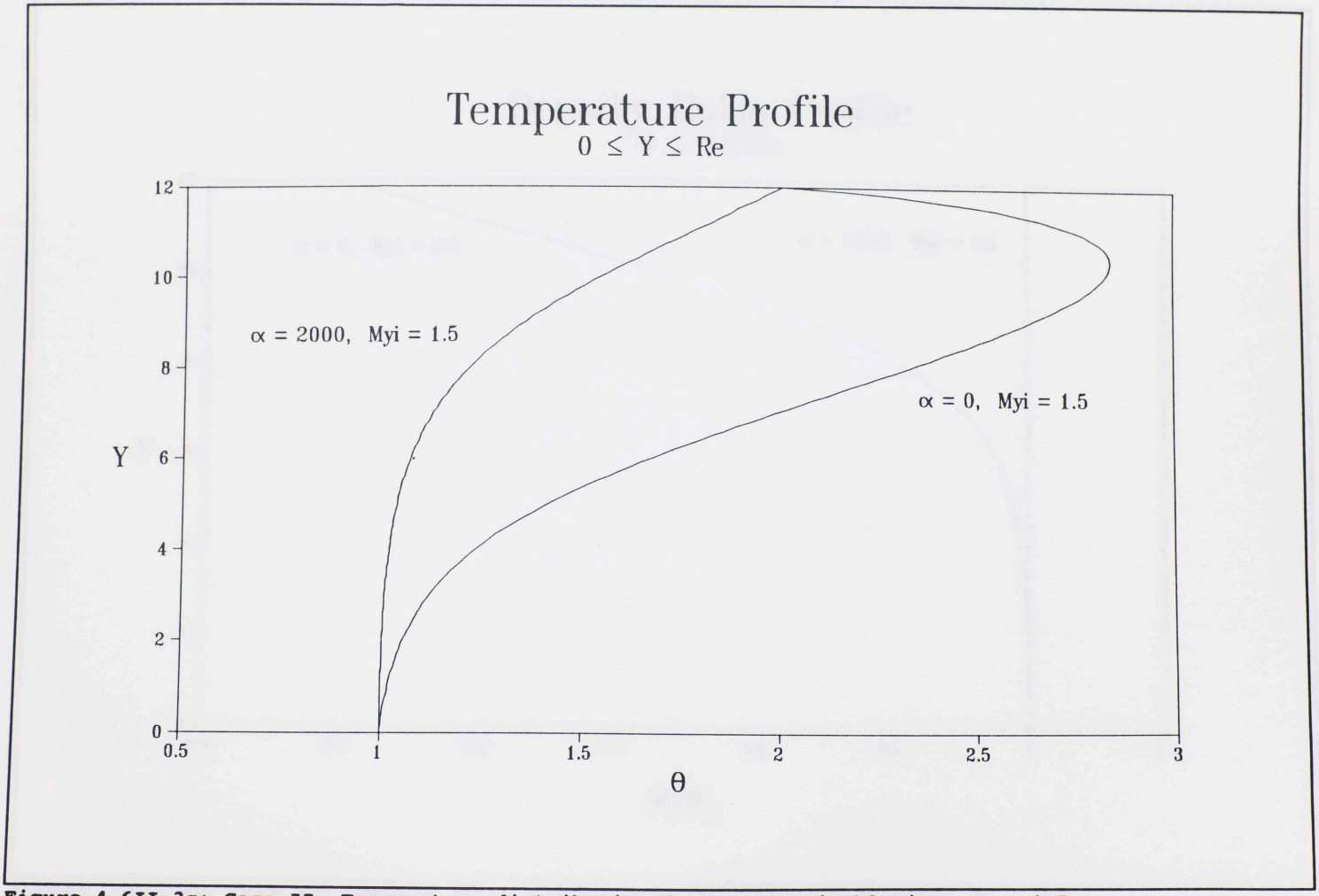

Figure 4.6II-3c: Case II: Temperature distribution for supersonic blowing, M_{yi} = 1.5

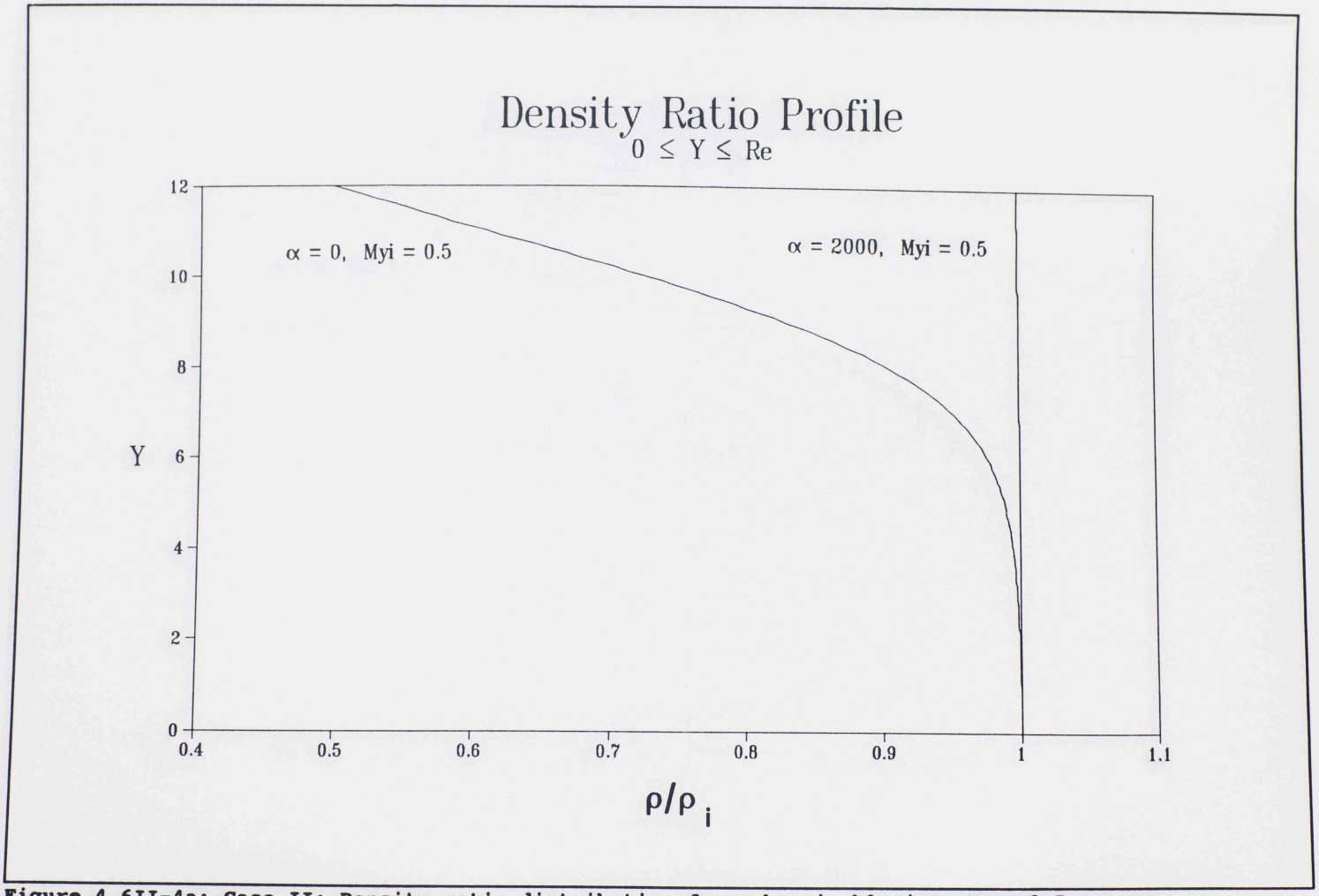

Figure 4.6II-4a: Case II: Density ratio distribution for subsonic blowing, M_{yi} = 0.5

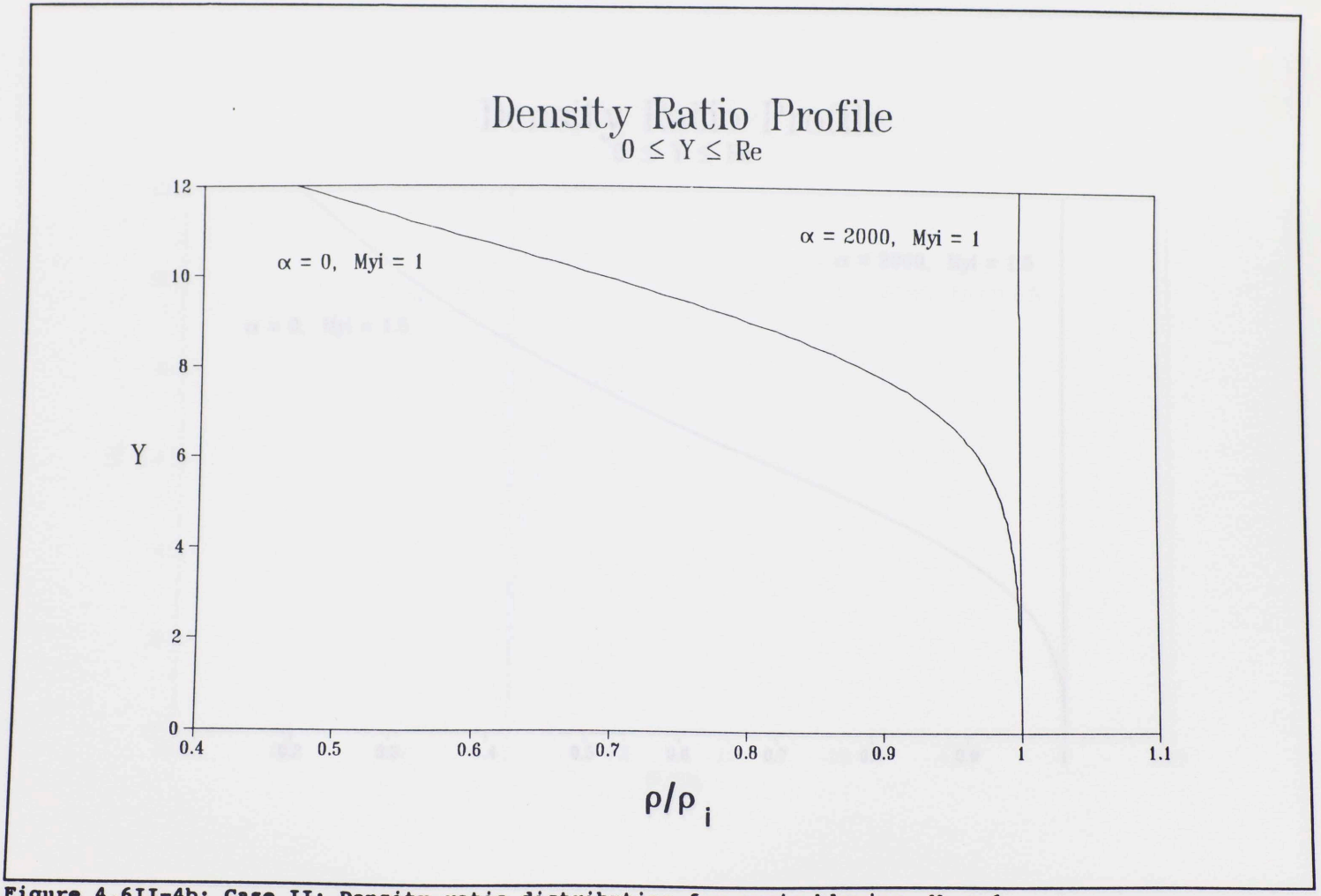

Figure 4.6II-4b: Case II: Density ratio distribution for sonic blowing, $M_{yi} = 1$

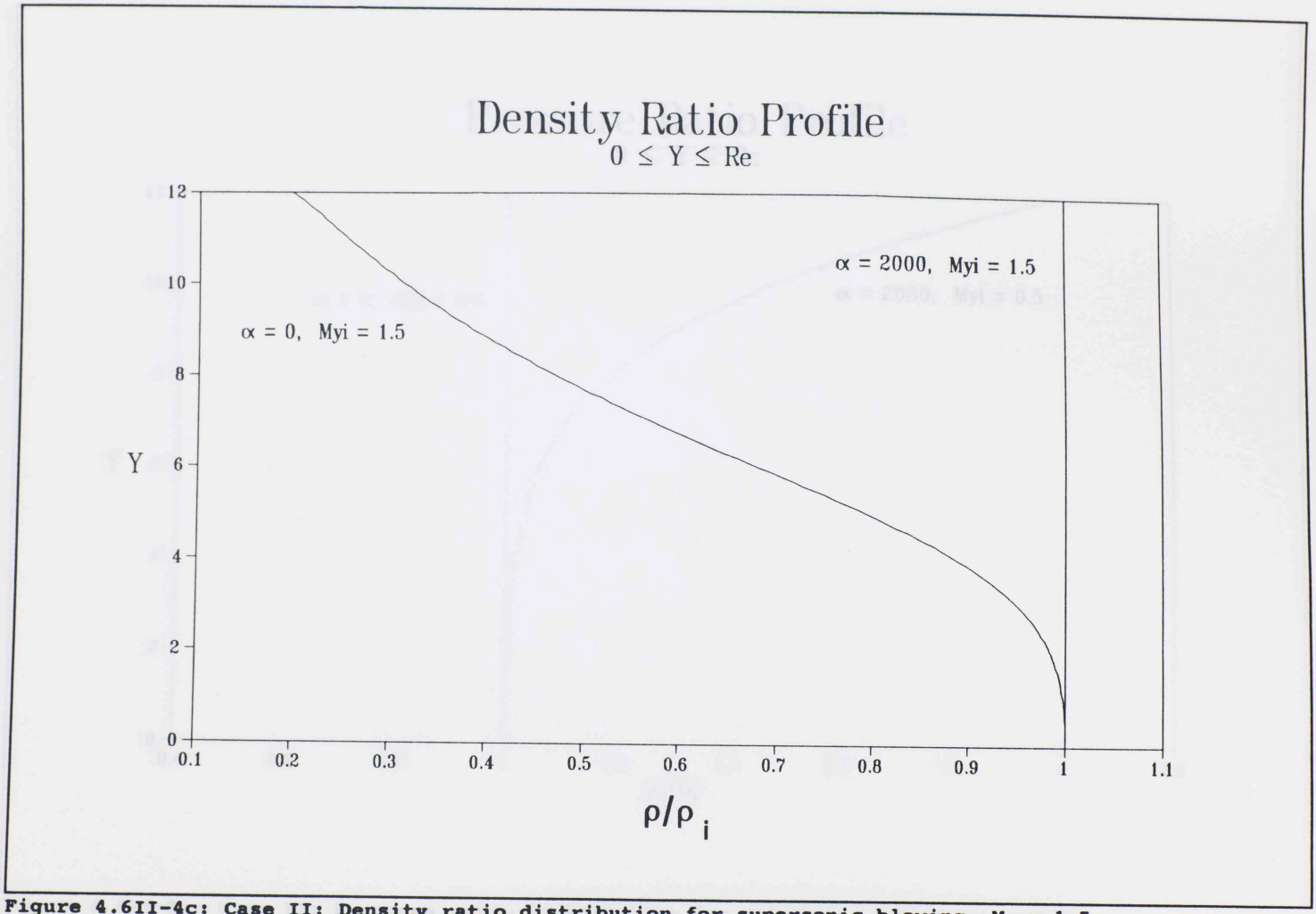

Figure 4.6II-4c: Case II: Density ratio distribution for supersonic blowing, $M_{yi} = 1.5$

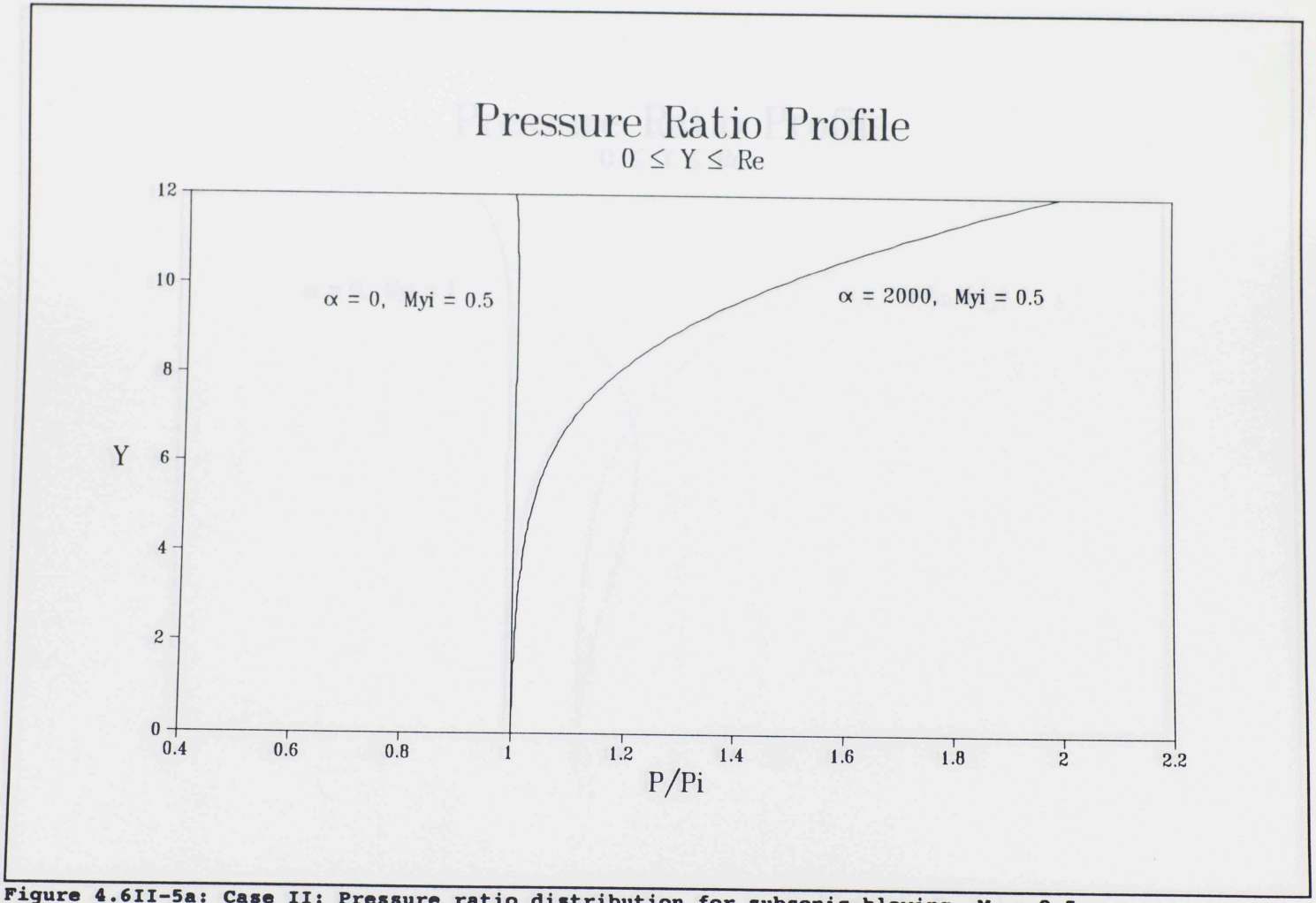

Figure 4.6II-5a: Case II: Pressure ratio distribution for subsonic blowing, $M_{yi} = 0.5$

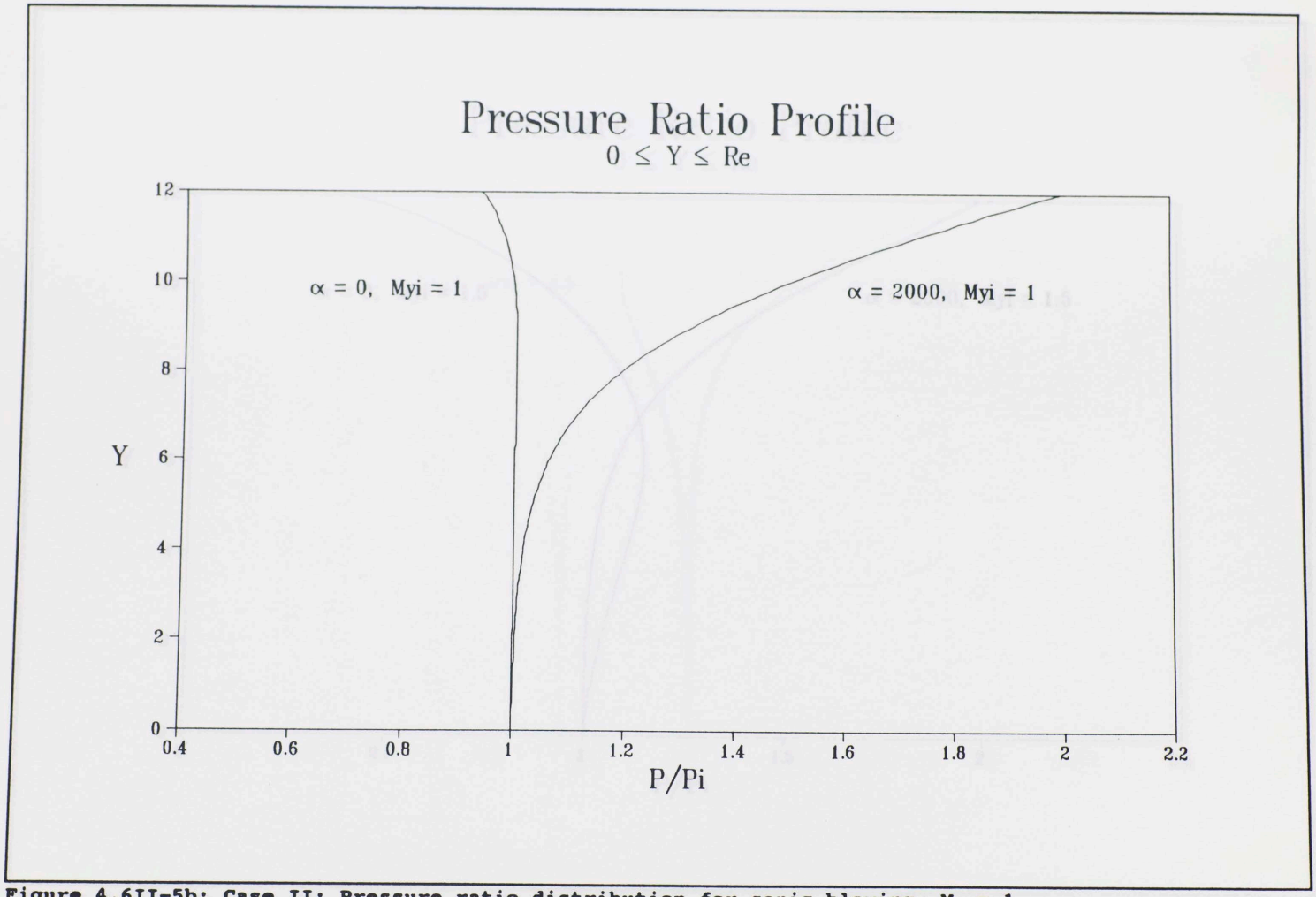

Figure 4.6II-5b: Case II: Pressure ratio distribution for sonic blowing, $M_{yi} = 1$

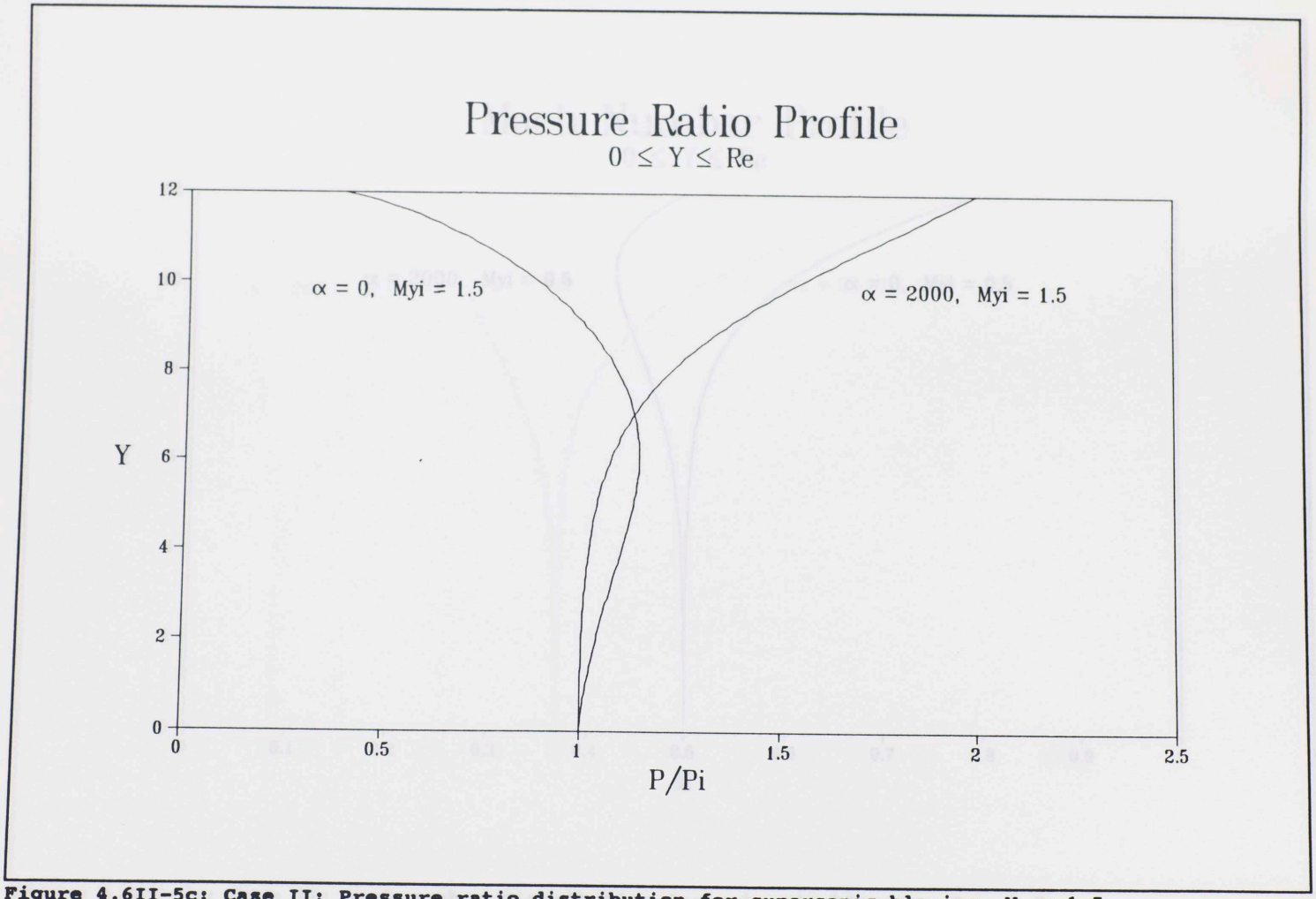

Figure 4.6II-5c: Case II: Pressure ratio distribution for supersonic blowing, M_{yi} = 1.5

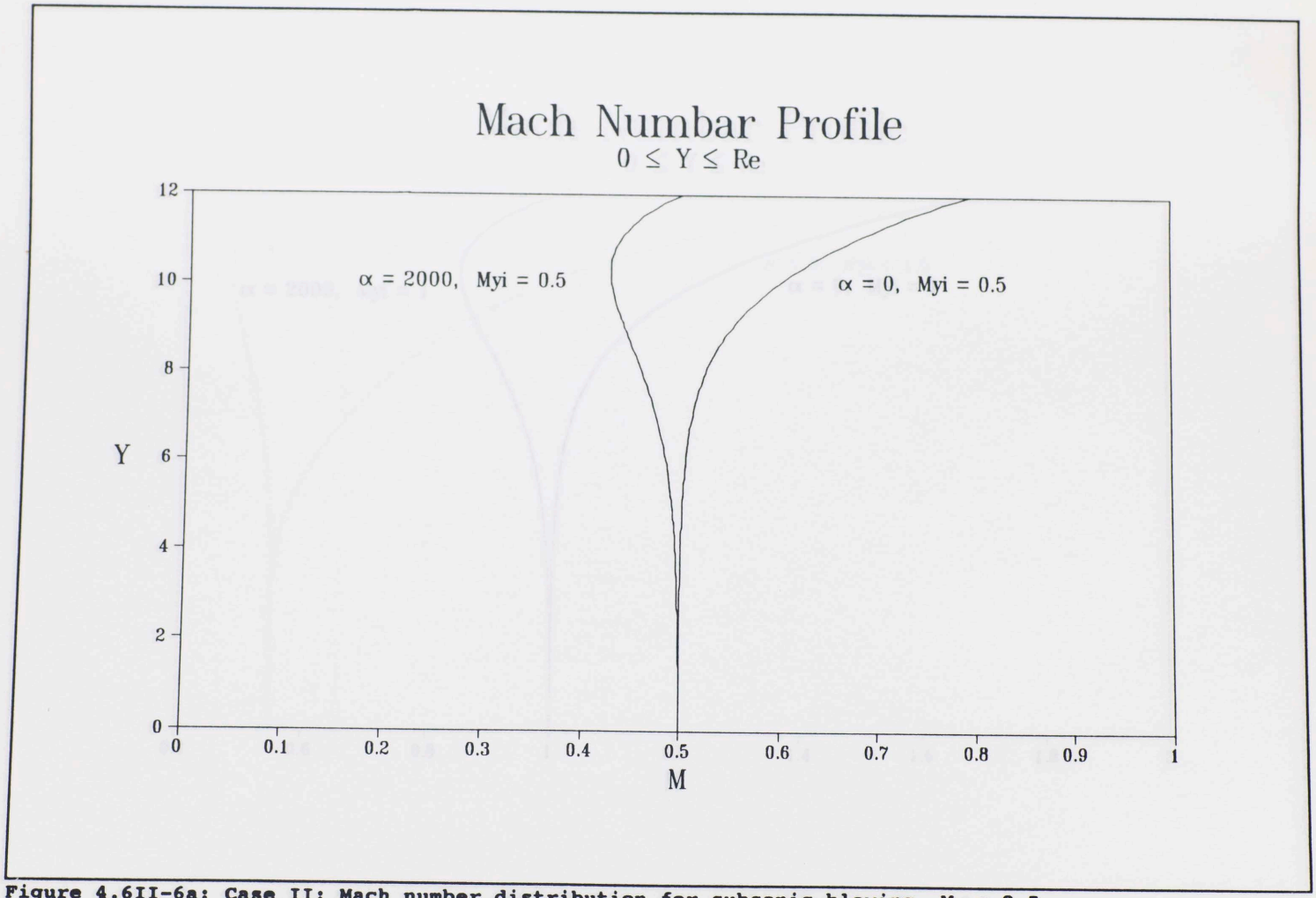

Figure 4.6II-6a: Case II: Mach number distribution for subsonic blowing, M_{yi} = 0.5

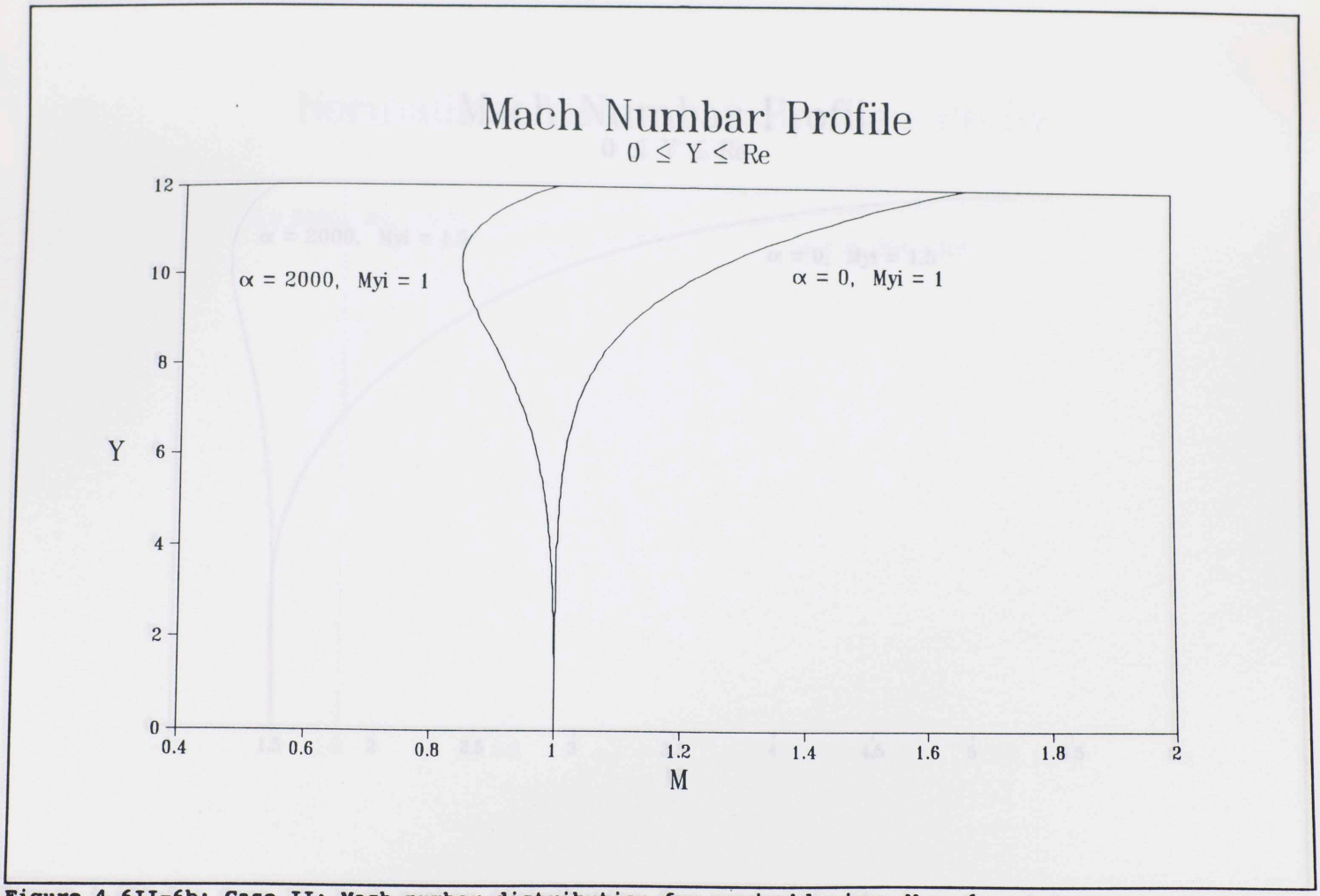

Figure 4.6II-6b: Case II: Mach number distribution for sonic blowing, $M_{yi} = 1$

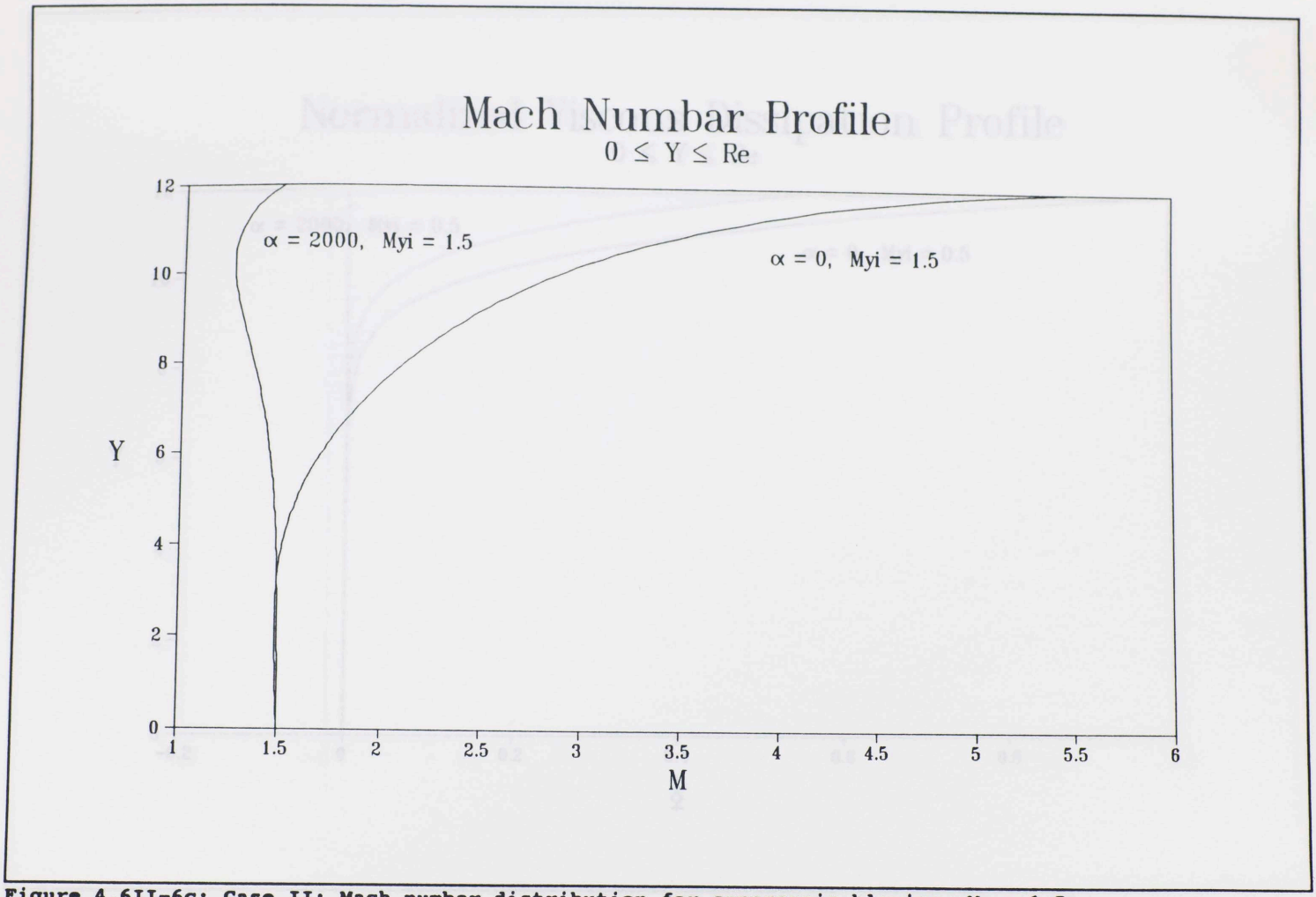

Figure 4.6II-6c: Case II: Mach number distribution for supersonic blowing, M_{yi} = 1.5

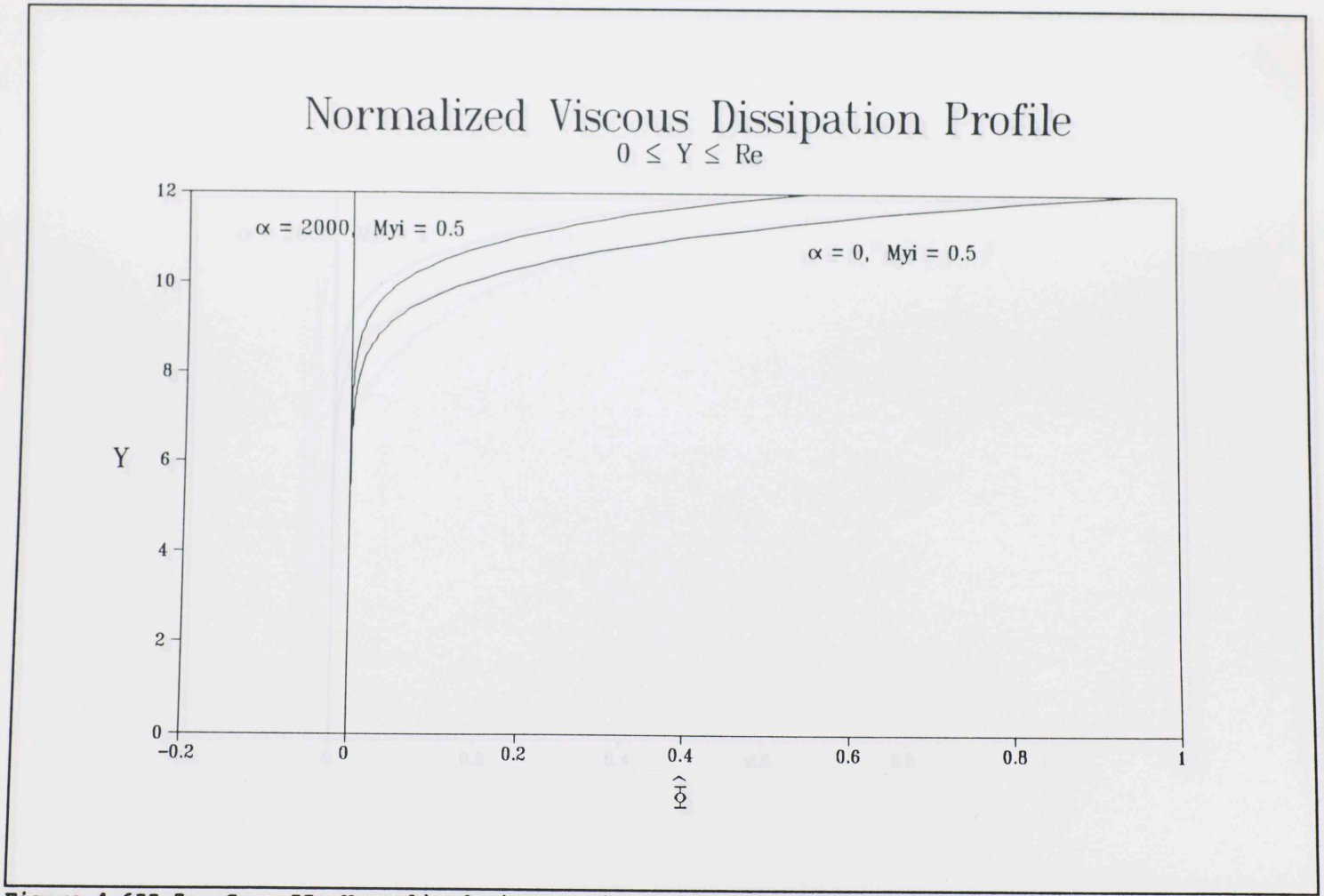

Figure 4.6II-7a: Case II: Normalized viscous dissipation distribution for subsonic blowing, M_{yi} = 0.5

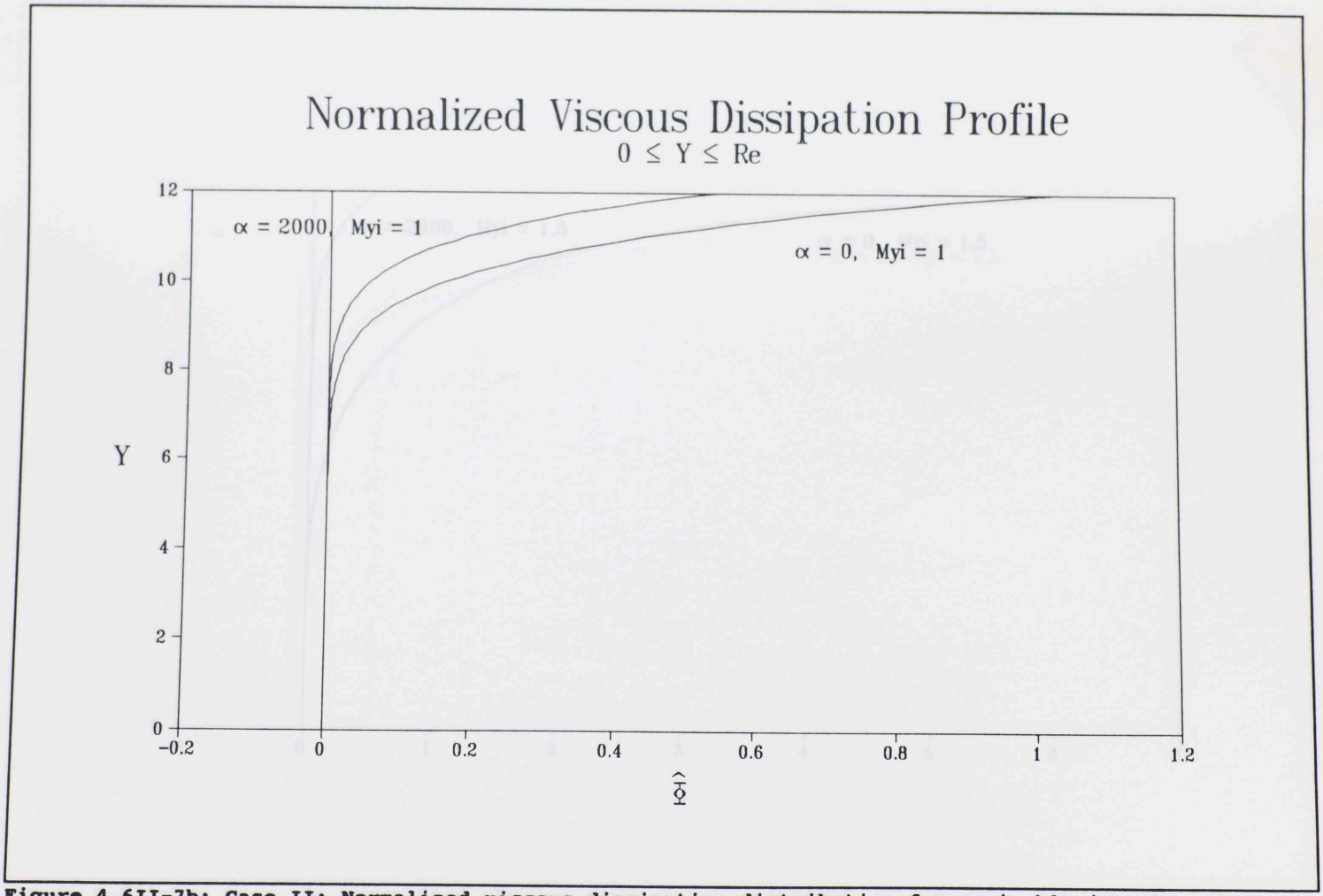

Figure 4.6II-7b: Case II: Normalized viscous dissipation distribution for sonic blowing, $M_{yi} = 1$

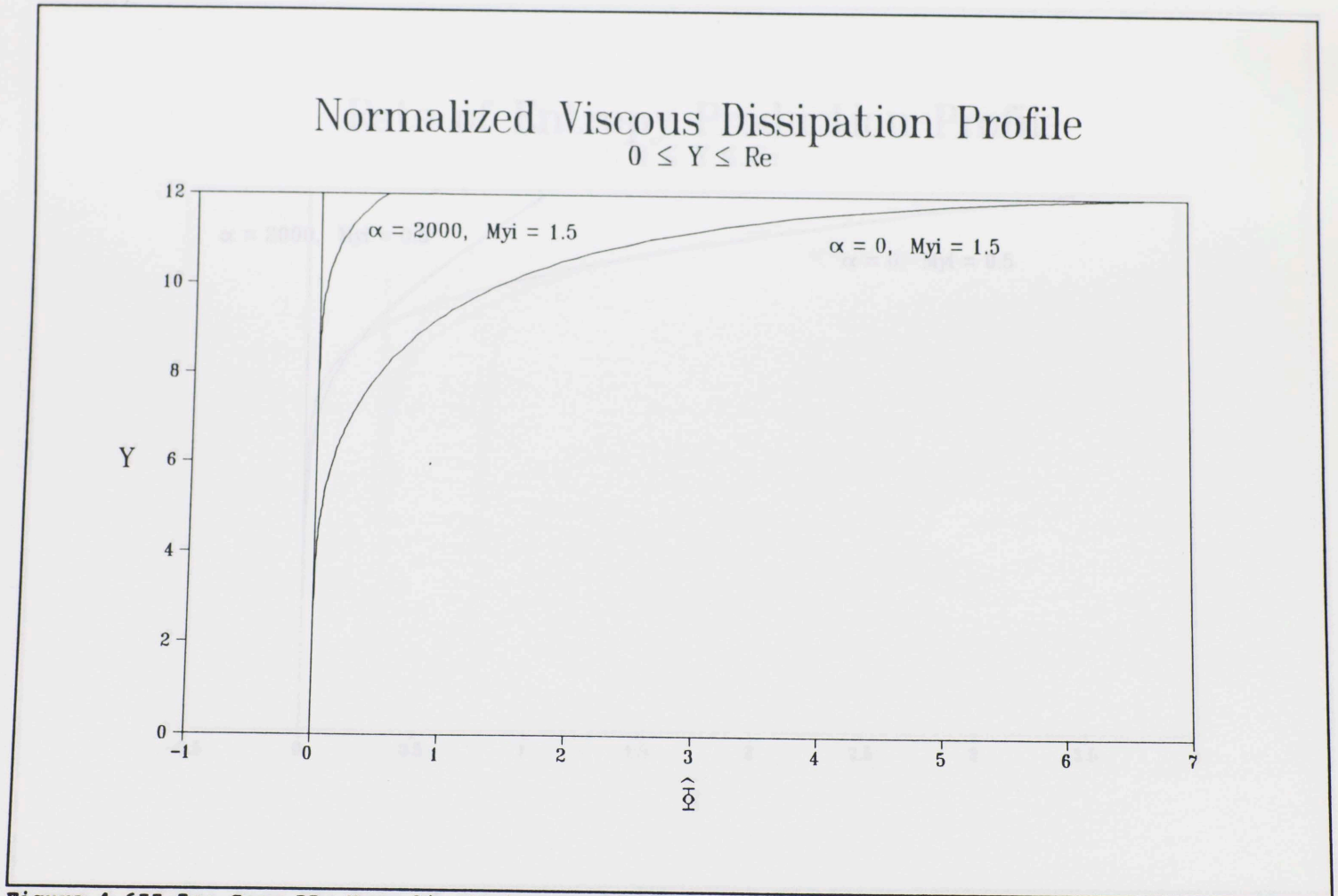

Figure 4.6II-7c: Case II: Normalized viscous dissipation distribution for supersonic blowing, M_{yi} = 1.5

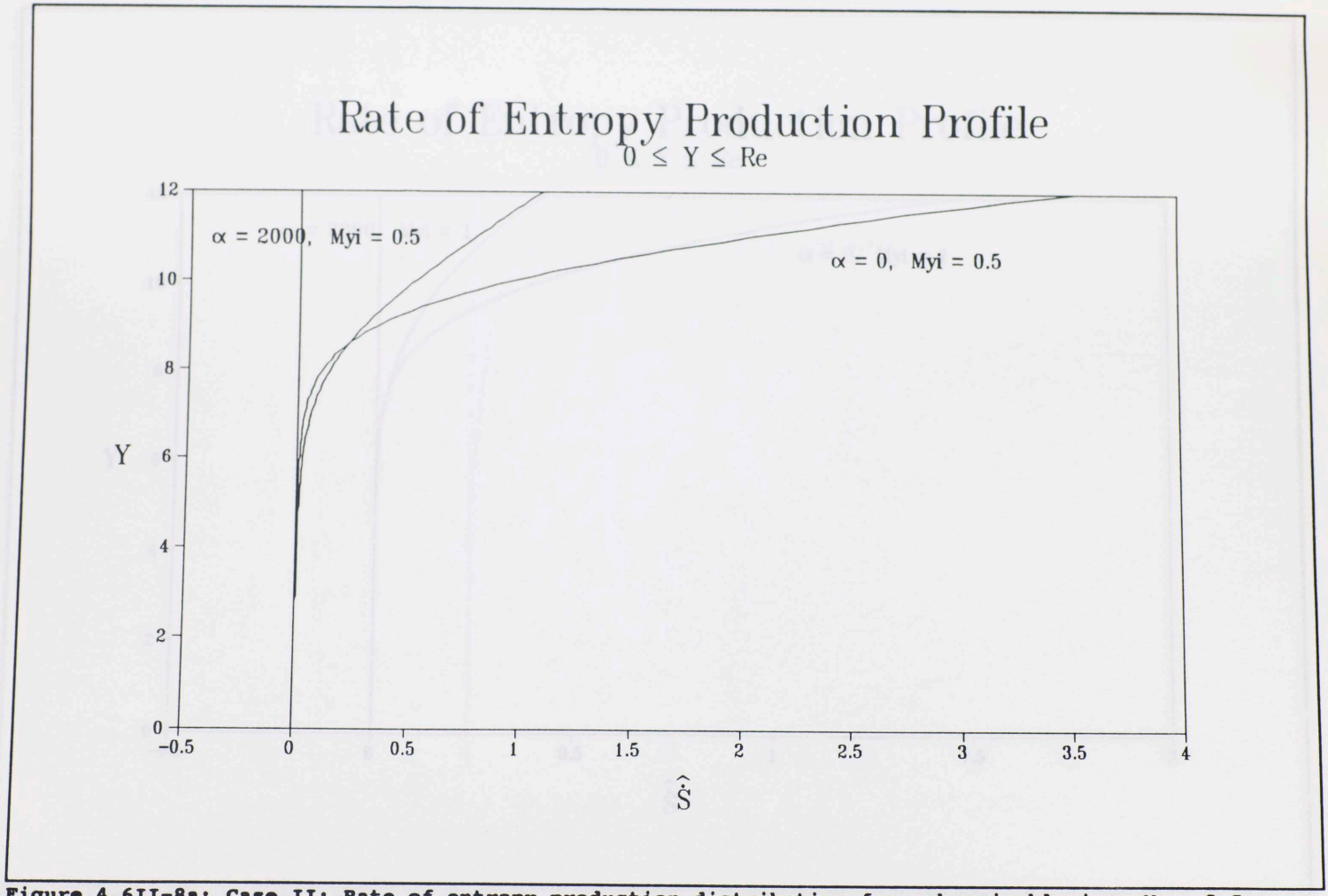

Figure 4.6II-8a: Case II: Rate of entropy production distribution for subsonic blowing, $M_{yi} = 0.5$

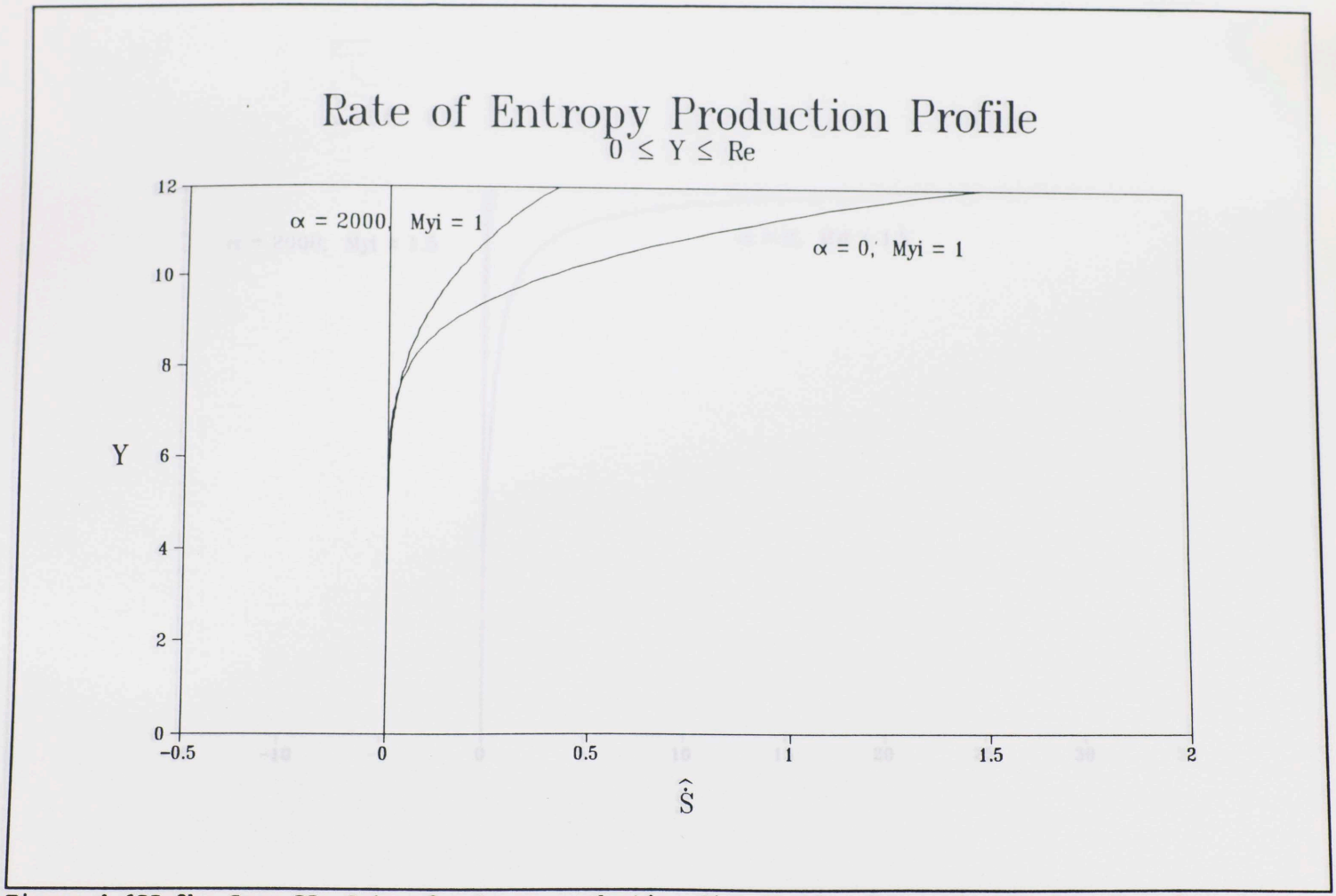

Figure 4.6II-8b: Case II: Rate of entropy production distribution for sonic blowing, $M_{yi} = 1$

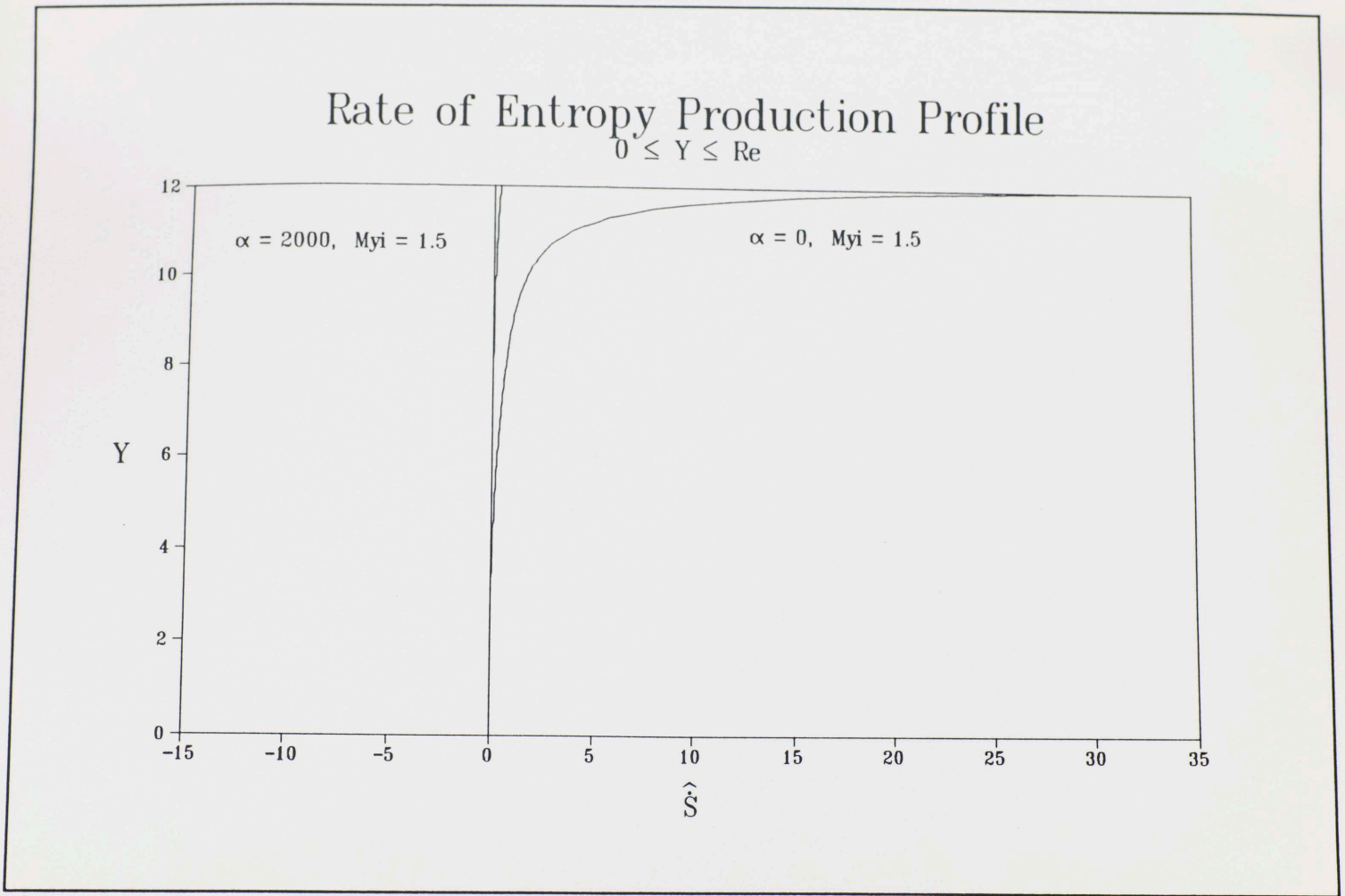

Figure 4.6II-8c: Case II: Rate of entropy production distribution for supersonic blowing, M_{yi} = 1.5